University of New Mexico
UNM Digital Repository

Electrical and Computer Engineering ETDs | Engineering ETDs

2-7-1961

A Development of an Equivalent Circuit of a Hall Generator Which Utilizes a Flux Concentrator

Laurence L. Rosier

Follow this and additional works at: https://digitalrepository.unm.edu/ece_etds

Part of the Electrical and Computer Engineering Commons

Recommended Citation
Rosier, Laurence L.. "A Development of an Equivalent Circuit of a Hall Generator Which Utilizes a Flux Concentrator." (1961).
https://digitalrepository.unm.edu/ece_etds/373

This Thesis is brought to you for free and open access by the Engineering ETDs at UNM Digital Repository. It has been accepted for inclusion in Electrical and Computer Engineering ETDs by an authorized administrator of UNM Digital Repository. For more information, please contact disc@unm.edu.

UNIVERSITY OF NEW MEXICO-GENERAL LIBRARY
A14419 458077

378.789
Un3Oro
1961
cop. 2

A DEVELOPMENT OF AN EQUIVALENT CIRCUIT OF A HALL GENERATOR WHICH UTILIZES A FLUX CONCENTRATOR - ROSIER

THE LIBRARY
UNIVERSITY OF NEW MEXICO

Call No.
378.789
Un30ro
1961
cop.2

Accession
Number
274241

UNIVERSITY OF NEW MEXICO LIBRARY

MANUSCRIPT THESES

Unpublished theses submitted for the Master's and Doctor's degrees and deposited in the University of New Mexico Library are open for inspection, but are to be used only with due regard to the rights of the authors. Bibliographical references may be noted, but passages may be copied only with the permission of the authors, and proper credit must be given in subsequent written or published work. Extensive copying or publication of the thesis in whole or in part requires also the consent of the Dean of the Graduate School of the University of New Mexico.

This thesis by Laurence L. Rosier
has been used by the following persons, whose signatures attest their acceptance of the above restrictions.

A Library which borrows this thesis for use by its patrons is expected to secure the signature of each user.

NAME AND ADDRESS	DATE

UNIVERSITY OF NEW MEXICO LIBRARY

MANUSCRIPT THESES

Unpublished theses submitted for the Master's and Doctor's degrees and deposited in the University of New Mexico Library are open for inspection, but are to be used only with due regard to the rights of the authors. Bibliographical references may be noted, but passages may be copied only with the permission of the authors, and proper credit must be given in subsequent written or published work. Extensive copying or publication of the thesis in whole or in part requires also the consent of the Dean of the Graduate School of the University of New Mexico.

This thesis by _____ has been used by the following persons, whose signatures attest their acceptance of the above restrictions.

A Library which borrows this thesis for use by its patrons is expected to secure the signature of each user.

NAME AND ADDRESS | DATE

A DEVELOPMENT OF AN EQUIVALENT CIRCUIT OF A HALL GENERATOR WHICH UTILIZES A FLUX CONCENTRATOR

By

Laurence L. Rosier

A thesis

Submitted in Partial Fulfillment of the

Requirements for the Degree

Master of Science in Electrical Engineering

The University of New Mexico

1960

This thesis, directed and approved by the candidate's committee, has been accepted by the Graduate Committee of the University of New Mexico in partial fulfillment of the requirements for the degree of

MASTER OF SCIENCE

E. L. Castetter
Dean

February 7, 1961
Date

Thesis committee

Wayne W. Grossmann
Chairman

Arnold H. Kaufmann

Ahmed Emley

378.789
Un30ro
1961
cop. 2

ACKNOWLEDGEMENTS

The author wishes to thank Dr. Wayne W. Grannemann, thesis advisor and director of the research described in this thesis, for his many helpful suggestions and guidance. Appreciation is also due to David L. Endsley and Jerrel Lochner for their helpful suggestions, and Allen Asselmier for his assistance in obtaining the experimental data.

274241

TABLE OF CONTENTS

CHAPTER		PAGE
I.	INTRODUCTION	1
	The Hall Effect	1
	Hall Effect Devices	6
	Specific Model Considered	11
II.	DEVELOPMENT OF THE EQUIVALENT CIRCUIT	16
	General Form of the Equivalent Circuit	16
	Parameters of Loop One	25
	Parameters of Loop Two	37
	Parameters of Loop Three	44
	Completed Equivalent Circuit	47
	Discussion of Assumptions	52
III.	EXPERIMENTAL VERIFICATION OF THE EQUIVALENT CIRCUIT	54
	Open-Circuit Impedance Approach	54
	Extension of the Open-Circuit Impedance Approach	67
	Transient Analysis	68
	Nonlinear Phenomena	70
IV.	SUMMARY AND CONCLUSIONS	78
	Summary	78
	Conclusions	89
BIBLIOGRAPHY		92
APPENDIXES		95

TABLE OF CONTENTS

CHAPTER PAGE

I. INTRODUCTION 1

The Hall Effect 1

Hall Effect Devices 6

Specific Model Considered 11

II. DEVELOPMENT OF THE EQUIVALENT CIRCUIT 16

General Form of the Equivalent Circuit 16

Parameters of Loop One 25

Parameters of Loop Two 37

Parameters of Loop Three 44

Completed Equivalent Circuit 47

Discussion of Assumptions 52

III. EXPERIMENTAL VERIFICATION OF THE EQUIVALENT CIRCUIT 54

Open-Circuit Impedance Approach 54

Extension of the Open-Circuit Impedance Approach 67

Transient Analysis 68

Nonlinear Phenomena 70

IV. SUMMARY AND CONCLUSIONS 78

Summary 78

Conclusions 89

BIBLIOGRAPHY 92

APPENDIXES 95

LIST OF FIGURES

FIGURE		PAGE
1.	Voltage Produced Due to a Flow of Current in a Magnetic Field	2
2.	Typical Flux Concentrator	7
3.	Hall Effect Amplifier	9
4.	Hall Effect Multiplier	10
5.	Specific Flux Concentrator Considered in This Study	12
6.	Specific Hall Generator Considered in This Study	13
7.	Arrangement of the Leads of the Hall Generator Considered in This Study	14
8.	Hall Generator and Flux Concentrator	17
9.	Three Loop Equivalent Circuit of the System Shown on Figure 8	18
10.	General Form of the Equivalent Circuit of Loop One	20
11.	General Form of the Equivalent Circuit of Loop Two	21
12.	General Form of the Equivalent Circuit of Loop Three	22
13.	Equivalent Circuit of a Hall Generator Which Utilizes a Flux Concentrator	23
14.	Current Carrying Conductor Located Between Two High Permeability Materials	31

FIGURE

FIGURE PAGE

15. Approximate Magnetic Field Distribution Due to a Current Carrying Conductor Located in an Air Gap 32

16. Simplified Magnetic Field Distribution Due to a Current Carrying Conductor Located in an Air Gap 33

17. Simplified Magnetic Field Distribution Due to Two Current Carrying Conductors Located in an Air Gap 34

18. Path of Integration Used to Obtain Equation (21) 35

19. Area Bounded by Loop Two 36

20. Area Bounded by Loop Three 37

21. Area Bounded by Loops Two and Three 40

22. Displacement Voltage Due to the Failure of the Input Electrodes to Cover the Entire End Faces of the Semiconductor 43

23. Displacement Voltage Produced in Loop Three Due to a Current in Loop Two 46

24. Various Areas Involved in the Parameters of the Equivalent Circuit 50

25. $|Z_{11}(j2\pi f)|$ Versus Frequency 58

26. $|Z_{12}(j2\pi f)|$ Versus Frequency 59

27. $|Z_{13}(j2\pi f)|$ Versus Frequency 60

FIGURE

15. Approximate Magnetic Field Distribution Due to a Current Carrying Conductor Located in an Air Gap . . . . . .

16. Simplified Magnetic Field Distribution Due to a Current Carrying Conductor Located in an Air Gap . . . . . .

17. Simplified Magnetic Field Distribution Due to Two Current Carrying Conductors Located in an Air Gap . . . . . .

18. Path of Integration Used to Obtain Equation

19. Area Bounded by Loop Two . . . . . .

20. Area Bounded by Loops Three . . . . . .

21. Area Bounded by Loops Two and Three . . . . . .

22. Displacement Voltage Due to the Capture of the Input Electrodes to Cover the Entire End Faces of the Semiconductor . . . . . .

23. Displacement Voltage Produced in Loop Three Due to a Current in Loop Two . . . . . .

24. Various Areas Involved in the Parameters of the Equivalent Circuit . . . . . .

25. $|Z_{11}(j2\pi f)|$ Versus Frequency . . . . . .

26. $|Z_{12}(j2\pi f)|$ Versus Frequency . . . . . .

27. $|Z_{13}(j2\pi f)|$ Versus Frequency . . . . . .

FIGURE PAGE

28. $|Z_{21}(j2\pi f)|$ Versus Frequency 61

29. $|Z_{22}(j2\pi f)|$ Versus Frequency 62

30. $|Z_{23}(j2\pi f)|$ Versus Frequency 63

31. $|Z_{31}(j2\pi f)|$ Versus Frequency 64

32. $|Z_{32}(j2\pi f)|$ Versus Frequency 65

33. $|Z_{33}(j2\pi f)|$ Versus Frequency 66

34. $|V_3(j2\pi f)/I_1(j2\pi f)|_{I_3(j2\pi f)=0}$ Versus Frequency . 69

35. $v_1(t)$ Versus t 71

36. V_3 Versus I_1 73

37. σ x10^{-4} Versus I_1 75

38. σ x10^{-4} Versus I_2 76

39. K_{2b} and K_{2a} $|H(j2\pi f)|^2$ Versus Frequency 101

FIGURE

CHAPTER I

INTRODUCTION

The development of the transistor has brought about a great deal of research in the field of semiconductors. One of the results of this research is the development of the Hall effect. A number of new devices which utilize the Hall effect have been proposed; however, more theoretical and experimental work is required to determine which of these devices are practical. The success of the equivalent circuit approach in the other fields of electrical engineering suggests that an equivalent circuit which would represent Hall effect devices would be useful. The development of such an equivalent circuit should be centered about a knowledge of the device and its possible applications. It is with this viewpoint in mind that some of the more pertinent aspects of the Hall effect and Hall effect devices will be discussed.

I. THE HALL EFFECT

The Hall effect is concerned with the force that a magnetic field exerts on a moving charge.[1] If a current

---

[1] John N. Shive, The Properties, Physics, and Design of Semiconductor Devices (Princeton, New Jersey: D.Van Nostrand Company, Inc., 1959), pp. 26-27.

carrying material is placed in a magnetic field which has a component of flux density normal to the flow of current, then the magnetic field will exert a force on the moving charge. This force tends to deflect the charge to the boundary of the material, thus creating an electric field and hence a voltage. The current carrying material is usually of a rectangular shape and situated such that the magnetic field is perpendicular to both the face of the material and the flow of current. If this is the case, the electric field produced is perpendicular to both the magnetic field and the flow of current.[2] This situation is illustrated by Figure 1.

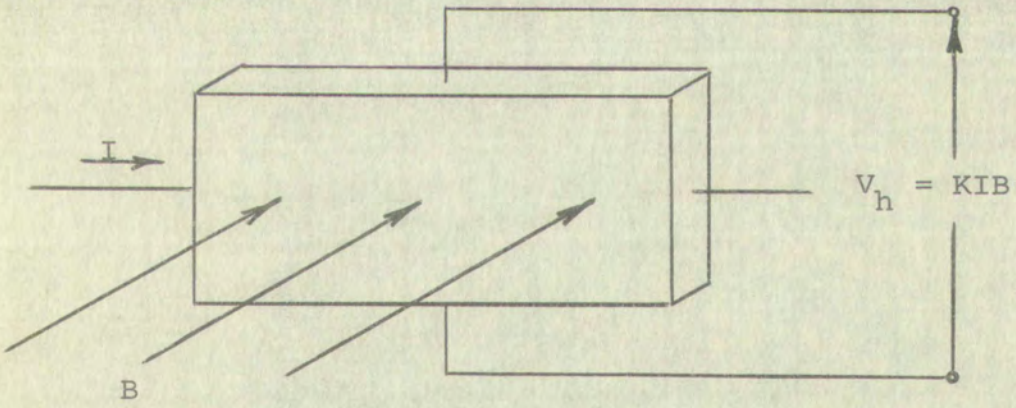

FIGURE 1

VOLTAGE PRODUCED DUE TO A FLOW OF CURRENT
IN A MAGNETIC FIELD

---

[2] Ibid.

---

[2] Ibid.

The voltage produced is often referred to as the Hall voltage and is directly proportional to the product of the current flowing in the material and the magnetic flux density.[3] This fact may be expressed by the equation,

$$V_h = KIB$$

where, V_h = Hall voltage,

K = constant of proportionality, meter^2/coulomb,

I = current flowing in the material, ampere,

B = magnetic flux density, weber/meter^2.

It may be shown that the constant of proportionality in equation (1) is given by[4],

$$K = \frac{\lambda}{N|e|} \qquad (2)$$

where, K = constant of proportionality in equation (1), volt meter/weber^2,

λ = constant determined by the geometry of the material, 1/meter,

N = carrier density, 1/meter^3,

---

[3] W. Crawford Dunlap, Jr., An Introduction to Semiconductors (New York: John Wiley and Sons, Inc., 1957), pp. 185-187.

[4] Olaf Lindberg, "Hall Effect," Proceedings of the I.R.E. 40: 1414, November, 1952.

e = electron charge, coulomb.

Therefore, the constant of proportionality, K, is inversely proportional to the carrier density.

From the previous discussion one might expect that insulating materials would make effective Hall devices since the carrier density of insulators is quite low. This, however, is only partially true since the Hall voltage also depends upon the current supplied to the material. Since the conductivity of insulators is quite low, small currents must be used to avoid excessive heating of the material. Thus, the combination of carrier density and conductivity is the real factor which determines the effectiveness of materials in producing a Hall voltage.

Although the Hall effect was discovered in 1879, it remained an idle curiosity until the introduction of the semiconductor.[5] This was primarily because the materials examined prior to the introduction of the semiconductor exhibited such an unfavorable combination of carrier density and conductivity that it was difficult to obtain a measureable Hall voltage. The majority of the semiconductors were found to have characteristics such that Hall

---

[5]E.H. Hall, "On a New Action of the Magnet on Electric Currents," American Journal of Mathematics, 2:287, 1879.

effect measurements could be made. Thus, the Hall effect became a valuable tool in the analysis of semiconductors since it could be used to determine carrier density, an important factor in the study and fabrication of semiconductors.

Further research indicated that certain high mobility compounds such as indium antimonide possessed a very desirable combination of carrier density and conductivity. These compounds made it possible to use the Hall effect in a number of new devices previously considered impractical.[6] In Hall effect applications indium antimonide is generally considered to be one of the more promising semiconductors, and it was selected as the experimental material in this study.

Before discussing Hall effect devices some of the terminology concerning the Hall effect should be mentioned. The semiconductor through which the Hall voltage is produced is often referred to as a Hall generator. The current which is supplied to the Hall generator is sometimes called the control current since it controls the Hall voltage. These terms have been used throughout the development of this study.

---

[6]Jerome Fox (ed.), Proceedings of the Symposium on the Role of Solid State Phenomena in Electric Circuits (New York: Interscience Publishers, 1957), pp. 116-117.

II. HALL EFFECT DEVICES

Since the Hall voltage is directly proportional to the product of the magnetic flux density and the control current, a number of devices are possible. One of the most obvious areas of Hall effect application is the measurement of magnetic fields. Fields ranging in magnitude from 10^{-4} weber/meter^2 to several weber/meter^2 may easily be measured.[7]

The Hall effect may also be used as an electrical compass since the output voltage is a function of the direction in which the magnetic flux density intersects the face of the semiconductor.[8] By the use of high permeability flux concentrators the attainable sensitivity is of the order of 10^{-8} watts of output power per degree change around the null position.[9] This figure is based on the use of indium antimonide.

A clip-on ammeter incorporating the Hall effect has also been proposed. With such a device the Hall effect

---

[7] E.W. Saker, F.A. Cunnell, and J.T. Edmonds, "Indium Antimonide as a Fluxmeter Material," British Journal of Applied Physics, 6: 218, June, 1955

[8] I.M. Ross, E.W. Saker, and N.A.C. Thompson, "The Hall-Effect Compass," Journal of Scientific Instruments, 34: 479-484, December, 1957.

[9] Ibid., p. 483.

II. HALL-EFFECT DEVICES

Since the Hall voltage is directly proportional to the product of the magnetic flux density and the control current, a number of devices are possible. One of the most obvious areas of Hall effect application is the measurement of magnetic fields. Fields ranging in magnitude from 10^{-4} weber/meter^2 to several webers/meter^2 may easily be measured.[7]

The Hall effect may also be used as an electronic compass since the output voltage is a function of the direction in which the magnetic flux density intersects the face of the semiconductor.[8] By the use of high mobility flux concentrators the obtainable sensitivity is of the order of 10^{-8} watts of output power per degree change around the null position.[9] This figure is based on the use of indium antimonide.

A clip-on ammeter incorporating the Hall effect has also been proposed. With such a device the Hall effect

---

[7] E.W. Saker, P.A. Cunnell, and G.T. Edmonds, "Indium Antimonide as a Fluxmeter Material," British Journal of Applied Physics, 6: 218, June 1955.

[8] I.M. Ross, E.W. Saker, and W.A.C. Thompson, "The Hall-Effect Compass," Journal of Scientific Instruments, 34: 479-484, December, 1957.

[9] Ibid., p. 483.

would be used to determine the magnetic field which exists about a current carrying wire. If a d.c. control current were supplied to the Hall generator, the Hall voltage would be directly proportional to the current flowing in the wire. Such an arrangement would be quite useful since the flow of current in the wire would not need to be interrupted by the insertion of a conventional current measuring device. A flux concentrator may be used to increase the flux density and hence the Hall voltage. A high permeability toroid with an air gap forms an efficient flux concentrator. Such an arrangement is shown in Figure 2. This device may

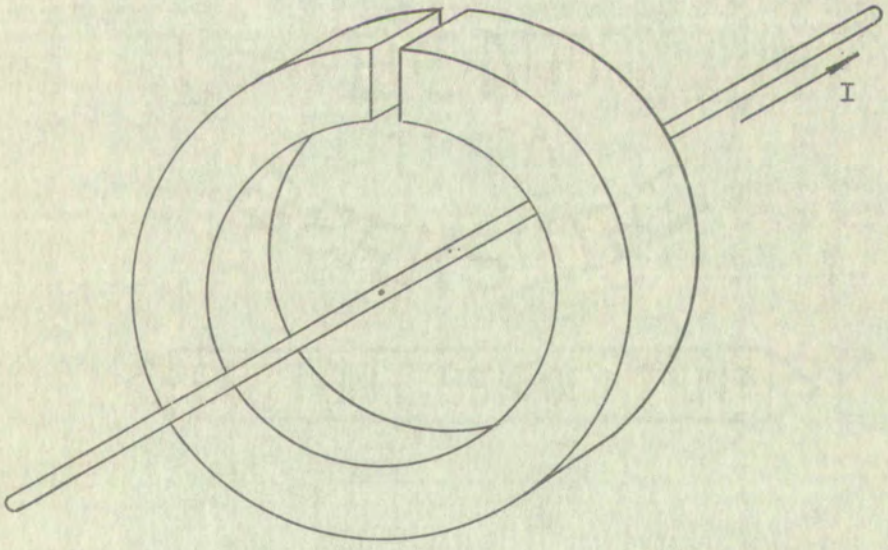

FIGURE 2

TYPICAL FLUX CONCENTRATOR

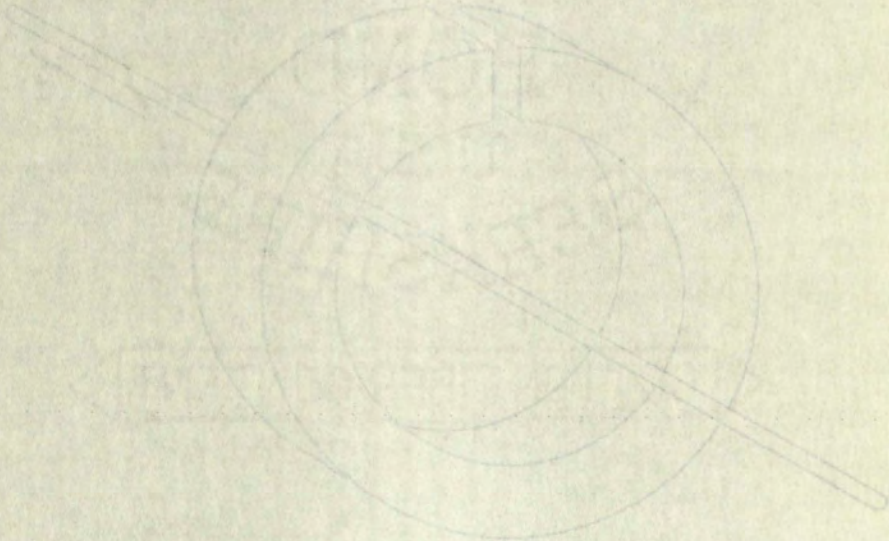

be used to measure both a.c. and d.c. currents.[10]

Amplification is also a possible application of the Hall effect.[11] A flux concentrator with an air gap would be used, and the input signal would then be applied to a coil wrapped around the concentrator. Flow of current in the windings would produce a magnetic flux density which in turn would cause a Hall voltage. If a d.c. current were supplied to the Hall generator, a voltage would be produced of approximately the same form as the current flowing in the windings surrounding the toroid. A suitable configuration is shown in Figure 3. Power gains of five have been obtained under both d.c. and low frequency conditions.[12]

Since the Hall voltage is directly proportional to the product of the magnetic flux density and the current flowing in the semiconductor, modulation is possible.[13] In this application an audio frequency signal would be supplied to the windings of a flux concentrator and a radio

---

[10] I.M. Ross, and E.W. Saker, "Application of Indium Antimonide," Journal of Electronics, 1:226-227, June, 1955.

[11] I.M. Ross, and N.A.C. Thompson, "An Amplifier Based on the Hall Effect," Nature, 175: 518, March, 1955.

[12] Ibid.

[13] M.J.O. Strutt, "Hall Effect in Semiconductor Compounds," Electronic and Radio Engineering, 36:9-10, January, 1959.

---

[10] I.M. Rose, and E.W. Baker, "Identification of Indium Antimonide," Journal of Electronics, [illegible] Univ. [illegible].

[11] I.M. Rose, and R.A.C. Thompson, "An Amplifier Based on the Hall Effect," Nature, [illegible] Sept. March 1955.

[12] Ibid.

[13] M.J.O. Strutt, "Data Sheet [illegible] Semiconductor Compounds," Electronic and Radio Engineering, Physic. Dec. [illegible] uary, 1955.

frequency signal would be supplied to the Hall generator. The Hall voltage would then consist of a radio frequency signal modulated by an audio frequency signal. The same approach may be used to obtain a d.c. to a.c. converter: the a.c. signal may be applied to the windings of the toroid or the input terminals of the Hall generator.

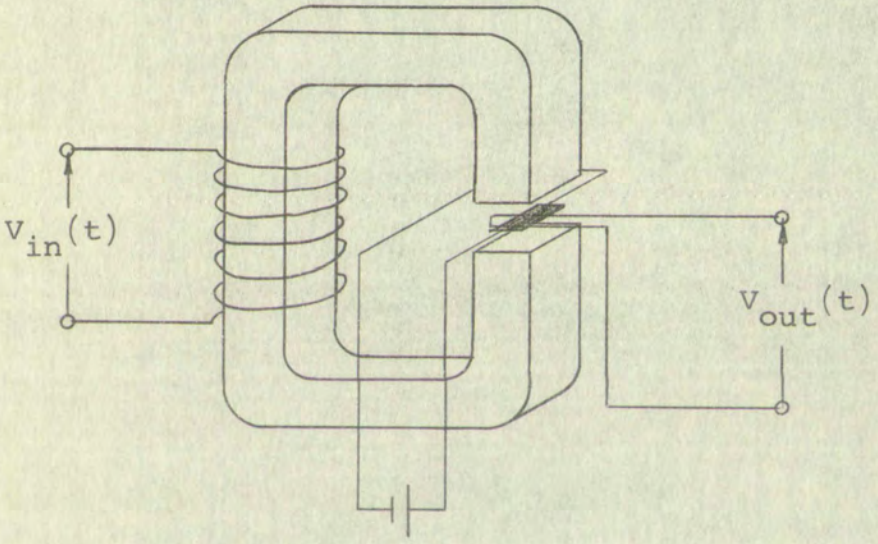

FIGURE 3

HALL EFFECT AMPLIFIER

The Hall generator may be used as a multiplication element in analog computers.[14] Figure 4 illustrates a

---

[14] Lars Lofgren, "Analog Multiplier Based on the Hall Effect," Journal of Applied Physics, 29: 158-166, February, 1958; and C. Hilsum, Multiplication by Semiconductors," Electronic Engineering, 30: 664-666, November, 1958.

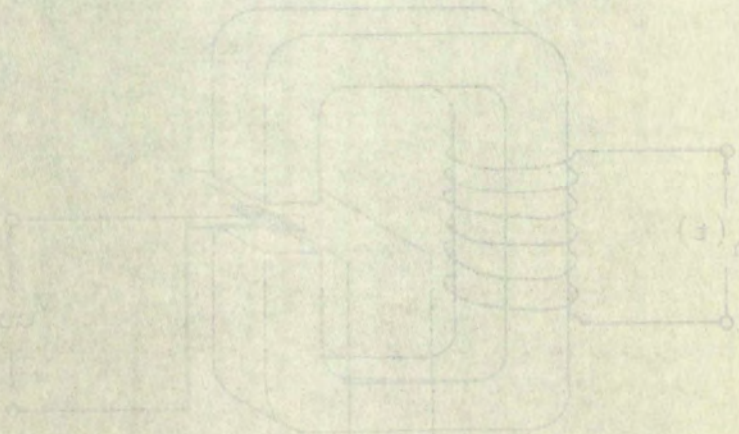
$V_{in}(t)$

typical arrangement. Again a flux concentrator would be used to increase the magnetic flux density. If the current supplied to the toroid windings were given by i_1, and the current supplied to the Hall generator were given by i_2, then over a certain frequency range the output voltage would be proportional to $i_1 \cdot i_2$. Thus, multiplication may be easily achieved.

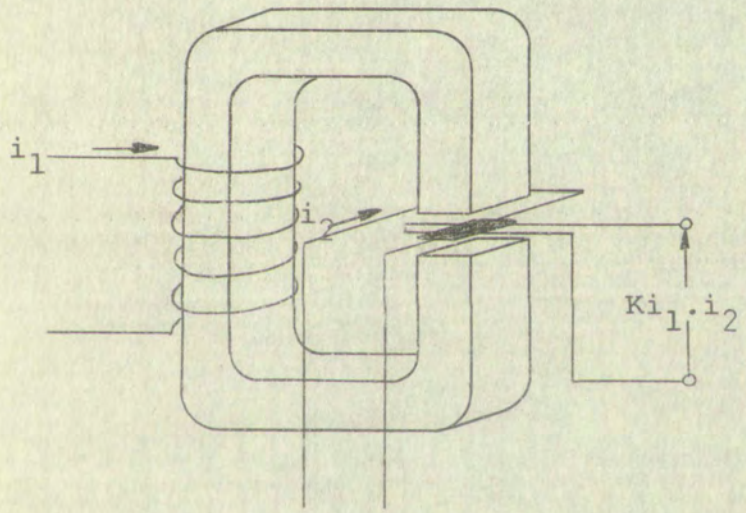

FIGURE 4

HALL EFFECT MULTIPLIER

Only a few of the possible applications have been discussed. The Hall effect may also be used in such devices as magnetometers, power meters, electric torque meters, impedance converters, and displacement gauges.

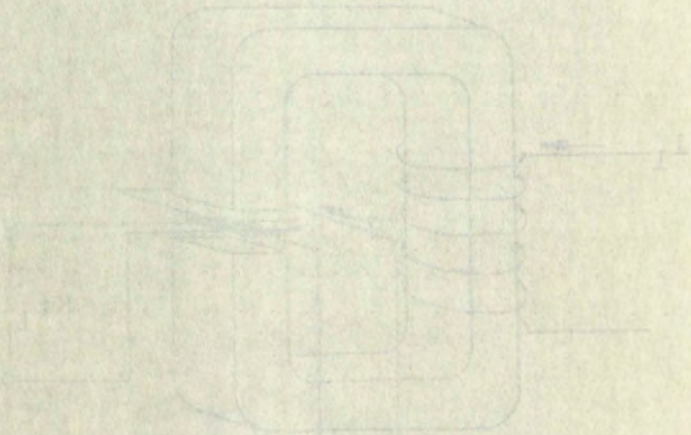

Many of the applications mentioned are only in an introductory state and further study is required to determine their significance.

III. SPECIFIC MODEL CONSIDERED

A number of applications of the Hall effect have been suggested. Many of the more promising devices incorporate some form of a high permeability material to confine the magnetic field to the general area of the Hall generator. This often takes the form of a high permeability toroid. An air gap is cut in the toroid, and the Hall generator is placed in the air gap. The following devices utilize this arrangement: clip-on ammeter, amplifier, modulator, chopper, impedance converter, power meter, and analog multiplier. Because a large number of devices utilize such a flux concentrator, it was decided that it should be included in the model selected for study. Figure 5 illustrates the flux concentrator considered in this study. Many of the results of this study may be extended to describe devices which utilize different types of flux concentrators.

Figure 6 illustrates the specific Hall generator considered in this study. The electrodes through which the control current entered the semiconductor covered the entire end faces of the material, and the electrodes from

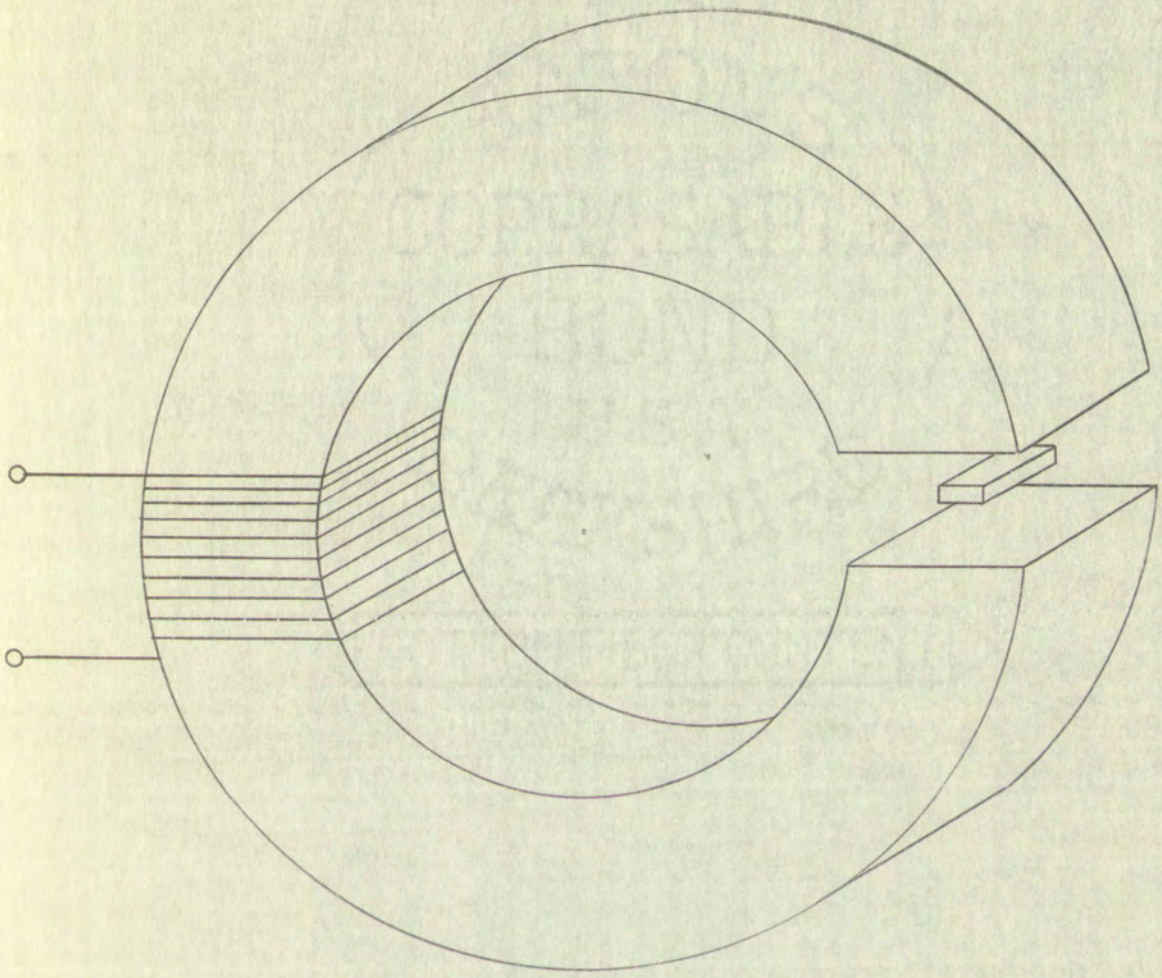

FIGURE 5

SPECIFIC FLUX CONCENTRATOR CONSIDERED

IN THIS STUDY

Note: The leads of the Hall generator have not been indicated in this figure. Figure 7 illustrates the arrangement of the Hall generator leads with respect to the boundary of the air gap.

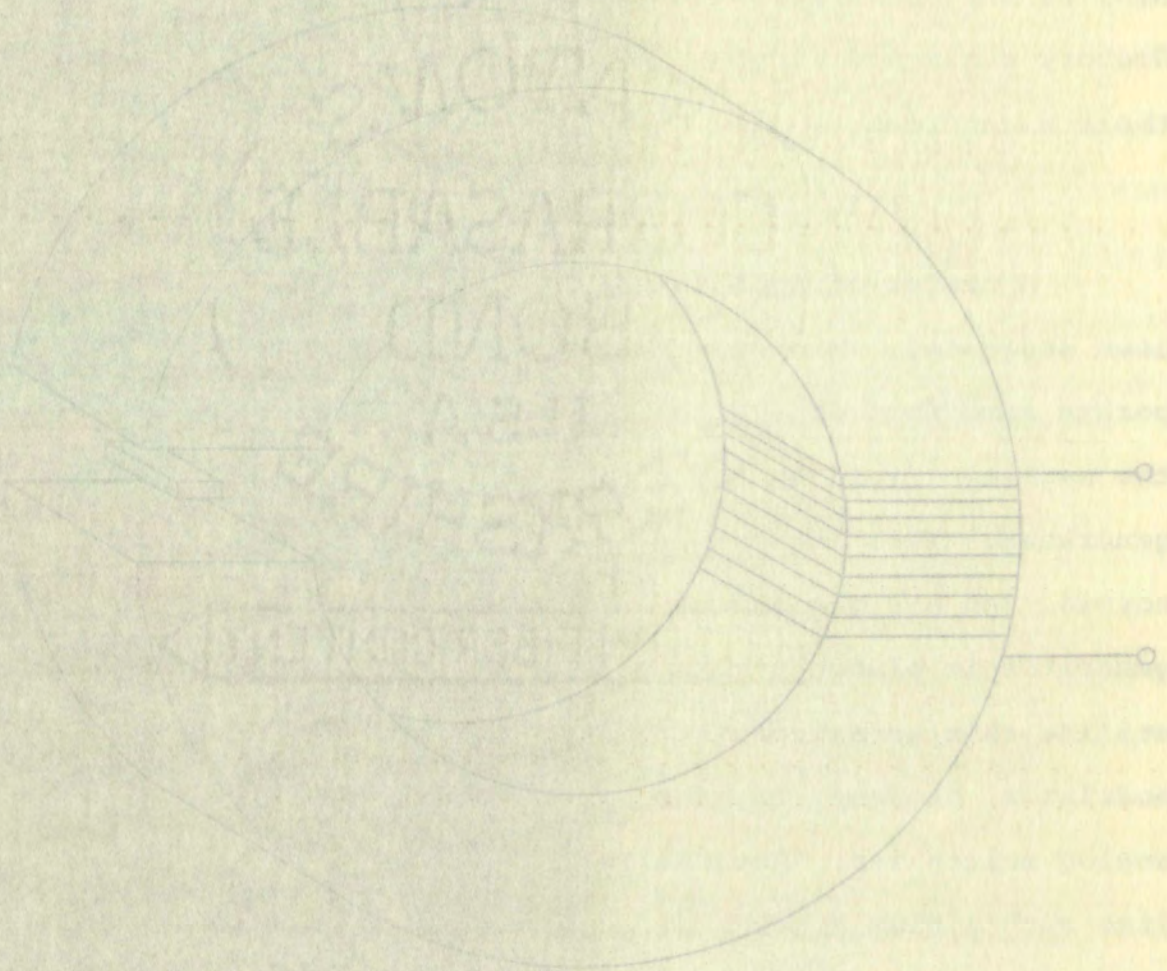

which the Hall voltage was obtained covered only a fraction of the length of the material. This particular Hall generator is the one most frequently used in Hall effect applications.

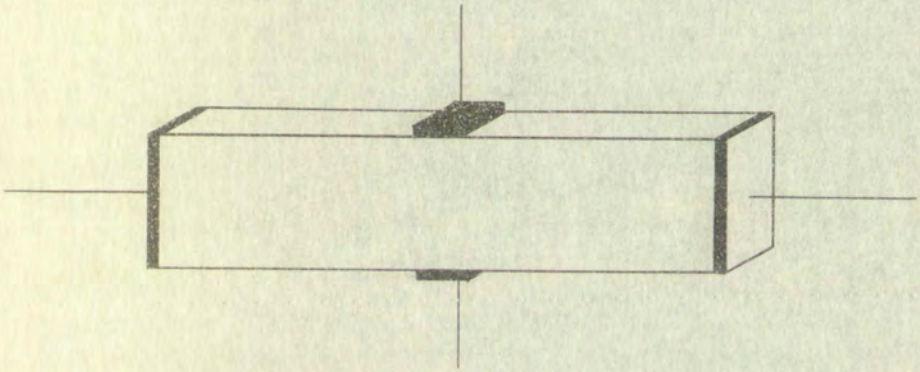

FIGURE 6

SPECIFIC HALL GENERATOR CONSIDERED IN THIS STUDY

As will be seen in Chapter two, the arrangement of the leads of the Hall generator is an important factor in the operation of the device. The model considered in this study had leads which formed closed loops within the air gap. Figure 7 illustrates such an arrangement of Hall generator leads. Although this particular arrangement of leads is not always used, the results of this study may be readily extended to include other lead configurations.

The Hall generator used in the experimental verification of the equivalent circuit was manufactured by Ohio

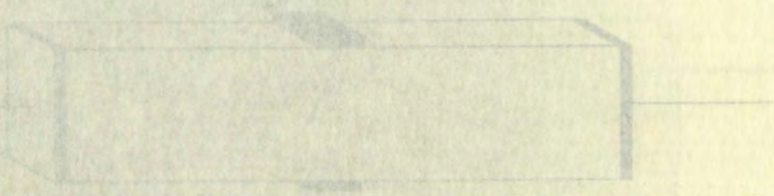

Semiconductors, Inc. The semiconductor used was indium antimonide, which is one of the high mobility compounds. The results of this study should be valid for any semiconductor one would choose to use.

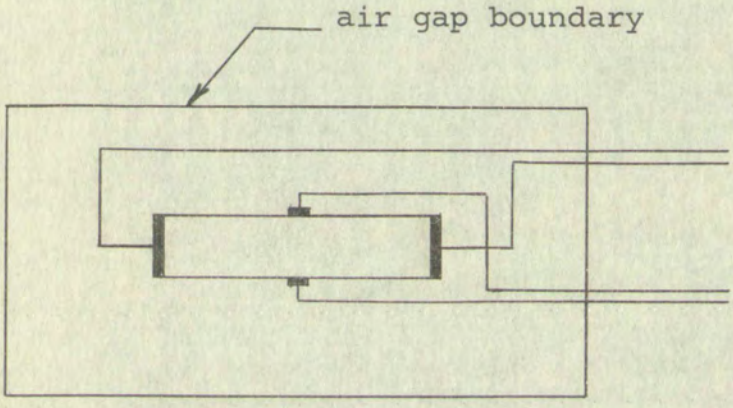

FIGURE 7

ARRANGEMENT OF THE LEADS OF THE HALL GENERATOR CONSIDERED IN THIS STUDY

In attempting to analyze devices which employ the Hall effect one is faced with a number of problems. The Hall effects must be considered as well as the various impedances of the Hall generator. Since the magnetic field is a basic factor in the Hall effect, it must also be considered. Thus, the analysis of Hall effect devices is complicated by several factors.

The purpose of this study has been the development of an a.c. equivalent circuit which would describe the

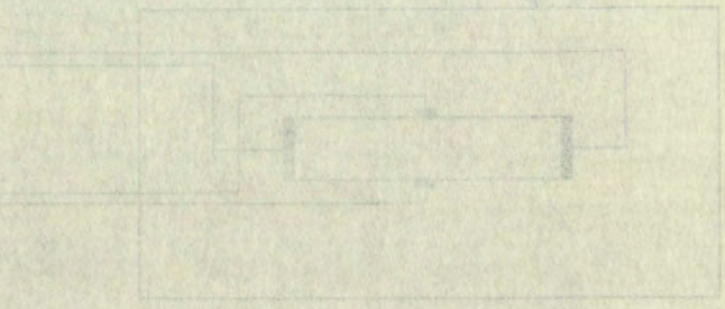

operation of many of the devices which utilize the Hall effect. Such an equivalent circuit should be useful in the analysis and design of Hall effect devices as well as the determination of which devices are practical. The equivalent circuit should place in evidence the effects of the various dimensions and electrical characteristics of the system. Several restrictions have been imposed upon the model under consideration; however, a review of the current literature indicates that the model selected is both sufficiently general to be of practical use and limited enough that a useful equivalent circuit may be obtained.

CHAPTER II

DEVELOPMENT OF THE EQUIVALENT CIRCUIT

The subject of this chapter is the development of an equivalent circuit which would represent the operation of Hall effect devices utilizing flux concentrators. The parameters of the equivalent circuit will be developed in terms of the various dimensions and electrical characteristic of the physical system.

I. GENERAL FORM OF THE EQUIVALENT CIRCUIT

A few introductory remarks concerning the units and symbols used in the development of the equivalent circuit should be mentioned. The M.K.S. system of units was used throughout the study. Since a large number of symbols were used in the development of the equivalent circuit, their definition was quite important. The practice generally followed consisted of defining each symbol as it was introduced. From that point on it was not defined again until the completion of the equivalent circuit. Upon completion of the equivalent circuit all of the symbols involved in the parameters of the equivalent circuit were again defined or indicated by the appropriate figures.

The basic system considered in this study is shown on Figure 8. The three loops 1-1', 2-2', and 3-3' suggest

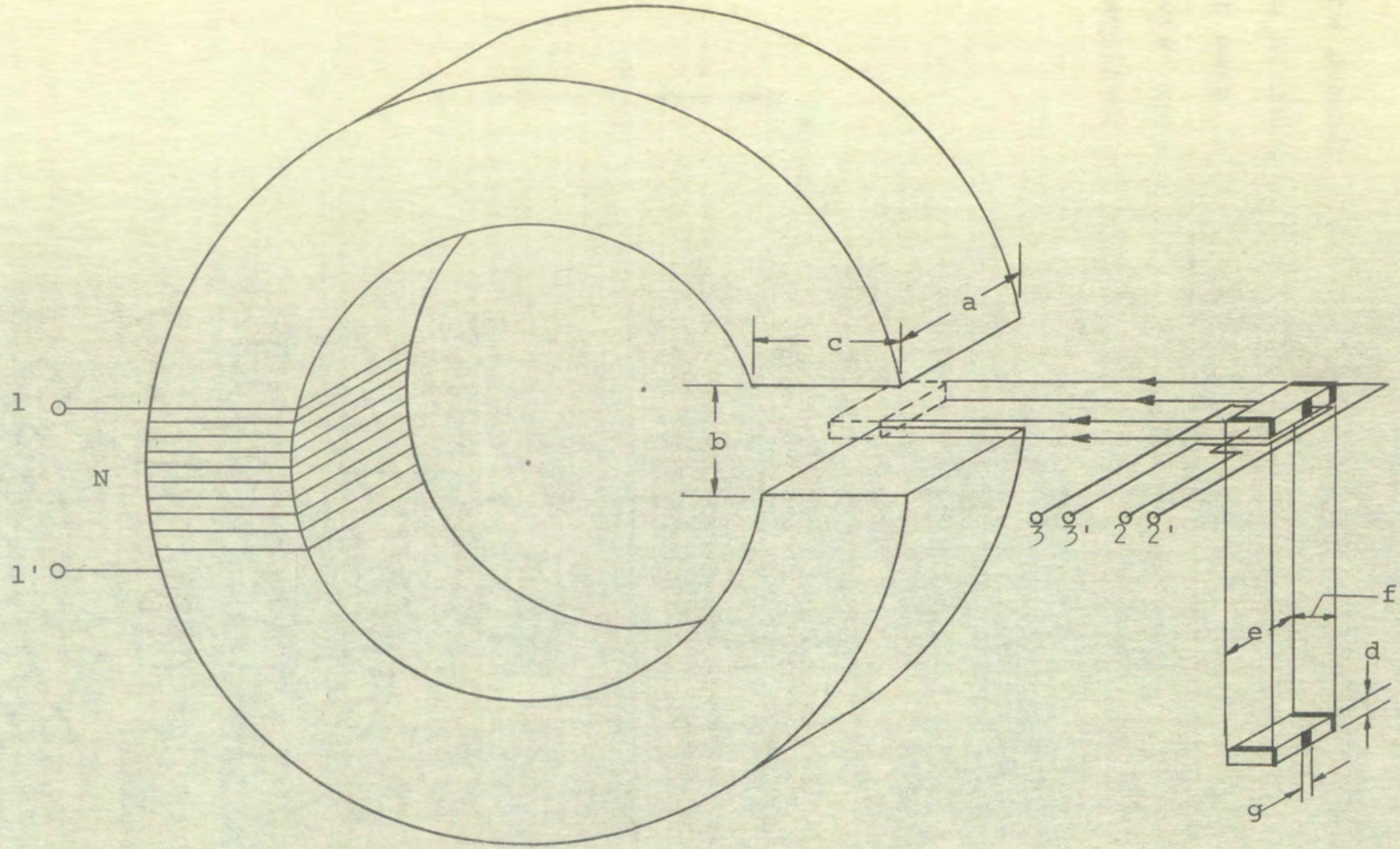

FIGURE 8

HALL GENERATOR AND FLUX CONCENTRATOR

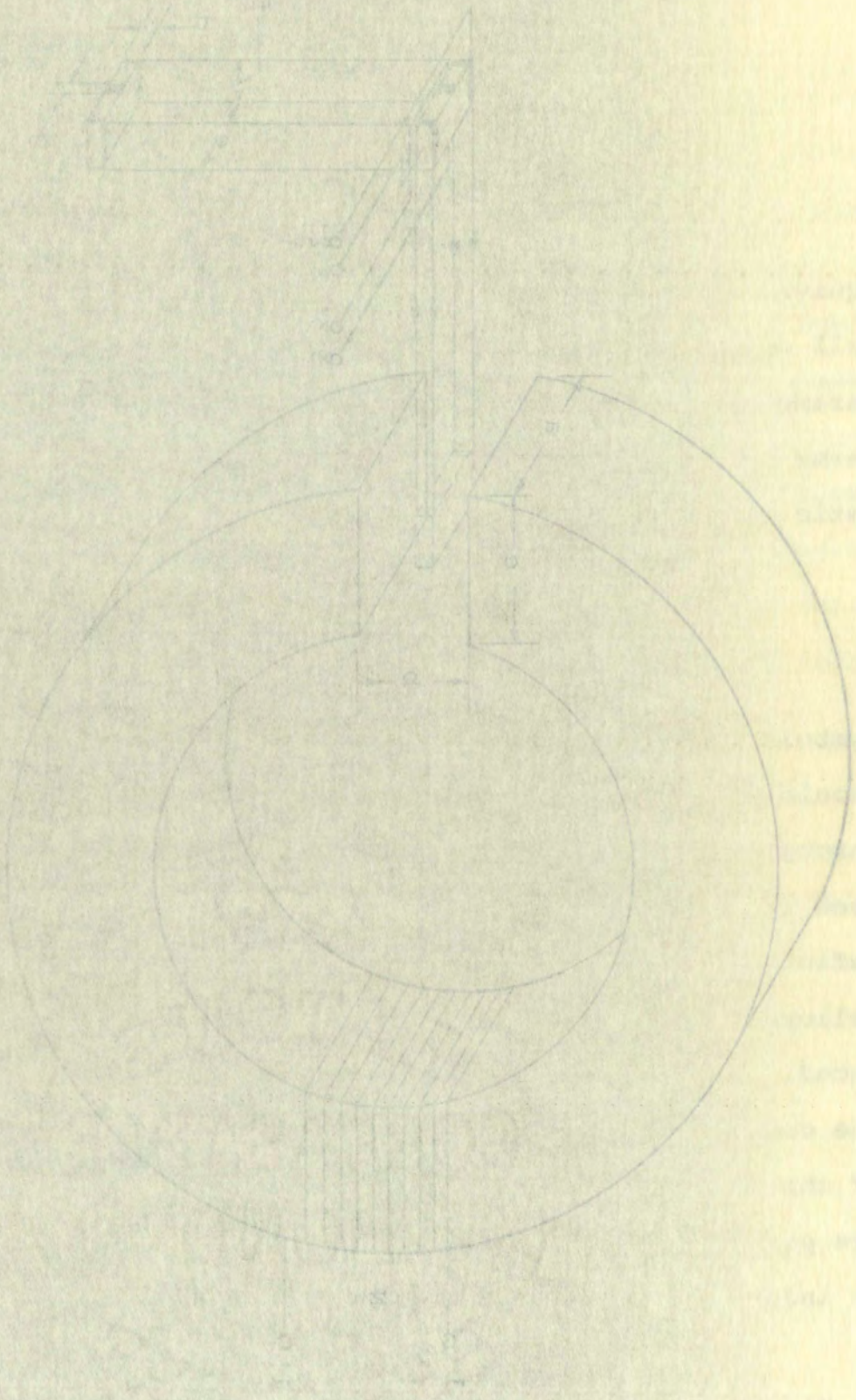

the possibility of a three loop equivalent circuit. Such an arrangement is shown on Figure 9. The boxes contained in each loop represent the various combinations of resistors, capacitors, inductors, and voltage generators required to describe the physical system.

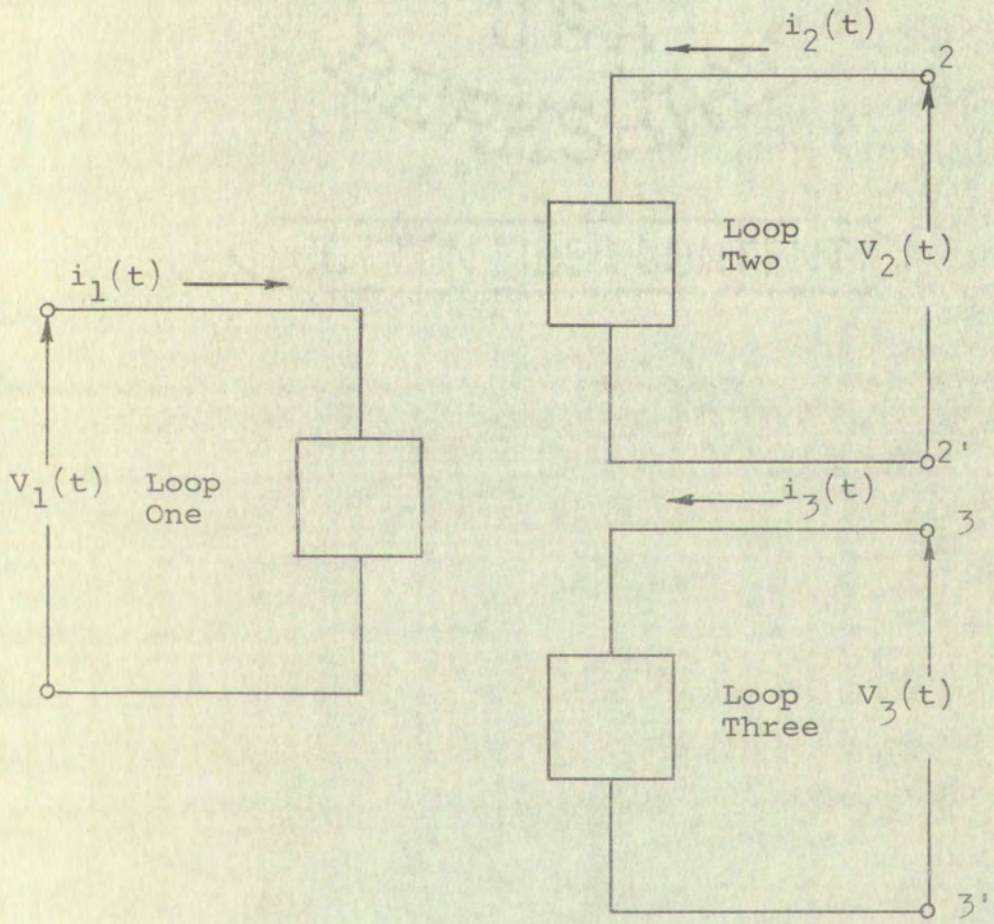

FIGURE 9

THREE LOOP EQUIVALENT CIRCUIT OF THE SYSTEM SHOWN ON FIGURE 8

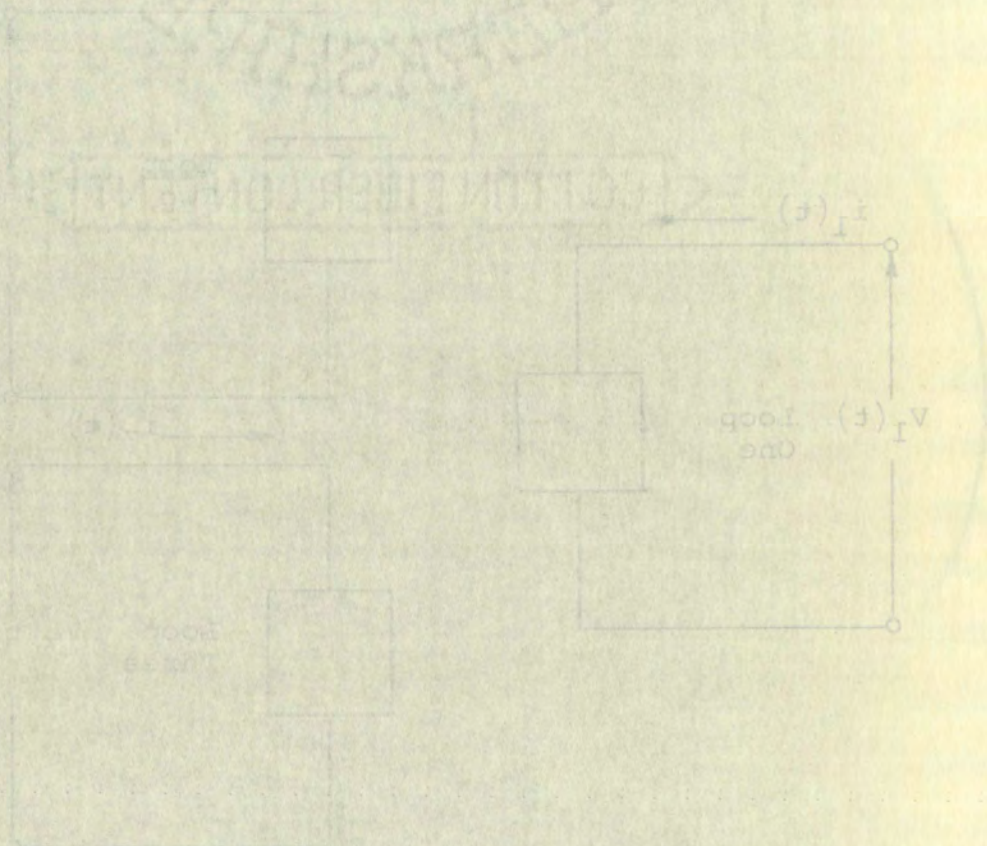

The parameters contained in loop one should represent the effects of current flow in loop one plus the coupling effects of current flow in loops two and three. Loop one should contain a small amount of resistance, R_{1a}, due to the resistance of the windings surrounding the toroid. Loop one should also contain an inductance parameter, L_1, due to the coil and the high permeability toroid. As a first approximation, these two parameters may be combined to form a series $R_{1a}L_1$ equivalent circuit.

The turns of the coil also produce a certain amount of capacitance, C_1, which tends to shunt the series $R_{1a}L_1$ combination. There is a further shunting effect due to the hysteresis and eddy-current losses of the toroid and the imperfect insulation between the coils.[1] This shunting effect may be represented by a resistance, R_{1b}, placed in parallel with the capacitance C_1. The mutual coupling between loops one, two, and three must also be included in the equivalent circuit. Mutual inductance parameters, M_{12} and M_{13}, may be used to represent this coupling. Therefore, the characteristics of loop one may be described by the equivalent circuit of Figure 10.

The parameters of loop two should represent the

---

[1]Melville B. Stout, Basic Electrical Measurements (New York: Prentice-Hall, Inc., 1950), p. 284.

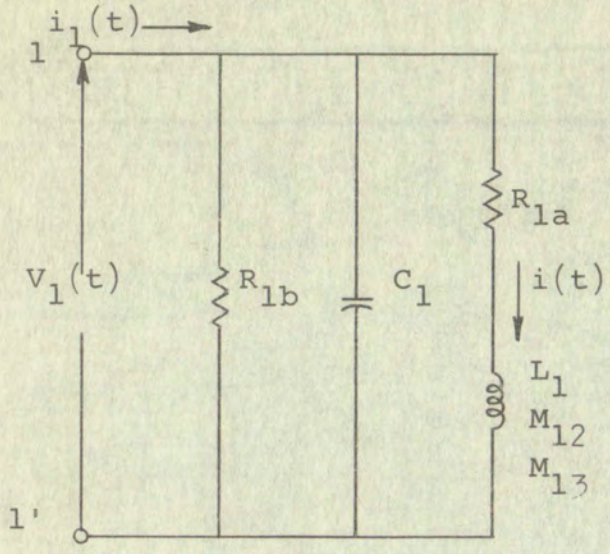

FIGURE 10

GENERAL FORM OF THE EQUIVALENT CIRCUIT OF LOOP ONE

effects of current flow in loop two plus the coupling effects of current flow in loops one and three. The equivalent circuit of loop two should contain a resistance parameter, R_2, to represent the resistance of the Hall generator as viewed from terminals 2-2'. An inductance parameter, L_2, should also be included to describe the effects of the toroid. Furthermore, mutual inductance parameters, M_{21} and M_{23}, are required to describe part of the coupling effects. The coupling effects due to the Hall voltage and displacement voltage must also be represented.

The Hall voltage produced in loop two is directly

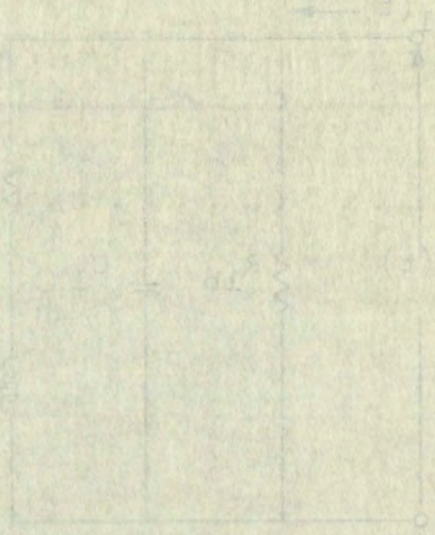

proportional to the product of current flow in loops one and three. Therefore, a voltage generator of the form $K_{2a}i \cdot i_3$ may be used to represent the Hall voltage.

The displacement voltage is due to the failure of the input electrodes of the Hall generator to cover the entire end faces of the semiconductor.* This effect may be represented by a voltage generator of the form $K_{2b}i_3$.

The various parameters of loop two may now be combined to form the equivalent circuit of loop two. The result is indicated by Figure 11.

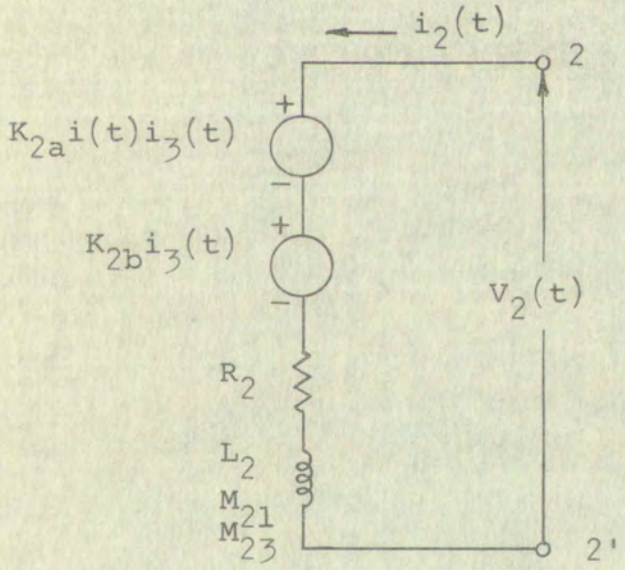

FIGURE 11

GENERAL FORM OF THE EQUIVALENT CIRCUIT OF LOOP TWO

*The term displacement voltage should not be confused with the term displacement current.

The equivalent circuit of loop three is quite similar to that of loop two. The circuit should contain all of the parameters of loop two; however, their values will in general be different. Therefore, the equivalent circuit of loop three is as shown on Figure 12.

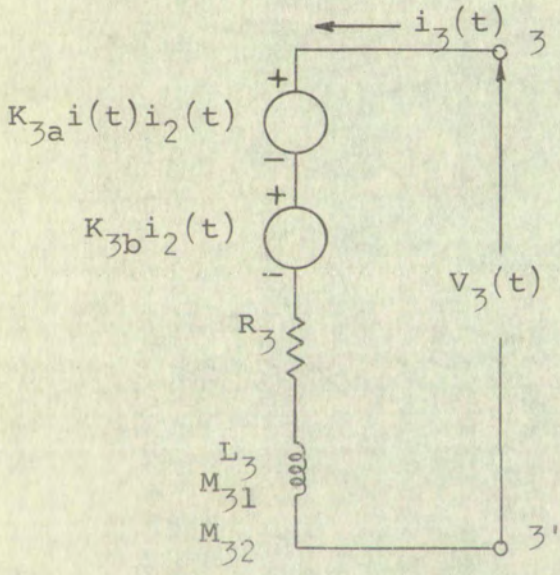

FIGURE 12

GENERAL FORM OF THE EQUIVALENT CIRCUIT OF LOOP THREE

The equivalent circuits of the three loops may now be combined to form the equivalent circuit of the system shown in Figure 8 page 17. The result is shown on Figure 13. The development of the general form of the equivalent circuit was based largely on reasonable

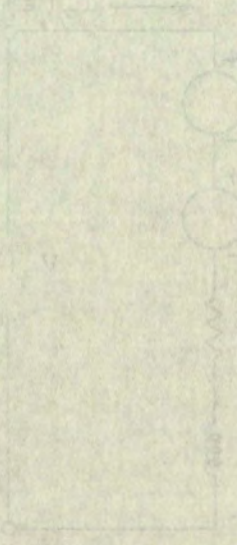

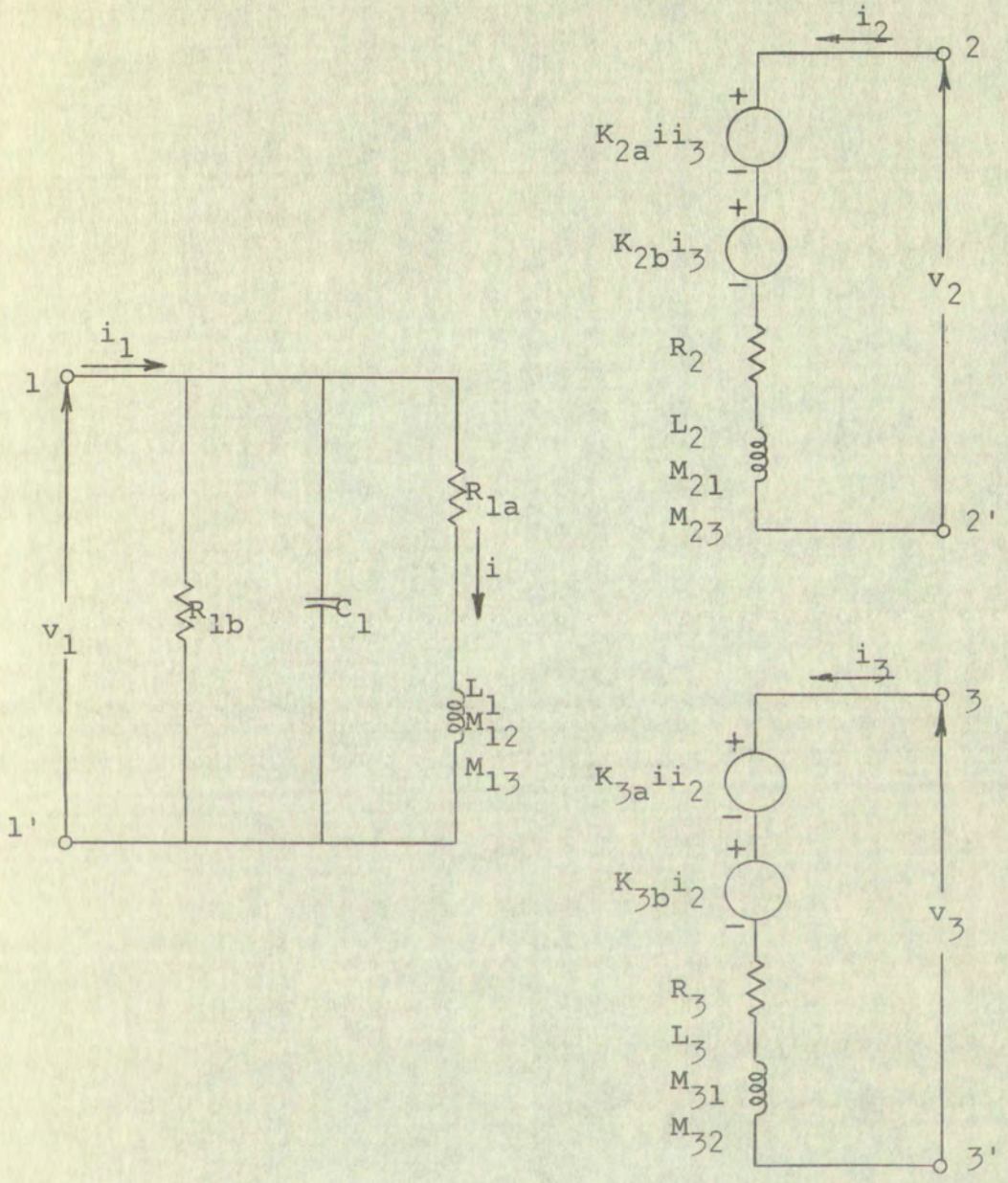

FIGURE 13

EQUIVALENT CIRCUIT OF A HALL GENERATOR
WHICH UTILIZES A FLUX CONCENTRATOR

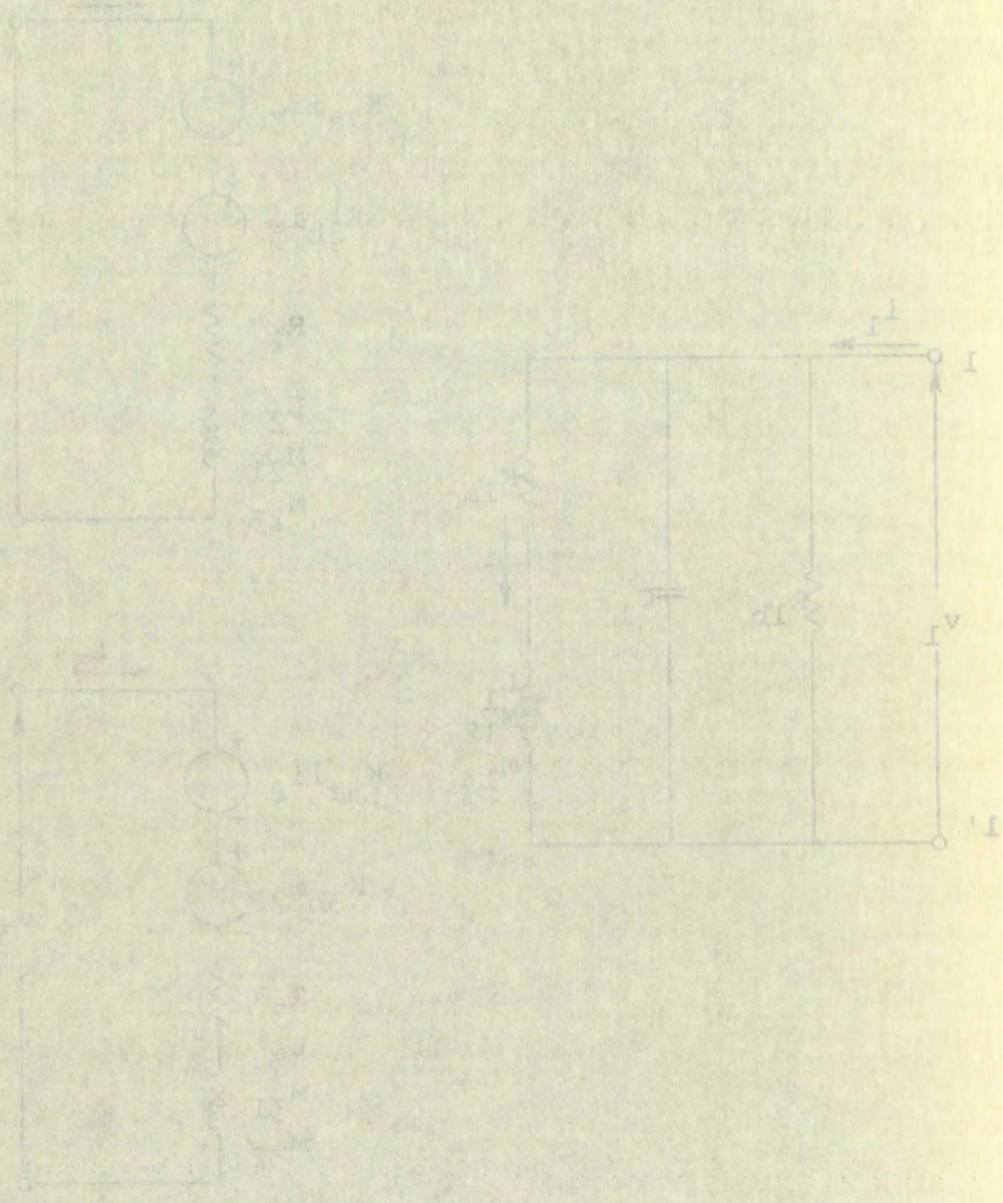

assumptions. Experimental verification was therefore required to justify these assumptions. In fact the equivalent circuit initially proposed did not contain all of the parameters of the equivalent circuit shown on Figure 13. Experimental study indicated that certain changes in the equivalent circuit were necessary. Thus, it may be said that the development of the equivalent circuit involved a certain amount of trial and error. The general form of the equivalent circuit shown on Figure 13 is the result of this trial and error investigation.

Some comment should be made concerning the various polarities involved in the equivalent circuit. The mutual inductance parameters have not been specified; their sign may be determined from an examination of the particular system. The four voltage generators have been designated; however, the constants involved may either be positive or negative depending on the particular system. More comment on this subject will follow.

The general form of the equivalent circuit has been suggested. The remainder of this chapter is devoted to a theoretical development of the parameters of the equivalent circuit. The parameters will be derived in terms of the various dimensions and electrical characteristics of the physical system.

II. PARAMETERS OF LOOP ONE

The parameters of loop one are as follows: R_{1a}, R_{1b}, L_1, M_{12}, M_{13}, and C_1. R_{1a} is simply the resistance of the coil surrounding the toroid. The experimental determination of this parameter is given by the equation,

$$R_{1a} = \left. \frac{V_1(j\omega)}{I_1(j\omega)} \right|_{\omega=0} \qquad (3)$$

where, R_{1a} = parameter of the equivalent circuit shown on Figure 13, ohm,

$V_1(j\omega)$ = phasor representation of a voltage applied to terminals 1-1 , volt,

$I_1(j\omega)$ = phasor representation of the current resulting in loop one due to $V_1(j\omega)$, ampere,

ω = angular frequency, radian/second.

This parameter may also be found from tables.

The parameter L_1 is the self inductance of loop one. This parameter is by definition equal to the total flux which links loop one due to a current in loop one divided by the current in loop one. Thus, to determine L_1 the flux must be found as a function of current in loop one.

Ampere's law may be used to determine the flux linking loop one due to a current in loop one. Ampere's law may be expressed by,

$$\oint \bar{H} \cdot d\bar{l} = I \qquad (4)$$

where, $\bar{H}$ = magnetic field intensity vector, ampere/meter,

$d\bar{l}$ = differential element of length vector, meter,

I = current inclosed by the path of integration, ampere.

By the application of Ampere's law the following equation may be obtained,

$$H_g b + (2\pi r - b) H_t = Ni \qquad (5)$$

where, H_g = magnetic field intensity within the air gap, ampere/meter,

H_t = magnetic field intensity within the toroid, ampere/meter,

b = width of the air gap, meter,

r = radial distance from the center of the toroid, meter,

N = number of turns surrounding the toroid,

i = current in loop one which produces the flux, ampere,

Since the normal component of magnetic flux density must be continuous,

$$B_g = B_t \qquad (6)$$

where, B_g = magnetic flux density within the air gap, weber/meter^2,

B_t = magnetic flux density within the toroid, weber/meter^2.

Using the relation $B = \mu H$ and combining equations (5) and (6) one may obtain,

$$B_t = \frac{Ni}{\frac{b}{\mu_o} + \frac{(2\pi r - b)}{\mu}} \tag{7}$$

where, μ = permeability of the toroid, henry/meter,

μ_o = permeability of free space, henry/meter.

If the permeability of the magnetic material is reasonably high,

$$\frac{\mu}{\mu_o} \gg \frac{(2\pi r - b)}{b} \tag{8}$$

or, $$\frac{b}{\mu_o} \gg \frac{(2\pi r - b)}{\mu}. \tag{9}$$

If this approximation is valid, then equation (7) becomes,

$$B_t = \frac{\mu_o Ni}{b} \tag{10}$$

The total flux which passes through the toroid may be found from the equation:

where, B_a = magnetic flux density within the air gap,

weber/meter^2,

B_f = magnetic flux density within the toroid,

weber/meter^2.

Using the relation $B = \mu H$ and continuity equations (5) and (6) one may obtain,

$$B_f = \frac{NI}{\frac{b}{\mu_o} + \frac{(2\pi r - b)}{\mu}}$$

where, μ = permeability of the toroid, henry/meter,

μ_o = permeability of free space, henry/meter.

If the permeability of the magnetic material is sufficiently high,

$$\frac{b}{\mu_o} \gg \frac{(2\pi r - b)}{\mu}$$

or, $b \gg \frac{(2\pi r - b)}{\mu}$

If this approximation is valid, then equation (7) becomes

$$B_f = \frac{\mu_o NI}{b}$$

The total flux which passes through the toroid may be found from the equation:

$$\Phi = BA \tag{11}$$

where, Φ = flux passing through the toriod, weber,

B = flux density within the toroid, weber/meter^2,

A = cross sectional area of the toroid, meter^2.

The self inductance of loop one is expressible as,

$$L_1 = \frac{N\Phi}{i} \tag{12}$$

where, L_1 = self inductance of loop one, henry.

Combining equations (10), (11), and (12) results in,

$$L_1 = \frac{\mu_o N^2 ac}{b} \tag{13}$$

where, a = depth of the toroid as shown in Figure 8, meter,

c = width of the toroid as shown in Figure 8, meter.

Thus, the parameter L_1 has been derived in terms of the dimensions of the physical system.

The capacitance parameter C_1 will now be discussed. This parameter depends primarily on the number of turns surrounding the toroid and the spacing of the turns. A theoretical derivation of this parameter is quite difficult, but it may easily be determined experimentally by the following approach.

The open-circuit impedance $Z_{11}(s)$ of the equivalent

where, Φ = flux passing through the toroid, webers

B = flux density within the toroid, webers/meter^2

A = cross sectional area of the toroid, meter^2

The self inductance of loop one is expressed as:

$$L_1 = \frac{N\Phi}{I}$$

where, L_1 = self inductance of loop one, henry

Combining equations (1), (2), and (3) results in:

$$L_1 =$$

where, a = depth of the toroid as shown in figure 6, meter

c = width of the toroid as shown in figure 6, meter

Thus, the parameter L_1 has been derived in terms of the dimensions of the physical system.

The capacitance parameter C_1 will now be discussed. This parameter depends primarily on the number of turns surrounding the toroid and the spacing of the turns. A theoretical derivation of this parameter is quite difficult, but it may easily be determined experimentally by the following approach.

The open-circuit impedance Z_{11} is the equivalent

circuit shown on Figure 13 is by definition,

$$Z_{11}(s) = \left.\frac{V_1(s)}{I_1(s)}\right| I_2(s)=I_3(s)=0. \qquad (14)$$

The various terms involved in equation (14) are the Laplace transforms of the voltages and currents shown in Figure 13. By applying equation (14) in conjunction with the equivalent circuit of Figure 13 the following equation results,

$$Z_{11}(s)= \frac{\frac{1}{C_1}\left(s + \frac{R_{1a}}{L_1}\right)}{s^2 + s\left(\frac{R_{1a}}{L_1} + \frac{1}{R_{1b}C_1}\right) + \frac{R_{1a}+R_{1b}}{R_{1b}L_1C_1}} \qquad (15)$$

If $R_{1b} \gg R_{1a}$, and $L_1/R_{1a} \gg R_{1b}C_1$,

$$Z_{11}(s) = \frac{\frac{1}{C_1}\left(s + \frac{R_{1a}}{L_1}\right)}{s^2 + s\left(\frac{1}{R_{1b}C_1}\right) + \frac{1}{L_1C_1}} . \qquad (16)$$

If practical values are substituted in equation (16), it may be shown that a highly underdamped frequency response results. The resonant frequency is given by,

$$\omega_r = \frac{1}{\sqrt{L_1C_1}} \qquad (17)$$

circuit shown on Figure 12 is by definition

$$Z_{11}(s) = \frac{V_1(s)}{I_1(s)} \Big|_{I_2(s)=0}$$

The various terms involved in Figure 12 (b) are the Laplace transforms of the voltages and currents shown in Figure 12a. By applying equation (12) to the section with the equivalent circuit of Figure 12 we obtain the following equation result:

$$Z_{11}(s) = \frac{s^2 + s\left(\frac{1}{C_a R_{1a}} + \frac{1}{C_b R_{1b}}\right) + \frac{1}{C_a C_b R_{1a} R_{1b}}}{s^2 + s\left(\frac{1}{C_a R_{1a}} + \frac{1}{C_b R_{1b}}\right)}$$

If $R_{1b} \gg R_{1a}$ and $R_{1a} C_a \gg R_{1b} C_b$

$$Z_{11}(s) = \frac{s^2 + s\left(\frac{1}{C_a R_{1a}}\right) + \frac{1}{C_a C_b R_{1a} R_{1b}}}{s^2 + s\left(\frac{1}{R_{1b} C_b}\right) + \frac{1}{C_a C_b R_{1a} R_{1b}}}$$

If practical values are substituted in equation (15), it may be shown that a highly underdamped frequency response results. The resonant frequency is given by

$$\omega_r^2 = \frac{1}{C_a C_b R_{1a} R_{1b}}$$

where, ω_r = resonant angular frequency of the coil surrounding the toroid, radian/second.

Therefore, C_1 may be determined from a knowledge of ω_r and L_1,

$$C_1 = \frac{1}{\omega_r^2 L_1} \tag{18}$$

Since L_1 may be found from equation (13), and ω_r may be determined experimentally, the parameter C_1 may be determined experimentally.

The parameter R_{1b} represents the effects of hysteresis loss, eddy-current loss, and imperfect insulation between the conductors surrounding the toroid. A theoretical derivation of this parameter would be quite difficult; however, it may be easily found experimentally by the following approach. If the open-circuit impedance $Z_{11}(j\omega)$ is evaluated at resonance,

$$Z_{11}(j\omega)\Big|_{\omega=\omega_r} = \frac{\frac{1}{C_1}\left(j\omega_r + \frac{R_{1a}}{L_1}\right)}{j\omega_r\left(\frac{1}{R_{1b}C_1}\right)}. \tag{19}$$

If $\omega_r \gg R_{1a}/L_1$, then

$$Z_{11}(j\omega)\Big|_{\omega=\omega_r} = R_{1b}. \tag{20}$$

where, ω_r = resonant angular frequency of the n^{th} mode

Therefore, C_1 may be determined from the slope of ω_r and L_1, where

$$C_1 = \frac{1}{\omega_r^2 L_1}$$

Since L_1 may be found from equation (17), and ω_r may be determined experimentally, the parameter C_1 may be determined experimentally.

The parameter R_{1a} represents the effects of hysteresis loss, eddy-current loss, and dimensional imperfections between the conductors surrounding the core. A theoretical derivation of this parameter would be quite difficult; however, it may be easily found experimentally by the following approach. If the input-driving impedance $Z_{11}(j\omega)$ is evaluated at resonance,

$$Z_{11}(j\omega)_{\omega=\omega_r} = \frac{\left(\frac{1}{j\omega C_1} + j\omega L_1\right)\left(R_{1a} + j\omega L_1\right)}{\left(R_{1a} + j\omega L_1\right)}$$

If $\omega_r \gg R_{1a}/L_1$, then

Therefore, the parameter R_{1b} may easily be determined experimentally.

The mutual inductance parameters, M_{12} and M_{13}, will now be determined. The mutual inductance M_{12} is by definition equal to the flux which links loop one due to a current in loop two divided by the current in loop two. To determine this quantity the magnetic field produced by a current in loop two must be found.

Figure 14 illustrates a current carrying conductor situated between two high permeability materials. The current carrying conductor will be assumed to be of infinite length. If the magnetic field due to this infinitely long current carrying conductor can be found, it may be used to determine the magnetic field existing in the physical system due to a current in loop two.

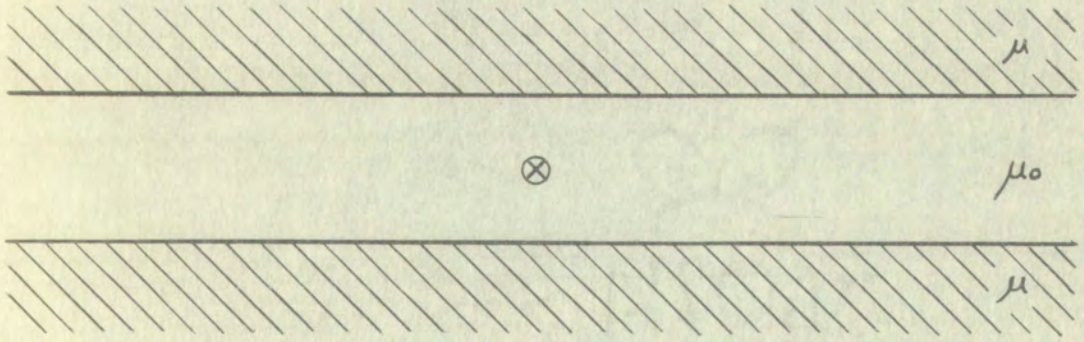

FIGURE 14

CURRENT CARRYING CONDUCTOR LOCATED BETWEEN TWO HIGH PERMEABILITY MATERIALS

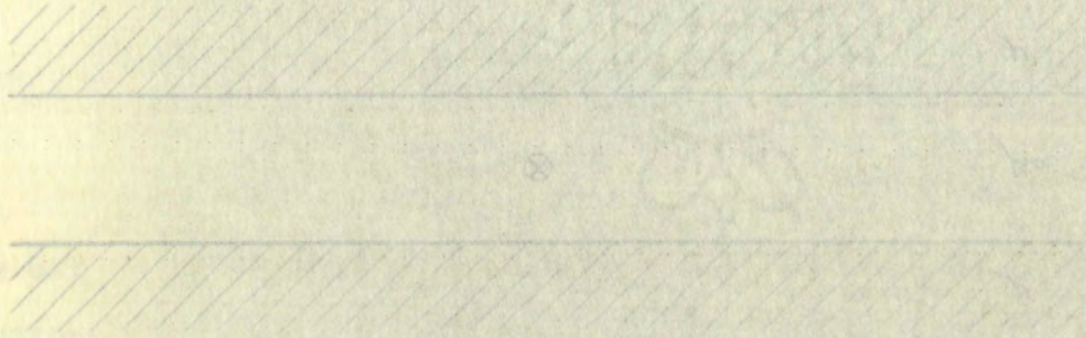

The magnetic field which exists in the configuration shown on Figure 14 will be argued rather than developed rigorously. At points very near the conductor the magnetic field should not be influenced by the presence of the high permeability material; therefore, the magnetic field should be circumferential at distances very near the conductor. If the permeability of the magnetic material is much greater than the permeability of air, then the magnetic field at the boundary between the air and the magnetic material should be very nearly vertical. If these two principles are combined, then the approximate magnetic field distribution within the air gap may be obtained.[2] The result is indicated by Figure 15.

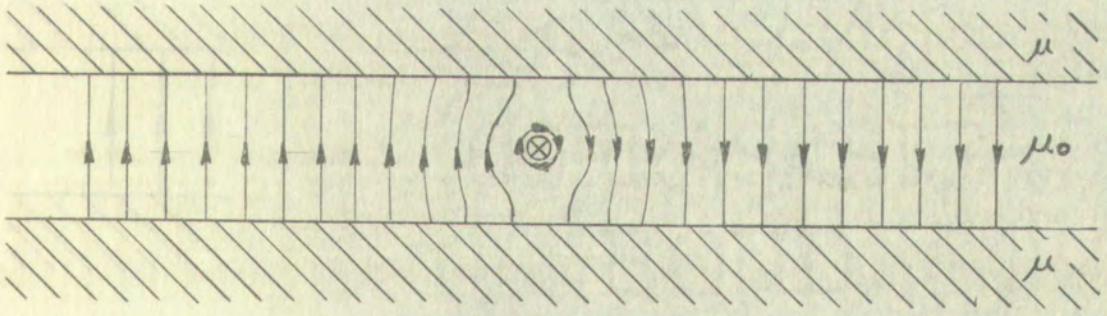

FIGURE 15

APPROXIMATE MAGNETIC FIELD DISTRIBUTION DUE TO A CURRENT CARRYING CONDUCTOR LOCATED IN AN AIR GAP

---

[2] John D. Kraus, Electromagnetics, (New York: McGraw-Hill Book Company, Inc., 1953), p. 258.

As can be seen from Figure 15, the magnetic field is very nearly vertical at distances from the conductor greater than several times the air gap width. Therefore, an approximate picture of the magnetic field distribution consists of a vertical array. This situation is illustrated in Figure 16. The approximation is very poor near the conductor; however, at distances from the conductor greater than several times the air gap width, the approximation is very good. The approximate magnetic field distribution shown on Figure 16 will be used in the development of the mutual inductance parameters.

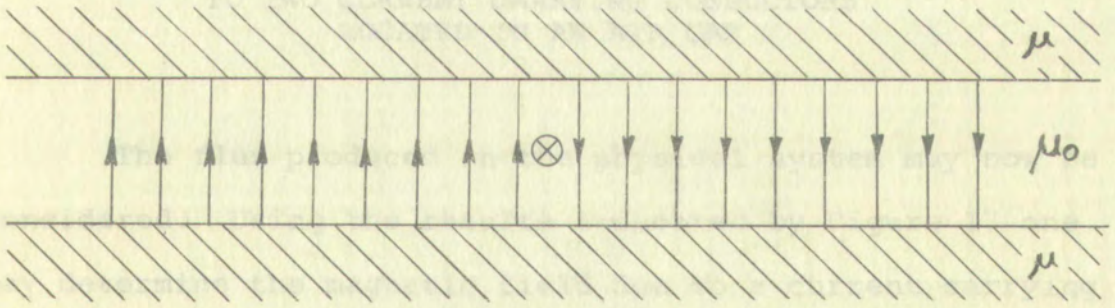

FIGURE 16

SIMPLIFIED MAGNETIC FIELD DISTRIBUTION DUE TO A CURRENT CARRYING CONDUCTOR LOCATED IN AN AIR GAP

Using the results shown on Figure 16 the magnetic field due to two current carrying conductors located between high permeability materials may be obtained. If

to obtain this information. If the path of integration is selected as shown on Figure 18, the following equation may be obtained,

$$H_t = \frac{i_2}{b} \tag{21}$$

where, H_t = magnetic field existing within the air gap due to i_2, ampere/meter,

i_2 = current in loop two, ampere,

b = width of the air gap, meter.

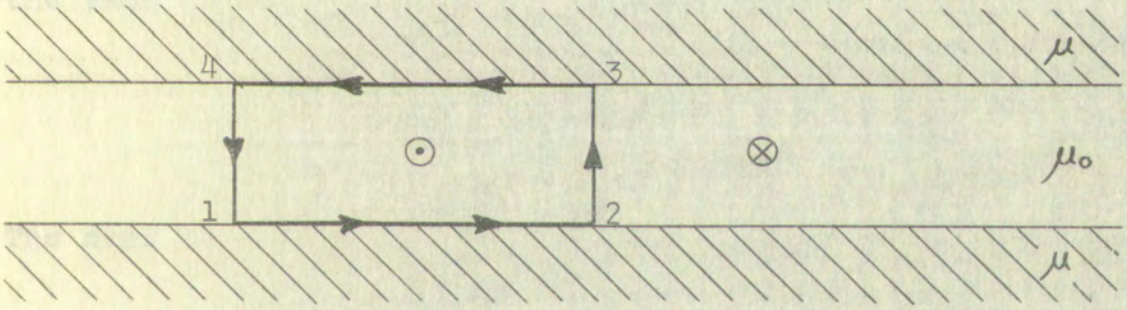

FIGURE 18
PATH OF INTEGRATION USED TO OBTAIN EQUATION (21)

Using the relations $B = \mu H$ and $\Phi = BA$, the flux which links loop one due to a current in loop two may be obtained,

$$\Phi_{12} = \frac{\mu_o A_2 i_2}{b} \tag{22}$$

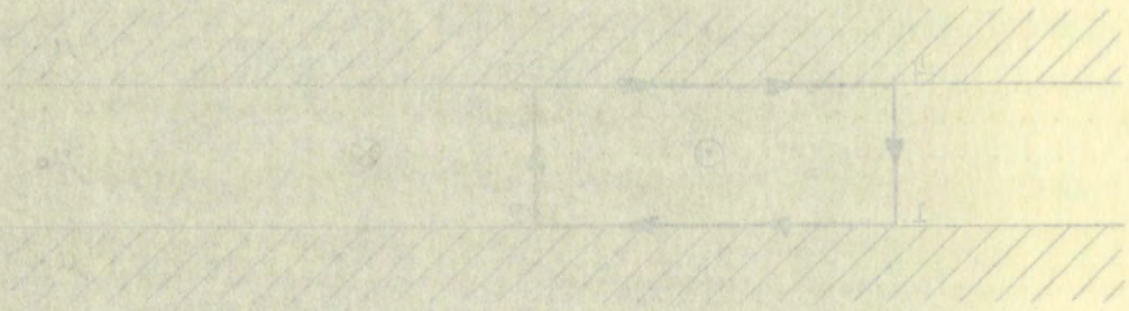

where, Φ_{12} = flux which links loop one due to a current in loop two, weber,

A_2 = area of loop two, meter^2.

The area of loop two is involved in equation (22). This quantity is shown on Figure 19. The mutual inductance parameter, M_{12}, may now be obtained,

$$M_{12} = \frac{\mu_o N A_2}{b}. \qquad (23)$$

The mutual inductance parameter, M_{13}, may be obtained by the same procedure used to determine M_{12}. The result is,

$$M_{13} = \frac{\mu_o N A_3}{b}.$$

The area of loop three, A_3, is shown on Figure 20.

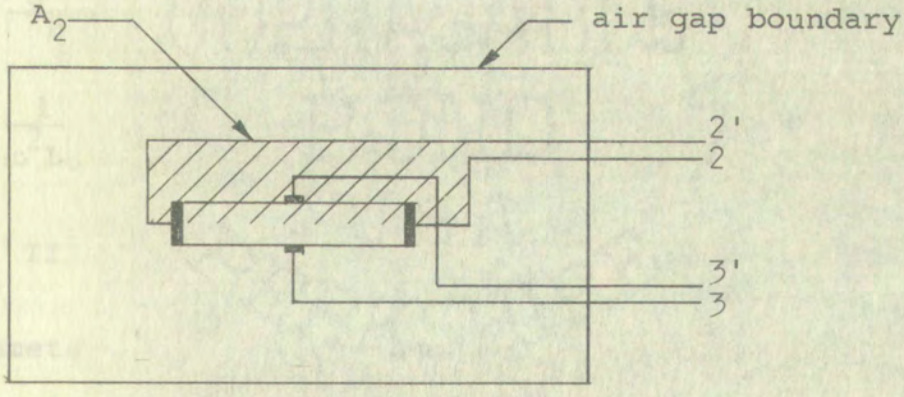

FIGURE 19

AREA BOUNDED BY LOOP TWO

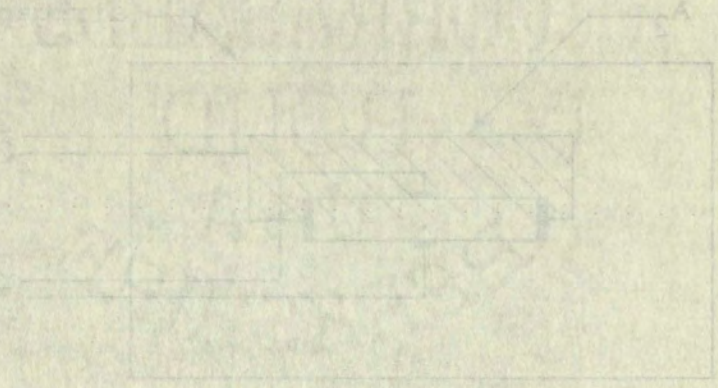

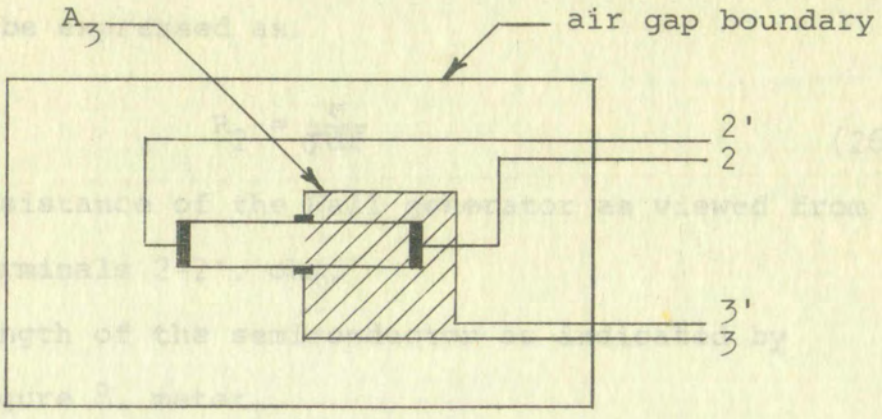

FIGURE 20

AREA BOUNDED BY LOOP THREE

All of the parameters of loop one have now been obtained. They are as follows:

$$L_1 = \frac{\mu_o N^2 ac}{b}, \qquad M_{12} = \frac{\mu_o N A_2}{b},$$

$$M_{13} = \frac{\mu_o N A_3}{b}, \qquad R_{1b} = \left| Z_{11}(j\omega) \right|_{\omega=\omega_r}, \qquad (25)$$

$$C_1 = \frac{1}{\omega^2 L_1}, \qquad R_{1a} = \left| \frac{V_1(j\omega)}{I_1(j\omega)} \right|_{\omega=0}.$$

III. PARAMETERS OF LOOP TWO

The parameters of loop two are as follows: R_2, L_2, M_{23}, M_{21}, K_{2a}, and K_{2b}. The parameter R_2 is simply the resistance of the Hall generator as viewed from terminals

inductance of loop two is expressible as,

$$L_2 = \frac{\mu_o A_2}{b}. \tag{28}$$

The mutual inductance M_{21} is by definition equal to the flux which links loop two due to a current in loop one divided by the current in loop one. It has been shown that a current in loop one produces a uniform flux density within the air gap given by,

$$B_g = \frac{\mu_o N i}{b} . \tag{29}$$

Therefore, the mutual inductance M_{21} is,

$$M_{21} = \frac{\mu_o N A_2}{b} \tag{30}$$

The mutual inductance M_{23} is by definition equal to the flux which links loop two due to a current in loop three divided by the current in loop three. A current in loop three produces a magnetic flux density within the air gap given by,

$$B_g = \frac{\mu_o i_3}{b} \tag{31}$$

where, B_g = magnetic flux density within the air gap due to i_3, weber/meter^2.

The amount of flux which links loop two depends on the area which is common to both loops two and three. This area is defined as A_{23} and is shown on Figure 21. Therefore, the mutual inductance M_{23} is,

$$M_{23} = \frac{\mu_o A_{23}}{b}. \qquad (32)$$

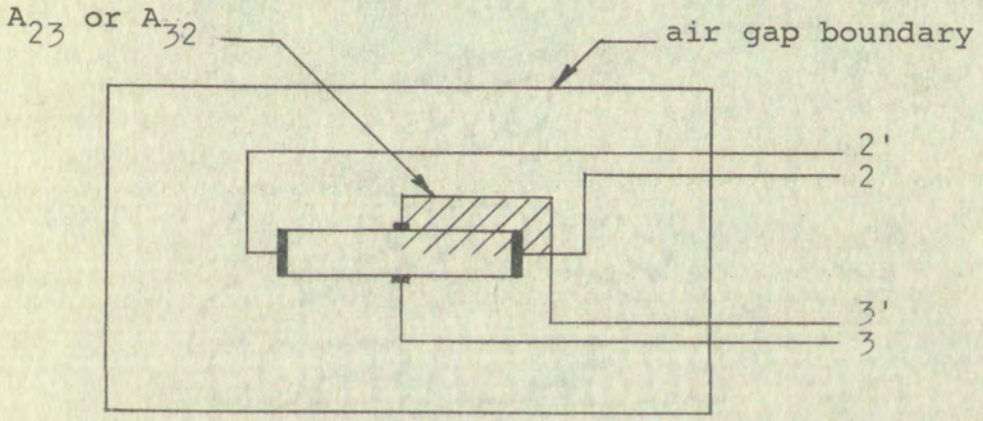

FIGURE 21

AREA BOUNDED BY LOOPS TWO AND THREE

The parameters R_2, L_2, M_{21}, and M_{23} have been determined. The constants, K_{2a} and K_{2b}, associated with the voltage generators of loop two will now be determined. The constant K_{2a} involves the Hall effect, and the constant K_{2b} involves the displacement voltage.

It may be shown that the Hall voltage equation is[3],

---

[3]Charles Kittel, Introduction to Solid State Physics (New York: John Wiley and Sons, Inc., 1953), p. 297.

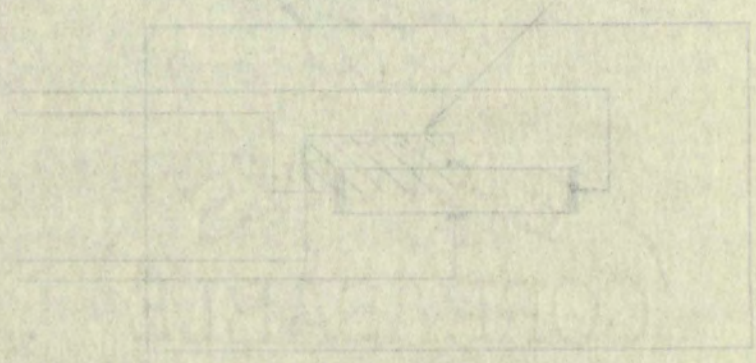

$$V_h = \frac{Ri_3B}{d} \tag{33}$$

where, V_h = voltage produced due to the Hall effect,

R = Hall constant, meter^3/coulomb,

i_3 = current flow in the semiconductor, ampere,

B = magnetic flux density normal to the face of the semiconductor, weber/meter^2,

d = thickness of the semiconductor as shown on Figure 13, meter.

The Hall constant, R, depends on the properties of the semiconductor. If the semiconductor is either predominantly n-type or predominantly p-type, then the Hall constant is[4],

$$R = \pm \frac{3\pi}{8} \cdot \frac{1}{N|e|} \tag{34}$$

where, N = carrier density, 1/meter^3,

e = charge on an electron, coulomb.

If both electrons and holes are present, the Hall constant is[5],

---

[4]William Shockley, Electrons and Holes in Semiconductors (Princeton, New Jersey, 1950), p. 215.

[5]Ibid., pp. 216-217

where, V_H = voltage produced due to the Hall effect,

R = Hall constant, meter^3/coulomb,

i_x = current flowing thru the semiconductor, ampere,

B = magnetic flux density normal to the face of the semiconductor, weber/meter^2,

d = thickness of the semiconductor, meter.

Figure 13. meter

The Hall constant, R, depends on the properties of the semiconductor. If the semiconductor is either deeply n-type or predominantly p-type then the Hall constant is[4],

$$R = \frac{1}{Ne}$$

where, N = carrier density, [illegible]

e = charge on an electron, coulomb.

If both electrons and holes are present, the Hall constant is[5],

---

[4] William Shockley, Electrons and Holes in Semiconductors (Princeton, New Jersey, 1950), pp. 216-217.

[5] Ibid., pp. 216-217.

$$R = \frac{3\pi}{8} \frac{-nb^2+p}{(nb+p)^2|e|} \tag{35}$$

where, n = electron carrier density, 1/meter^3,

p = hole carrier density, 1/meter^3,

b = ratio of electron to hole mobility.

As can be seen from equations (34) and (35), the Hall constant may be either positive or negative depending on the type of carriers present. Therefore, the constants K_{2a} and K_{3a} may be either positive or negative. Their polarity may be found from an inspection of the physical system and an application of the equation,

$$\overline{F} = Q\overline{V}x\overline{B} \tag{36}$$

where, $\overline{F}$ = force vector acting on a charge Q, newton,

Q = charge, coulomb,

$\overline{V}$ = velocity vector of the charge Q, meter/second,

$\overline{B}$ = magnetic flux density vector, weber/meter^2.

This equation enables one to determine the direction of carrier deflection and hence the polarity of the resulting Hall voltage.

The magnetic flux density within the air gap due to a current in loop one has been shown to be,

$$B_g = \frac{\mu_o Ni}{b} \tag{37}$$

$$K = \frac{p - nb^2}{p + nb^2}$$

where, n = electron carrier density, 1/meter^3

p = hole carrier density, 1/meter^3

b = ratio of electron to hole mobility

As can be seen from equations (3a) and (3b) the Hall constant may be either positive or negative depending on the type of carriers present. Therefore the constants K and K_{Ja} may be either positive or negative. Their polarity may be found from an inspection of the physical system and an application of the equation

$$\bar{F} = Q\bar{V} \times \bar{B}$$

where, $\bar{F}$ = force vector acting on a charge, newton

Q = charge, coulomb

$\bar{V}$ = velocity vector of the charge, meter/second

$\bar{B}$ = magnetic flux density vector, weber/meter^2

This equation enables one to determine the direction of carrier deflection and hence the polarity of the resulting Hall voltage.

The magnetic flux density within the air gap due to a current in loop one has been shown to be

$$B_d = \frac{\mu_o I}{2\pi r}$$

If equations (33) and (37) are combined,

$$V_h = \frac{\mu_o NRii_3}{bd}. \tag{38}$$

Therefore, the constant K_{2a} is given by,

$$K_{2a} = \frac{\mu_o NR}{bd}. \tag{39}$$

The constant K_{2b} is due to the displacement voltage produced by a current in loop three. Figure 22 illustrates the Hall generator and the displacement voltage. A theoretical derivation of K_{2b} would be quite difficult;

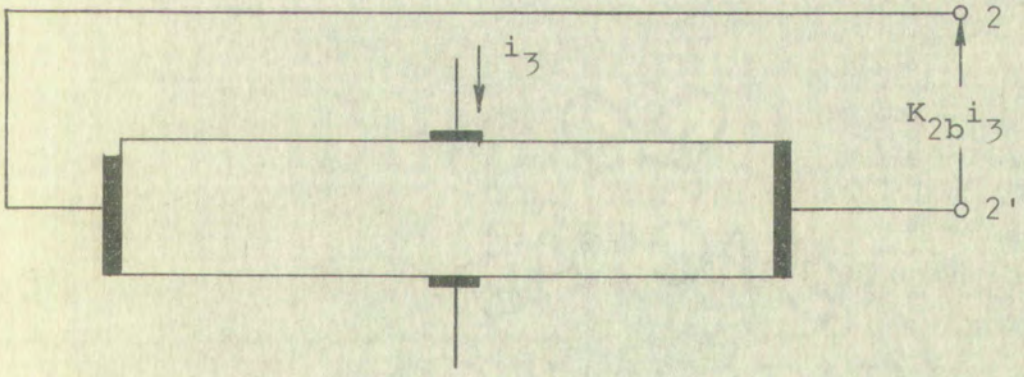

FIGURE 22

DISPLACEMENT VOLTAGE DUE TO THE FAILURE OF THE INPUT ELECTRODES TO COVER THE ENTIRE END FACES OF THE SEMICONDUCTOR

however, it may easily be determined experimentally. The experimental determination of K_{2b} may be expressed by the

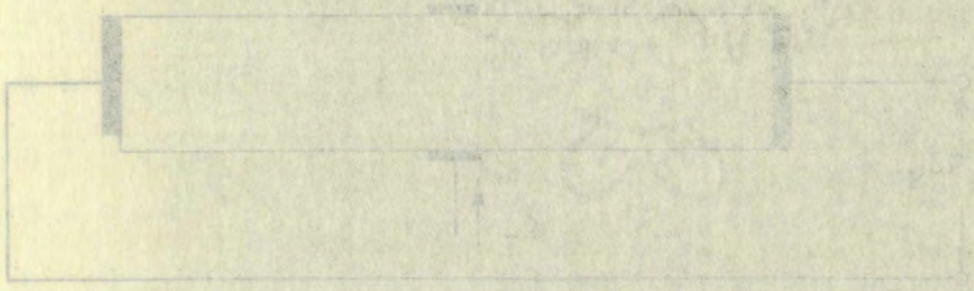

equation,

$$K_{2b} = \frac{V_2(j\omega)}{I_3(j\omega)}\Big|_{\omega=0}, \tag{40}$$

where, K_{2b} = displacement voltage constant, ohm,

$I_3(j\omega)$ = phasor representation of a current applied to loop three, ampere,

$V_2(j\omega)$ = phasor representation of the voltage resulting at terminals 2-2' due to $I_3(j\omega)$.

All of the parameters of loop two have now been determined. They are as follows.

$$L_2 = \frac{\mu_o A_2}{b}, \qquad M_{21} = \frac{\mu_o N A_2}{b},$$

$$M_{23} = \frac{\mu_o A_{23}}{b}, \qquad R_2 = \frac{e}{\sigma df}, \tag{41}$$

$$K_{2a} = \frac{\mu_o NR}{bd}, \qquad K_{2b} = \frac{V_2(j\omega)}{I_3(j\omega)}\Big|_{\omega=0}.$$

IV. PARAMETERS OF LOOP THREE

The parameters of loop three are as follows: R_3, L_3, M_{32}, M_{31}, K_{3a}, and K_{3b}. R_3 is the resistance of the semiconductor as viewed from terminals 3-3'. The development of this parameter is complicated by the fact that the output electrodes of the Hall generator cover only a fraction of the length of the semiconductor. If certain

$$L_2 = \frac{\mu_o A_2}{b}$$

$$M_{23} = \frac{\mu_o A_{23}}{b}$$

$$K_{2a} = \frac{\mu_o h_R}{bd}$$

assumptions are made, it may be shown that the resistance R_3 may be expressed by[6],

$$R_3 = \frac{2}{\sigma \pi d} \ln \left[\frac{\epsilon^{\pi g/f} + 1}{\epsilon^{\pi g/f} - 1} \right] \tag{42}$$

where, g = width of the output electrodes as indicated by Figure 8, meter,

R_3 = resistance of the semiconductor as viewed from terminals 3-3', ohm.

The validity of equation (42) is based on the following assumptions: (1) The thickness of the output electrodes and the semiconductor is essentially the same. (2) The width of the output electrodes is small compared with the length of the semiconductor. (3) The output electrodes are parallel. These assumptions are usually quite valid.

The development of the parameters L_3, M_{32}, M_{31}, and K_{3b} is very similar to the development of the parameters of loop two. Therefore, the value of these parameters will be stated without proof.

$$L_3 = \frac{\mu_o A_3}{b}, \qquad M_{31} = \frac{\mu_o N A_3}{b}, \tag{43}$$

---

[6] David L. Endsley and W.W. Grannemann, "A Theoretical and Experimental Analysis of a Hall Generator" (Technical Report EE-27, The University of New Mexico Engineering Experiment Station, Albuquerque, 1959), pp. 31-37.

$$M_{32} = \frac{\mu_o A_{32}}{b}, \qquad K_{3a} = \frac{\mu_o NR}{bd}. \tag{43}$$

The parameter K_{2b} involves the displacement voltage produced in loop three due to a current in loop two. Figure 23 illustrates the Hall generator and the displacement of the output electrodes. If the output electrodes

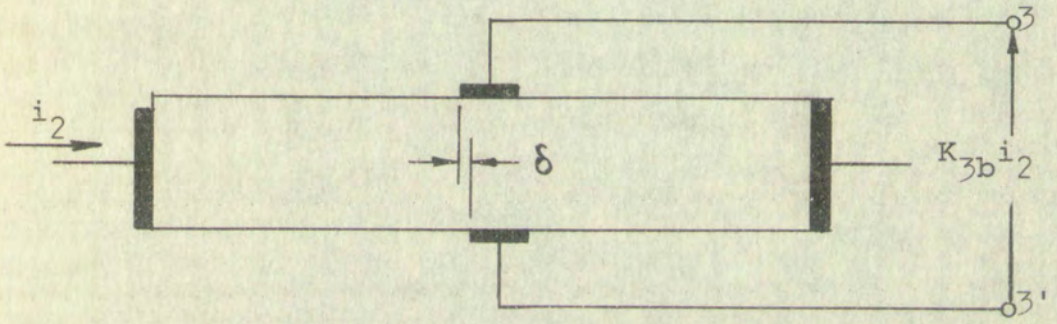

FIGURE 23

DISPLACEMENT VOLTAGE PRODUCED IN LOOP THREE DUE TO A CURRENT IN LOOP TWO

are displaced by a distance δ, then a current in loop two produces a voltage in loop three given by,

$$V_3 = \frac{\delta R_2 i_2}{e} \tag{44}$$

where, V_3 = voltage produced in loop three due to a current i_2,

δ = displacement of the output electrodes as indicated by Figure 23, meter,

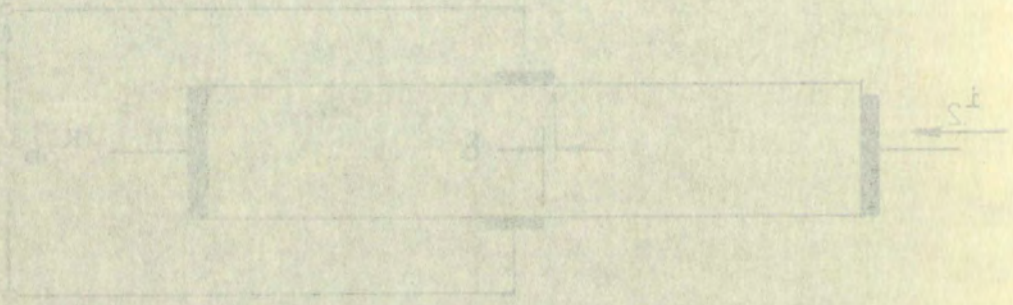

R_2 = resistance of the Hall generator as viewed from terminals 2-2', ohm,

e = length of the semiconductor as indicated by Figure 8, meter,

i_2 = current in loop two, ampere.

Combining equations (44) and (26) results in,

$$K_{3b} = \frac{\delta}{\sigma df}. \tag{45}$$

All of the parameters of loop three have now been determined. They are as follows.

$$L_3 = \frac{\mu_o A_3}{b}, \qquad M_{31} = \frac{\mu_o N A_3}{b},$$

$$M_{32} = \frac{\mu_o A_{32}}{b}, \qquad K_{3a} = \frac{\mu_o NR}{bd},$$

$$R_3 = \frac{2}{\sigma \pi d} \ln\left[\frac{\epsilon^{\pi g/f} + 1}{\epsilon^{\pi g/f} - 1}\right] \qquad K_{3b} = \frac{\delta}{\sigma df}. \tag{46}$$

V. COMPLETED EQUIVALENT CIRCUIT

The physical system considered in this study is illustrated on Figure 8 which has been repeated and is shown on page 48. The equivalent circuit of this system is shown on Figure 13 which has been repeated and is shown on page 49. The parameters of the equivalent circuit are

R_2 = resistance of the small primary coil, as viewed from terminals 2-2', ohms

ℓ = length of the secondary coil as indicated in Figure 8, meter,

i_2 = current in loop two, ampere.

Combining equations (94) and (25) results in

$$X_{3b} = \frac{\omega L}{c}$$

All of the parameters of loop three have now been determined. They are as follows:

$$L_3 = \frac{\mu_o \lambda_3}{b}$$

$$M_{32} = \frac{\mu_o A_2 z}{b}$$

$$R_3 = \frac{z}{\sigma \pi a} \ln\left[\frac{e^{\pi a/\ell} + 1}{e^{\pi a/\ell} - 1}\right]$$

V. COMPLETED MOUTVALVE CIRCUIT

The physical system considered in this study is illustrated on Figure 8 which has been repeated and is shown on page 46. The equivalent circuit of this system is shown on Figure 13 which has been repeated and is shown on page 49. The parameters of the equivalent circuit are

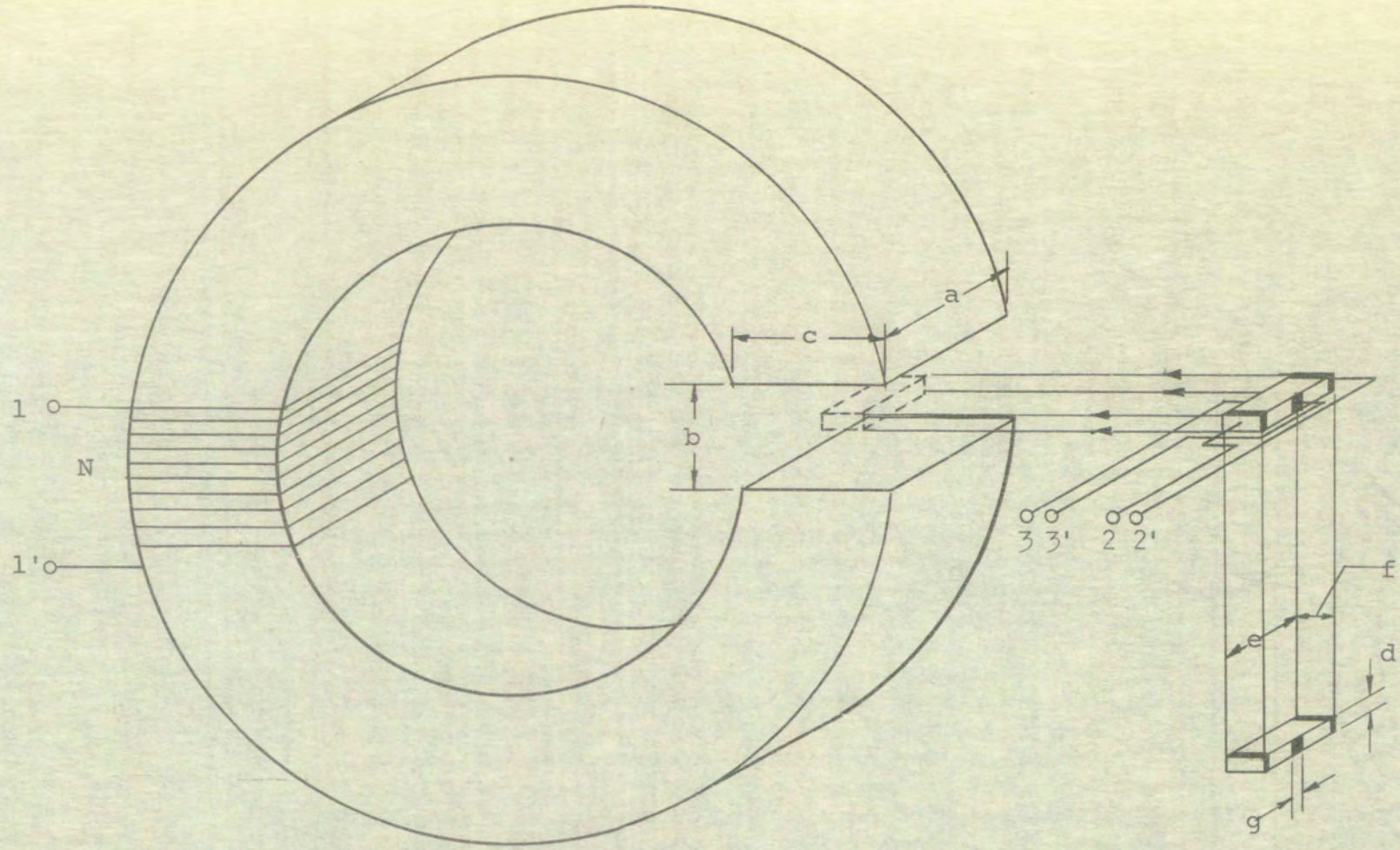

FIGURE 8 (REPEAT)

HALL GENERATOR AND FLUX CONCENTRATOR

HALF GENERATOR AND ITS CONSEQUENCES

FIGURE 8 (KELEVA)

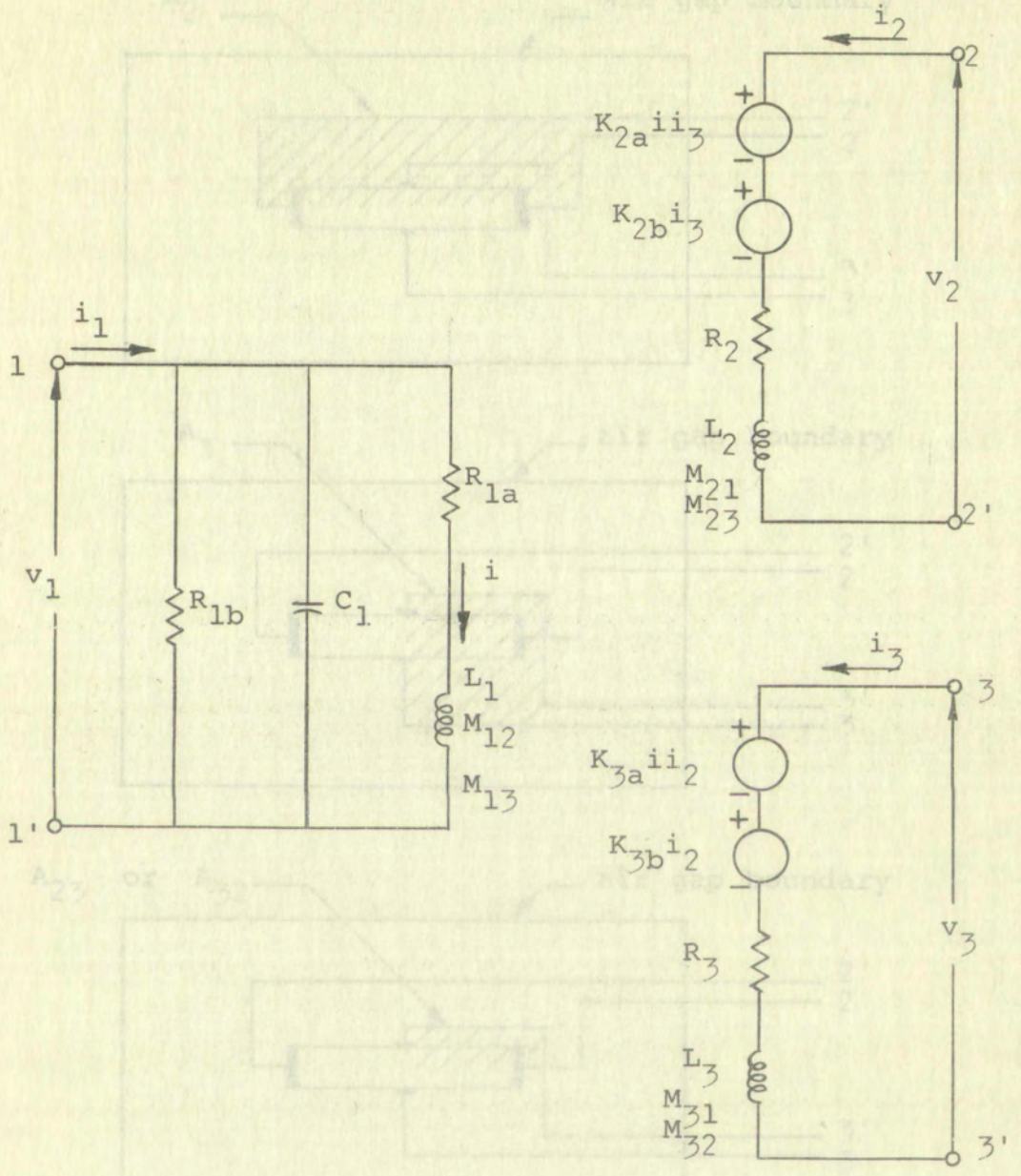

FIGURE 13 (REPEAT)

EQUIVALENT CIRCUIT OF A HALL GENERATOR
WHICH UTILIZES A FLUX CONCENTRATOR

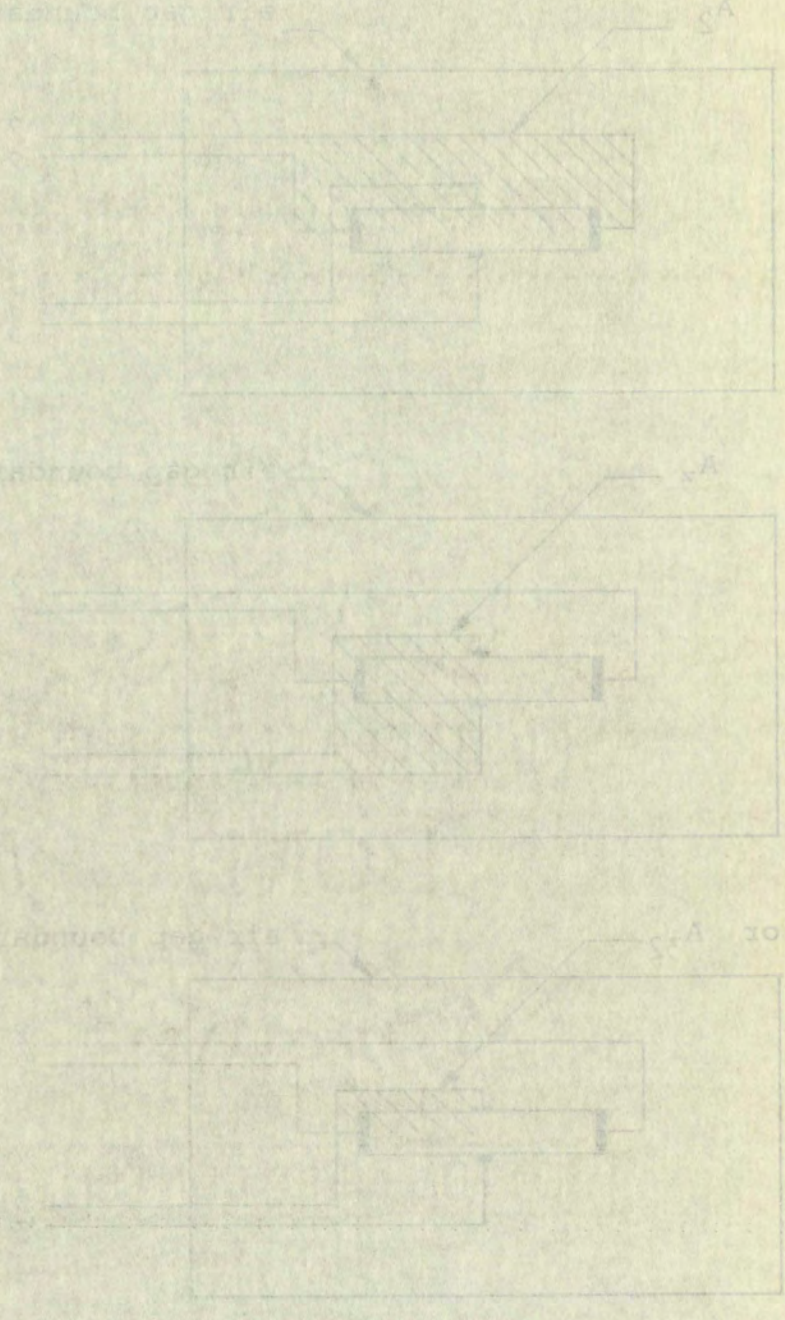

given by the following set of equations:

$$L_1 = \frac{\mu_o N^2 ac}{b}, \qquad L_2 = \frac{\mu_o A_2}{b}, \qquad L_3 = \frac{\mu_o A_3}{b},$$

$$M_{12} = \frac{\mu_o N A_2}{b}, \qquad M_{13} = \frac{\mu_o N A_3}{b}, \qquad M_{21} = \frac{\mu_o N A_2}{b},$$

$$M_{31} = \frac{\mu_o N A_3}{b}, \qquad M_{23} = \frac{\mu_o A_{23}}{b}, \qquad M_{32} = \frac{\mu_o A_{32}}{b},$$

$$C_1 = \frac{1}{\omega_r^2 L_1} \qquad K_{2a} = \frac{\mu_o NR}{bd}, \qquad K_{2b} = \left.\frac{V_2(j\omega)}{I_3(j\omega)}\right|_{\omega=0}, \tag{47}$$

$$K_{3a} = \frac{\mu_o NR}{bd} \qquad K_{3b} = \frac{\delta}{\sigma df}, \qquad R_{1a} = \left.\frac{V_1(j\omega)}{I_1(j\omega)}\right|_{\omega=0},$$

$$R_3 = \frac{2}{\sigma \pi d} \ln\left[\frac{\epsilon^{\pi g/f} + 1}{\epsilon^{\pi g/f} - 1}\right], \qquad R_2 = \frac{e}{\sigma df}, \qquad R_{1b} = \left|Z_{11}(j\omega)\right|_{\omega=\omega_r},$$

where, R = Hall constant, meter^3/coulomb,

σ = conductivity of the semiconductor, 1/ohm meter,

μ_o = permeability of free space, henry/meter,

ω = angular frequency, radian/second,

ω_r = resonant angular frequency of the coil surrounding the toroid, radian/second,

δ = displacement of the output electrodes, meter,

$$Z_{11}(j\omega) = \left.\frac{V_1(j\omega)}{I_1(j\omega)}\right|_{I_2(j\omega) = I_3(j\omega) = 0}, \text{ ohm.}$$

The various dimensions involved in the parameters of the equivalent circuit are shown on Figure 8. The parameters

given by the following set of equations:

$$L_1 = \frac{\mu_o N^2 ac}{b}, \qquad L_2 = \frac{}{}$$

$$M_{12} = \frac{\mu_o NA}{b}, \qquad M_{23} = \frac{}{}$$

$$M_{31} = \frac{\mu_o NA}{b}, \qquad M_{23} = \frac{}{}$$

$$C_1 = \frac{1}{\omega_r^2 L_1}, \qquad K_{23} = \frac{}{}$$

$$K_{3a} = \frac{\mu_o NR}{bd}, \qquad K_{3b} = \frac{}{}$$

$$R_3 = \frac{\sigma \pi d}{2} \ln \left[\frac{\varepsilon \pi d / t + 1}{\varepsilon \pi d / t - 1} \right], \qquad R_4 = \frac{}{}$$

where, R = Hall constant, vers

σ = conductivity of circuit

μ_o = permeability of free

ω = angular frequency

ω_r = resonant angular

δ = displacement

$$Z_{11}(j\omega) = \frac{I_1(j\omega)}{V_1(j\omega)}$$

The various dimensions involved in the construction of the

equivalent circuit are shown on Page 5. The parameters

of the equivalent circuit also involve several of the areas bounded by the leads of the Hall generator. These various areas are indicated by Figure 24.

VI. DISCUSSION OF ASSUMPTIONS

A number of assumptions have been made throughout the development of the equivalent circuit. Some of the more important assumptions warrant discussion.

The first assumption concerns the parameter R_{1a}. It was stated that this parameter is simply the resistance of the coil surrounding the toroid. This is true only if $R_{1b} \gg R_{1a}$. Such an approximation should be true for almost all systems of practical interest.

It was also assumed that $L_1/R_{1a} \gg R_{1b}C_1$. A study of the characteristics of the physical system indicates that this assumption should be true for the majority of applications.

In the development of the parameter L_1 it was assumed that $\mu/\mu_o \gg (2\pi r-b)/b$. This approximation should be satisfied provided that high permeability toroids are used; however, the use of low permeability toroids and thin air gaps may result in the failure of this approximation. If this approximation is not satisfied, the flux density within the air gap will not be uniform. This factor greatly complicates the analysis of the Hall effect.

of the equivalent circuit also involve several of the areas bounded by the leads of the Hall generator. These various areas are indicated by Figure 24.

VI. DISCUSSION OF ASSUMPTIONS

A number of assumptions have been made throughout the development of the equivalent circuit. Some of the more important assumptions warrant discussion.

The first assumption concerns the parameter R_{Ia}. It was stated that this parameter is simply the resistance of the coil surrounding the toroid. This is true only if $R_{Ib} \gg R_{Ia}$. Such an approximation should be true for almost all systems of practical interest.

It was also assumed that $L_1 / R_{Ia} \gg R_{Ib} C_1$. A study of the characteristics of the physical system indicates that this assumption should be true for the majority of applications.

In the development of the parameter L_1 it was assumed that $\mu / \mu_o \gg (2\pi - b) / b$. This approximation should be satisfied provided that high permeability toroids are used; however, the use of low permeability toroids and thin air gaps may result in the failure of this approximation. If this approximation is not satisfied, the flux density within the air gap will not be uniform. This factor greatly complicates the analysis of the Hall effect.

Therefore, one would probably be interested in using high permeability toroids to simplify the analysis.

The major assumption used in the development of the equivalent circuit concerns the magnetic field produced by a current carrying conductor located in an air gap. Since the solution of this problem was to some extent argued, experimental verification was quite important. The experimental verification of the inductance parameters indicates that this assumption was valid.

In conclusion it is believed that the assumptions used in the development of the parameters of the equivalent circuit are quite reasonable.

Therefore, one would probably be interested in having high permeability toroids to simplify the analysis.

The major assumption used in the development of the equivalent circuit concerns the magnetic field produced by a current carrying conductor located in an air gap. Figure the solution of this problem was to some extent argued.

experimental verification was quite important. The experimental verification of the inductance parameters indicates that this assumption was valid.

In conclusion it is believed that the material parameters used in the development of the parameters of the equivalent circuit are quite reasonable.

CHAPTER III

EXPERIMENTAL VERIFICATION OF THE EQUIVALENT CIRCUIT

A number of assumptions were made throughout the development of the equivalent circuit; therefore, the experimental verification was quite important. The equivalent circuit of a specific model was developed from the results of chapter two. The study of the validity of this equivalent circuit was centered about an open-circuit impedance approach. The open-circuit impedances of the physical system were calculated by an inspection of the equivalent circuit. The validity of these impedances was then experimentally verified by a sinusoidal steady-state analysis of the physical system. Since this procedure failed to place in evidence the effects of all of the parameters of the equivalent circuit, a d.c. and an a.c. signal were applied to two inputs of the system simultaneously. The response as a function of frequency obtained from the physical system was then compared with that predicted by the equivalent circuit. Finally, the transient and nonlinear aspects of the system were investigated.

I. OPEN-CIRCUIT IMPEDANCE APPROACH

The physical system considered in this study is

illustrated in Figure 8, page 48. The equivalent circuit of this system is shown in Figure 13, page 49, and the parameters of the equivalent circuit are given by the set of equations (47), page 51.

An experimental model incorporating an indium antimonide Hall generator was selected for study. The dimensions and electrical characteristics of the experimental model are listed in appendix one. By application of the results of the previous chapter the parameters of the equivalent circuit of the experimental model were determined; these parameters are listed in appendix two. The experimental investigation was concerned with determining the accuracy of this equivalent circuit.

The validity of the equivalent circuit was first studied by an open-circuit impedance approach. The operation of a three-port system may be described by the following set of equations;

$$\begin{aligned} V_1(s) &= Z_{11}(s)I_1(s) + Z_{12}(s)I_2(s) + Z_{13}(s)I_3(s), \\ V_2(s) &= Z_{21}(s)I_1(s) + Z_{22}(s)I_2(s) + Z_{23}(s)I_3(s), \\ V_3(s) &= Z_{31}(s)I_1(s) + Z_{32}(s)I_2(s) + Z_{33}(s)I_3(s). \end{aligned} \tag{48}$$

The various open-circuit impedances involved in equation (48) are defined by:

illustrated in Figure [illegible]. The nonlinear circuit
of this system is shown in Figure [illegible]. The numerical
parameters of the equivalent circuit are given by the solution
of equations (47), page [illegible].

An experimental model incorporating transistors and
monide Hall generator was selected for study. The characteris-
sions and electrical characteristics of the experimental
model are listed in Appendix [illegible]. A comparison of the
results of the previous chapter for the parameters of the
equivalent circuit of the experimental model were determined
mined; these parameters are listed in Appendix [illegible]. The
experimental investigation was concerned with determining
the accuracy of this equivalent circuit.

The validity of the equivalent circuit may be
studied by an open-circuit impedance experiment. The opera-
tion of a three-port system may be described by the follow-
ing set of equations:

$$V_1(s) = Z_{11}(s)I_1(s) + Z_{12}(s)I_2(s) + Z_{13}(s)I_3(s)$$

$$V_2(s) = Z_{21}(s)I_1(s) + Z_{22}(s)I_2(s) + Z_{23}(s)I_3(s)$$

$$V_3(s) = Z_{31}(s)I_1(s) + Z_{32}(s)I_2(s) + Z_{33}(s)I_3(s)$$

The various open-circuit impedances involved in equa-
tion (48) are defined by:

$$
\begin{aligned}
Z_{11}(s) &= \left.\frac{V_1(s)}{I_1(s)}\right|_{I_2(s)=I_3(s)=0'} \\
Z_{12}(s) &= \left.\frac{V_1(s)}{I_2(s)}\right|_{I_1(s)=I_3(s)=0'} \\
Z_{13}(s) &= \left.\frac{V_1(s)}{I_3(s)}\right|_{I_1(s)=I_2(s)=0'} \\
Z_{21}(s) &= \left.\frac{V_2(s)}{I_1(s)}\right|_{I_2(s)=I_3(s)=0'} \\
Z_{22}(s) &= \left.\frac{V_2(s)}{I_2(s)}\right|_{I_1(s)=I_3(s)=0'} \\
Z_{23}(s) &= \left.\frac{V_2(s)}{I_3(s)}\right|_{I_1(s)=I_2(s)=0'} \\
Z_{31}(s) &= \left.\frac{V_3(s)}{I_1(s)}\right|_{I_2(s)=I_3(s)=0'} \\
Z_{32}(s) &= \left.\frac{V_3(s)}{I_2(s)}\right|_{I_1(s)=I_3(s)=0'} \\
Z_{33}(s) &= \left.\frac{V_3(s)}{I_3(s)}\right|_{I_1(s)=I_2(s)=0'}
\end{aligned}
\tag{49}
$$

The set of equations (49) was used to determine the open-circuit impedances of the equivalent circuit. The development of the majority of these impedances was straightforward; however, the impedances $Z_{32}(s)$ and $Z_{23}(s)$ required special consideration.

$$Z_{11}(s) = \left.\frac{I_1(s)}{V_1(s)}\right|_{I_2(s)=I_3(s)=0}$$

$$Z_{12}(s) = \left.\frac{I_2(s)}{V_1(s)}\right|_{I_1(s)=I_3(s)=0}$$

$$Z_{13}(s) = \left.\frac{I_3(s)}{V_1(s)}\right|_{I_1(s)=I_2(s)=0}$$

$$Z_{21}(s) = \left.\frac{I_1(s)}{V_2(s)}\right|_{I_2(s)=I_3(s)=0}$$

$$Z_{22}(s) = \left.\frac{I_2(s)}{V_2(s)}\right|_{I_1(s)=I_3(s)=0} \qquad (49)$$

$$Z_{23}(s) = \left.\frac{I_3(s)}{V_2(s)}\right|_{I_1(s)=I_2(s)=0}$$

$$Z_{31}(s) = \left.\frac{I_1(s)}{V_3(s)}\right|_{I_2(s)=I_3(s)=0}$$

$$Z_{32}(s) = \left.\frac{I_2(s)}{V_3(s)}\right|_{I_1(s)=I_3(s)=0}$$

$$Z_{33}(s) = \left.\frac{I_3(s)}{V_3(s)}\right|_{I_1(s)=I_2(s)=0}$$

The set of equations (49) was used to determine the open-circuit impedances of the equivalent circuit. The development of the majority of these impedances was straightforward; however, the impedances $Z_{32}(s)$ and $Z_{23}(s)$ required special consideration.

It should be noted that the determination of a voltage produced at terminals 3-3' (refer to Figure 13, page 49) due to a current in loop two involves nonlinear differential equations. A similar situation occurs in the determination of a voltage produced at terminals 2-2' due to a current in loop three. Therefore, the concept of $Z_{23}(s)$ and $Z_{32}(s)$ actually has no meaning. The cause of the nonlinear differential equations is the Hall voltage generators. It is shown in appendix four that in the determination of a voltage produced at terminals 3-3' due to a current in loop two the effects of the Hall voltage generator are negligible in comparison with the other voltages present; therefore, they may be neglected. It should be emphasized that the validity of this approximation depends upon the particular system. Thus, the parameters $Z_{23}(s)$ and $Z_{32}(s)$ were determined without consideration of the Hall voltage generators.

The validity of the theoretically derived open-circuit impedances was experimentally investigated. The open-circuit impedances of the experimental model were measured as a function of frequency over a range extending from one c.p.s. to one m.c.p.s. The results of these tests are indicated by Figure 25 through 33. As can be seen from these figures, the experimentally determined open-circuit

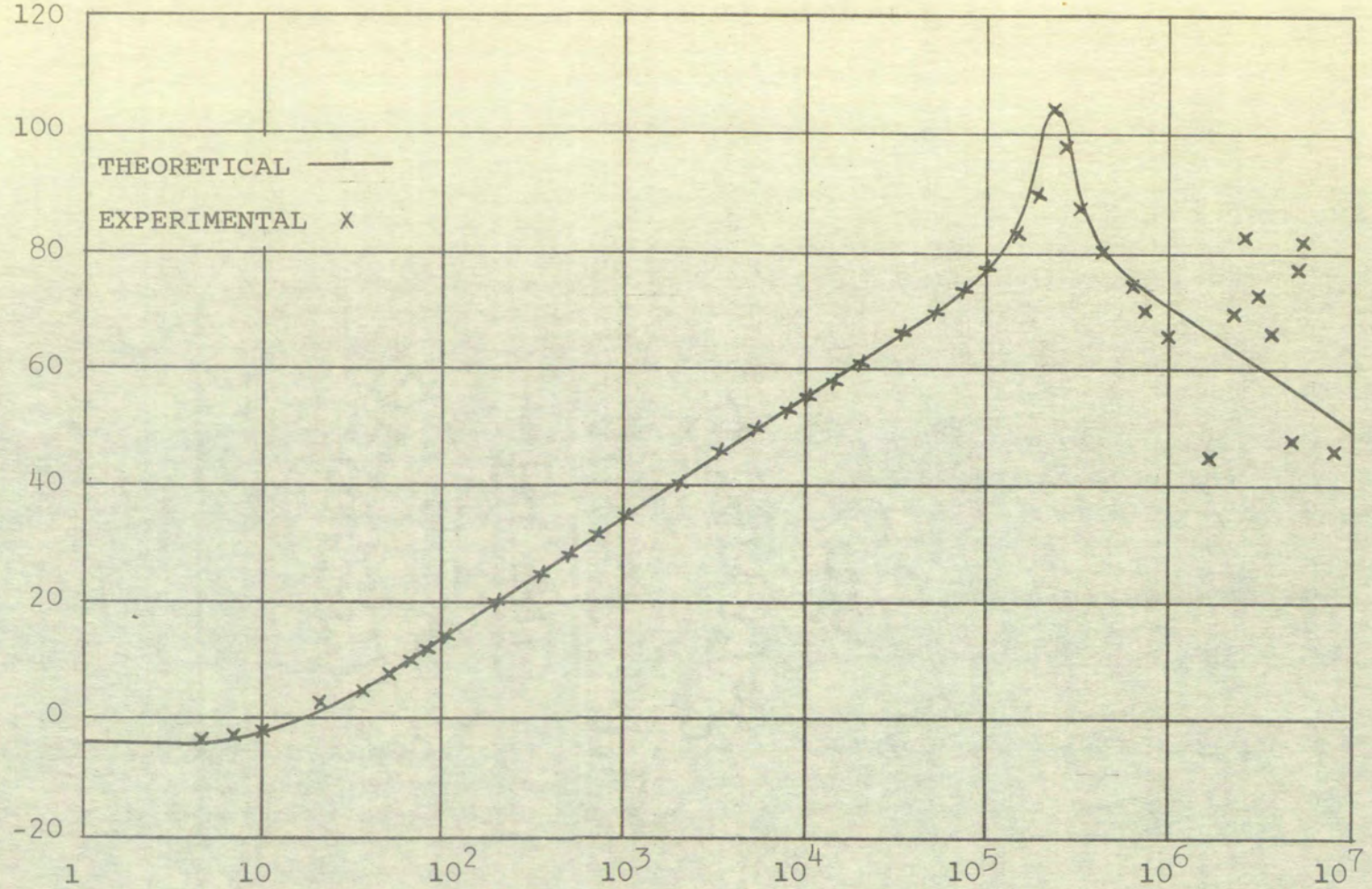

FIGURE 25

$|Z_{11}(j2\pi f)|$ VERSUS FREQUENCY

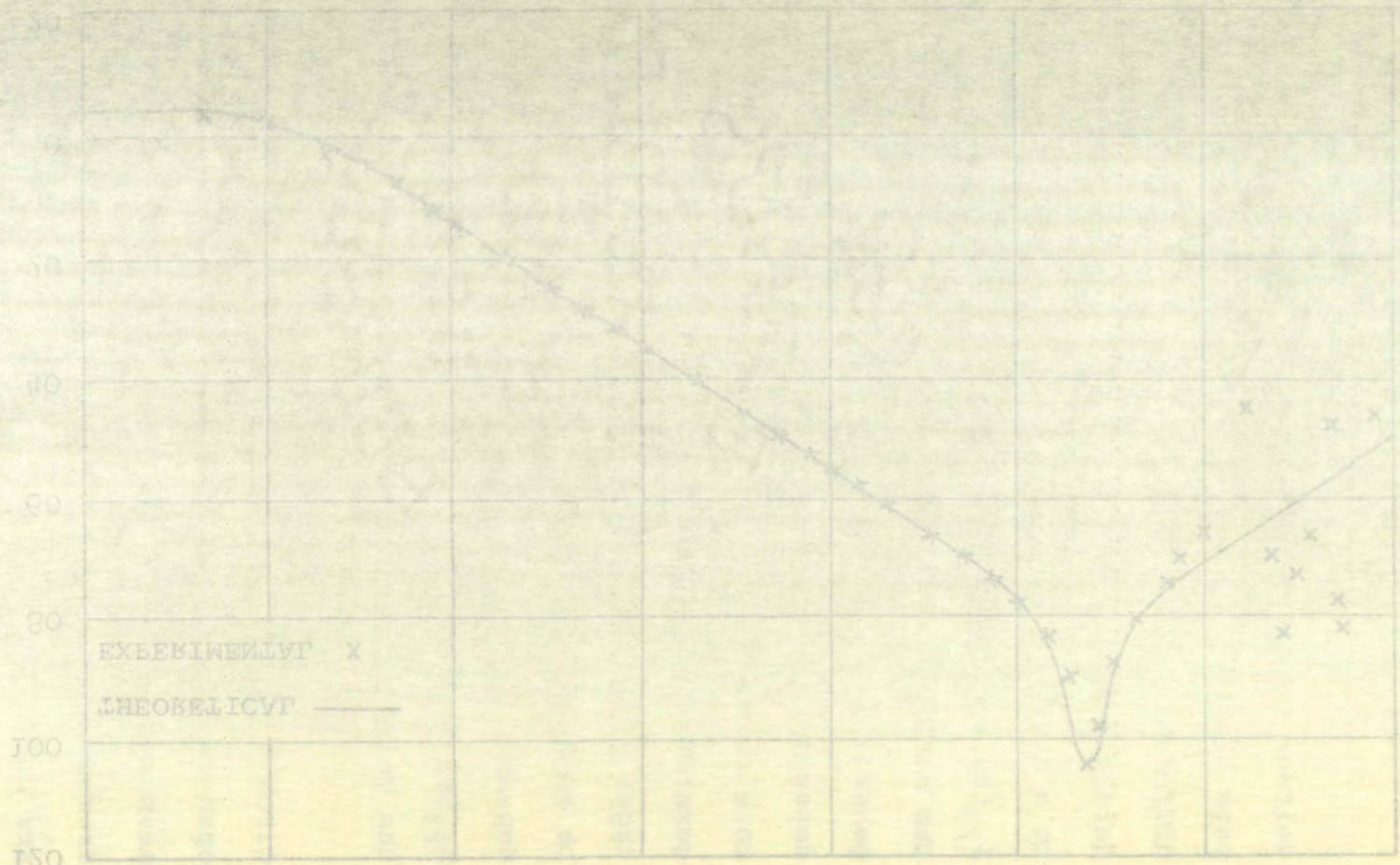
EXPERIMENTAL x
THEORETICAL ———

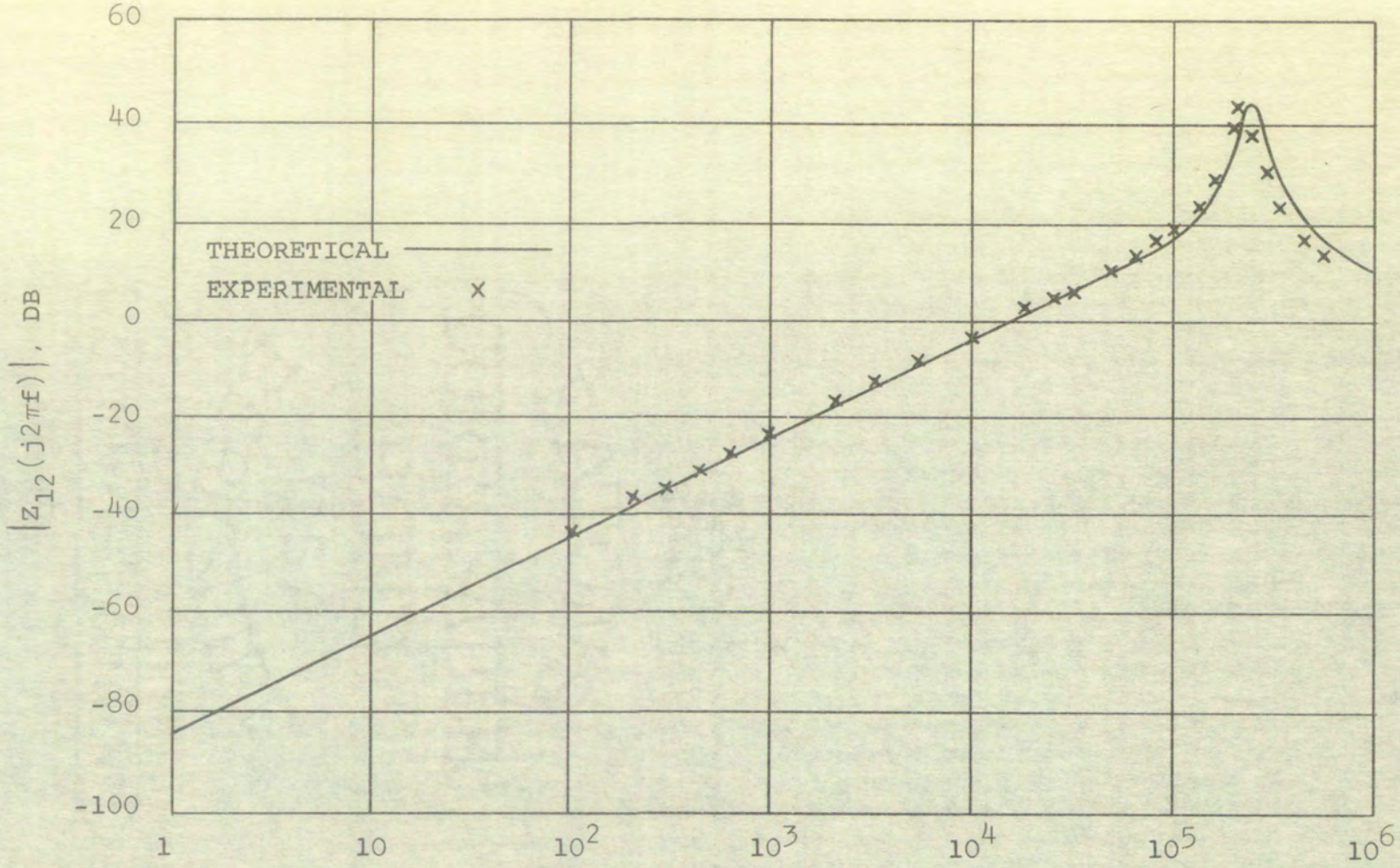

FIGURE 26

$|Z_{12}(j2\pi f)|$ VERSUS FREQUENCY

EXPERIMENTAL
THEORETICAL
60
50

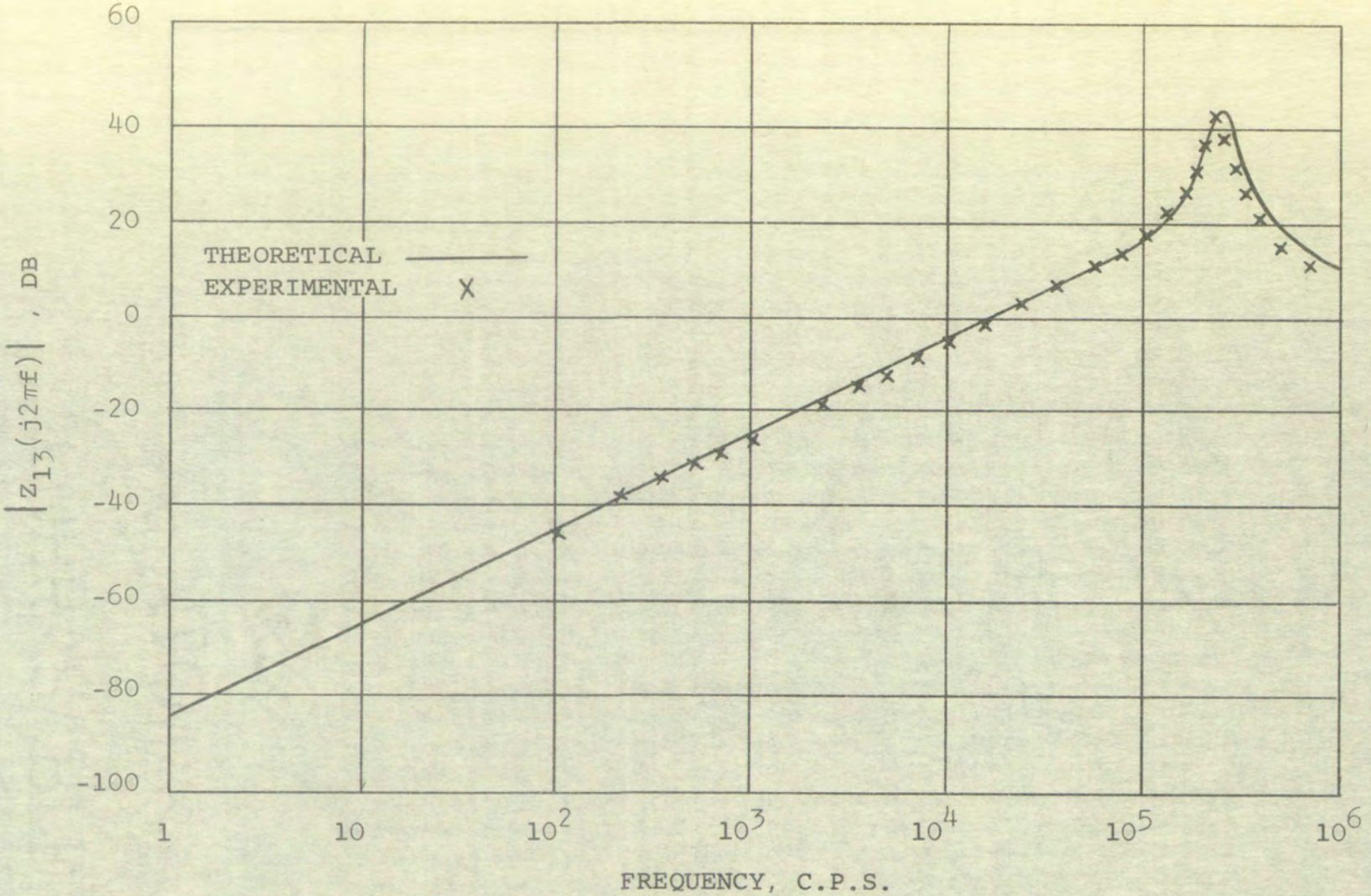

FIGURE 27

$|Z_{13}(j2\pi f)|$ VERSUS FREQUENCY

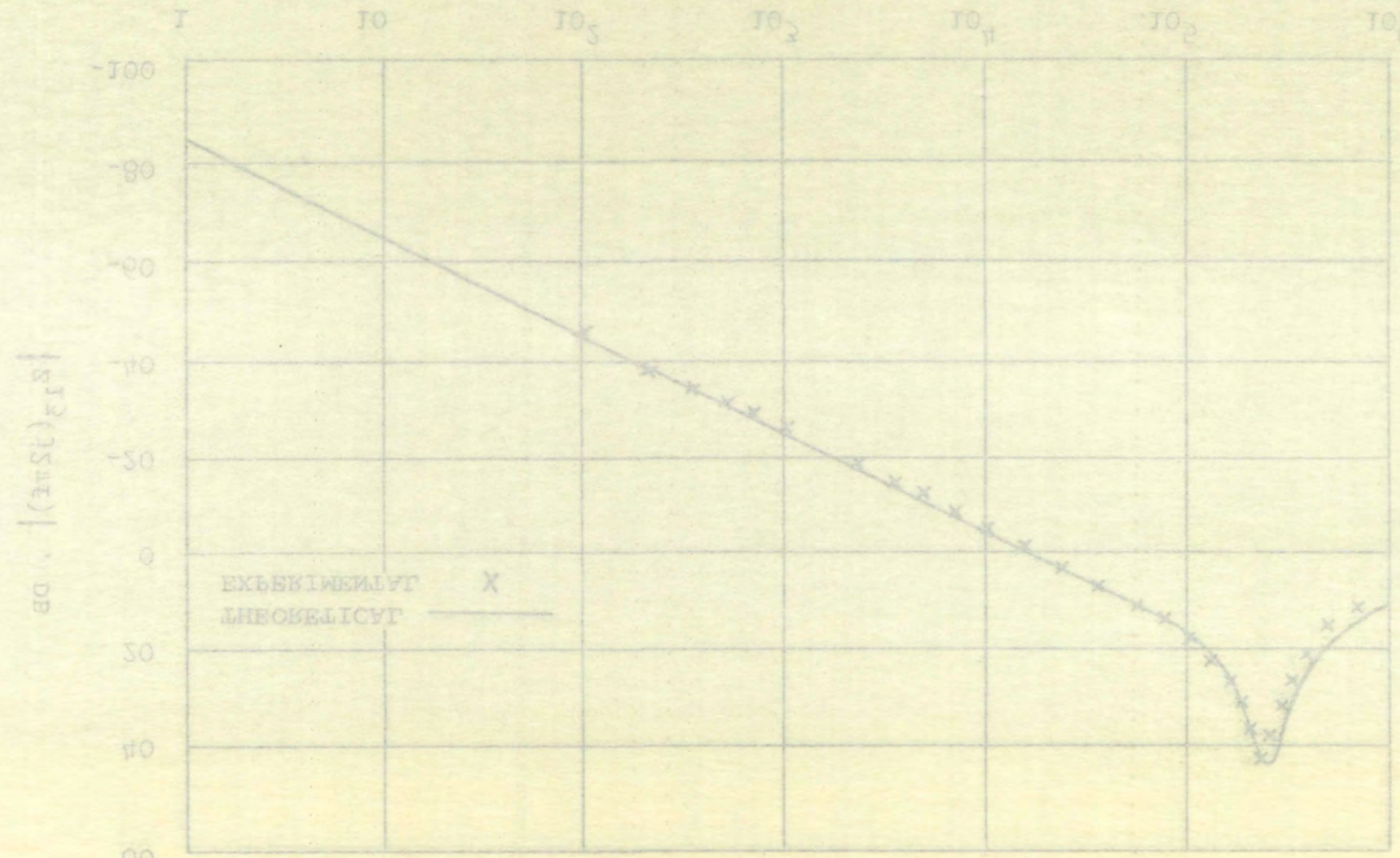
EXPERIMENTAL X
THEORETICAL

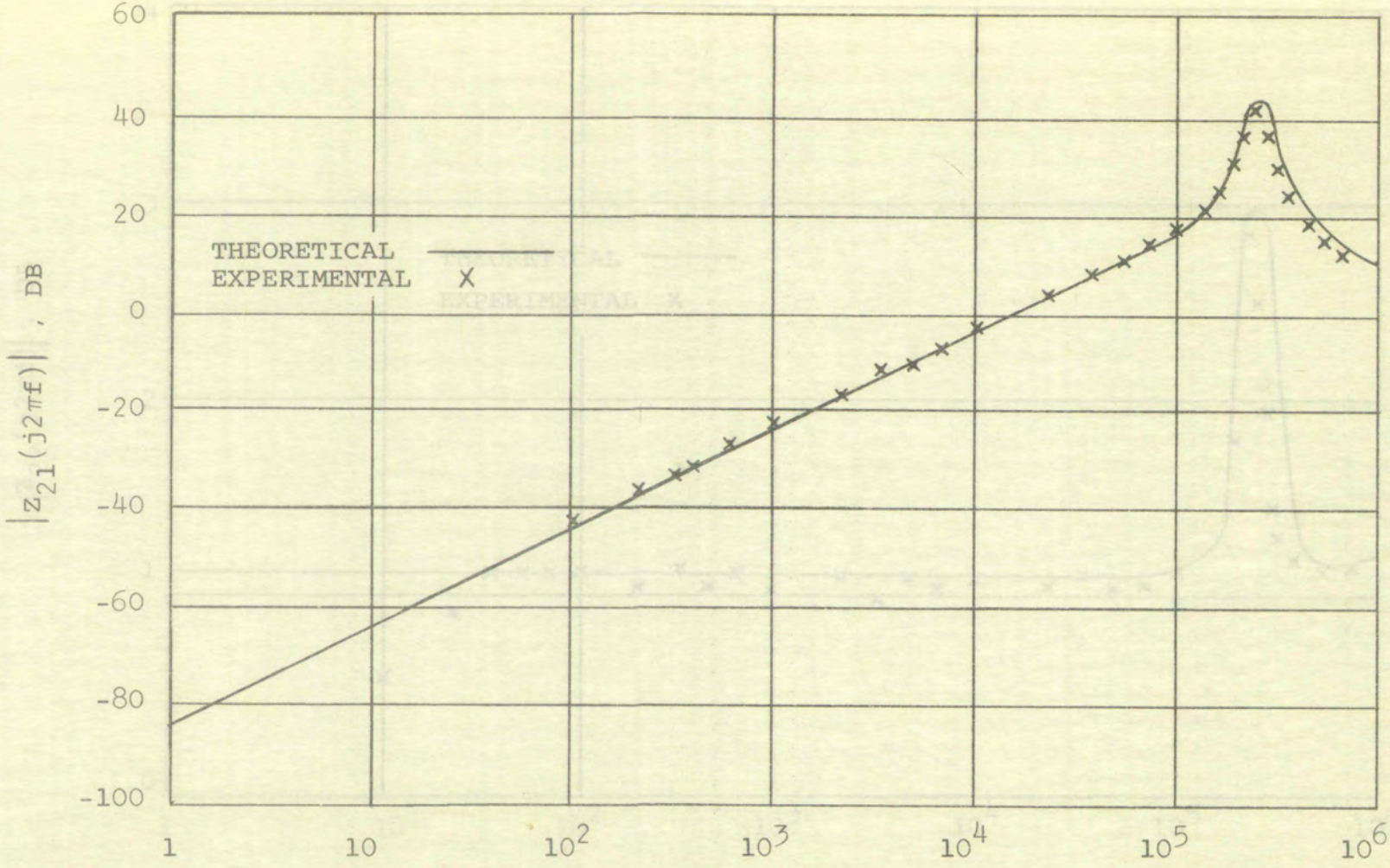

FIGURE 28

$|Z_{21}(j2\pi f)|$ VERSUS FREQUENCY

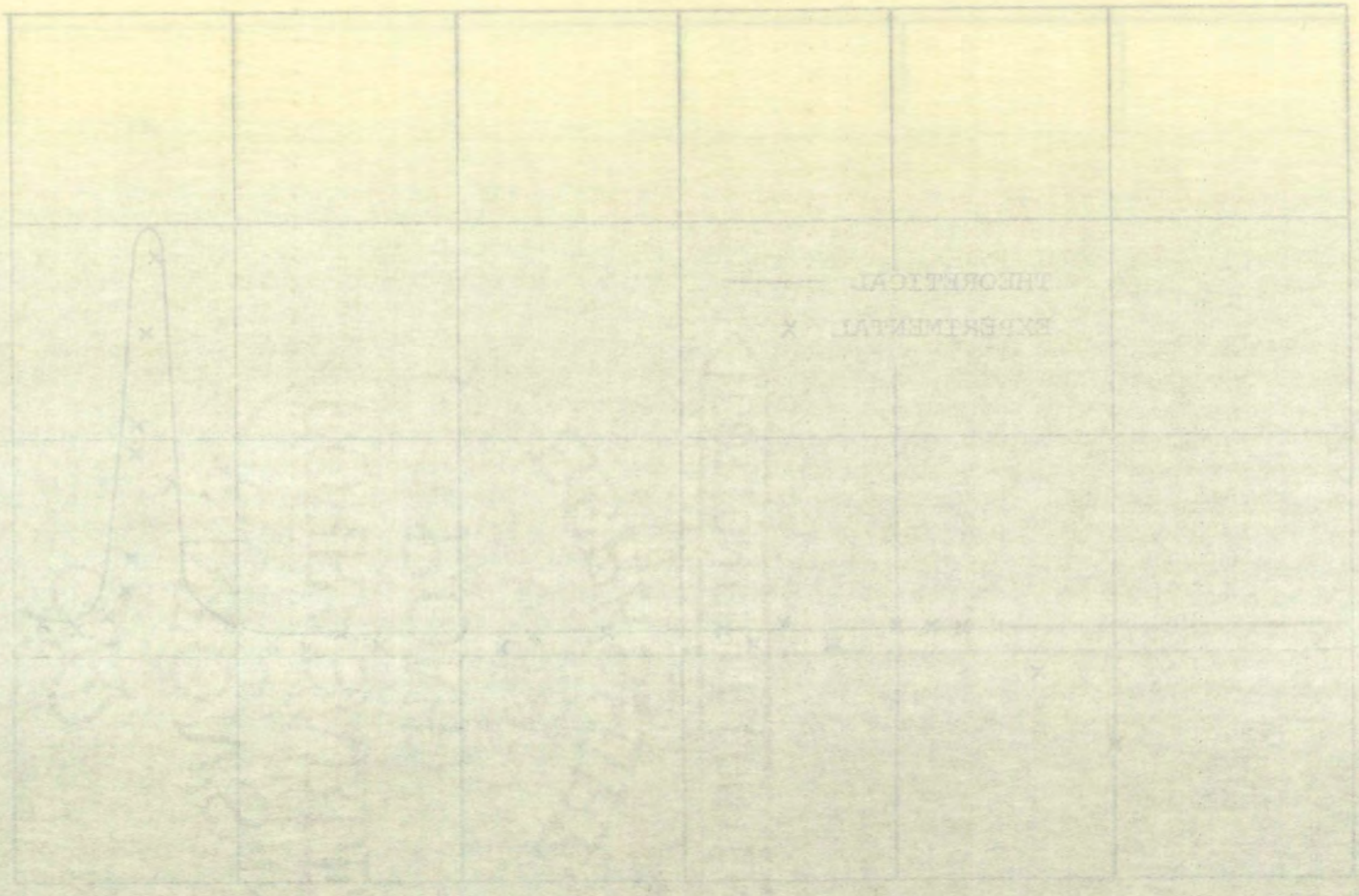

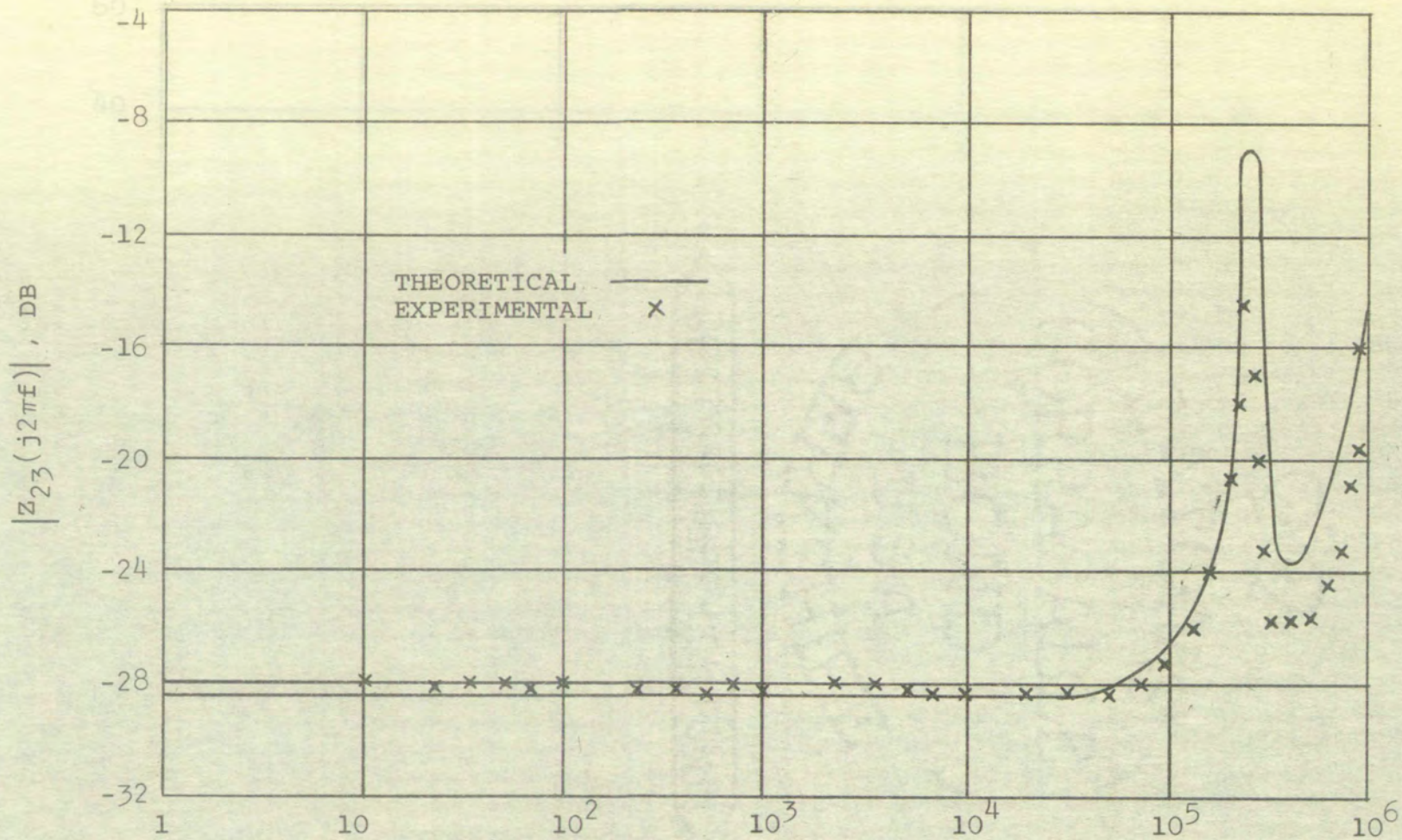

FIGURE 30

$|Z_{23}(j2\pi f)|$ VERSUS FREQUENCY

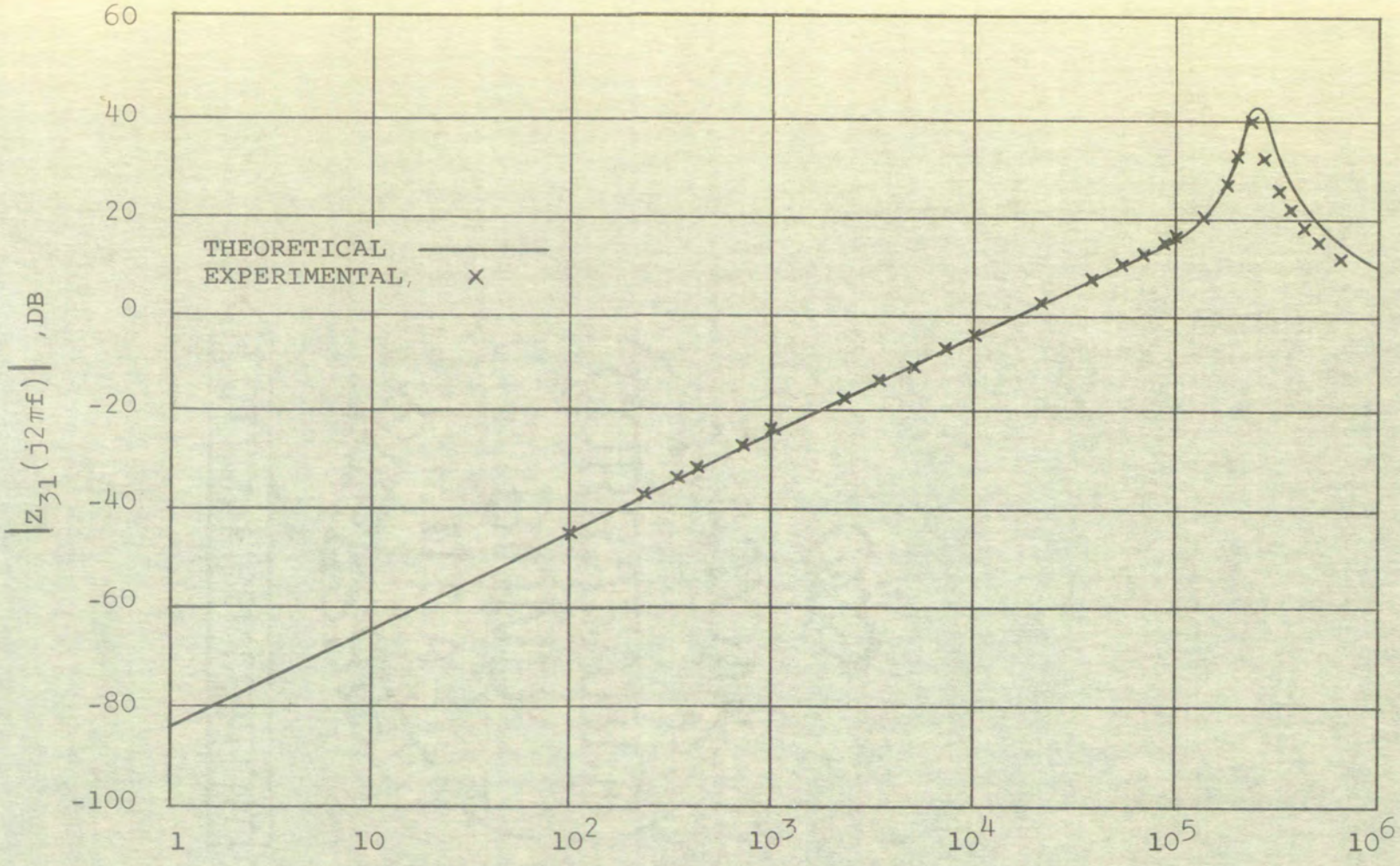

FIGURE 31

$|Z_{31}(j2\pi f)|$ VERSUS FREQUENCY

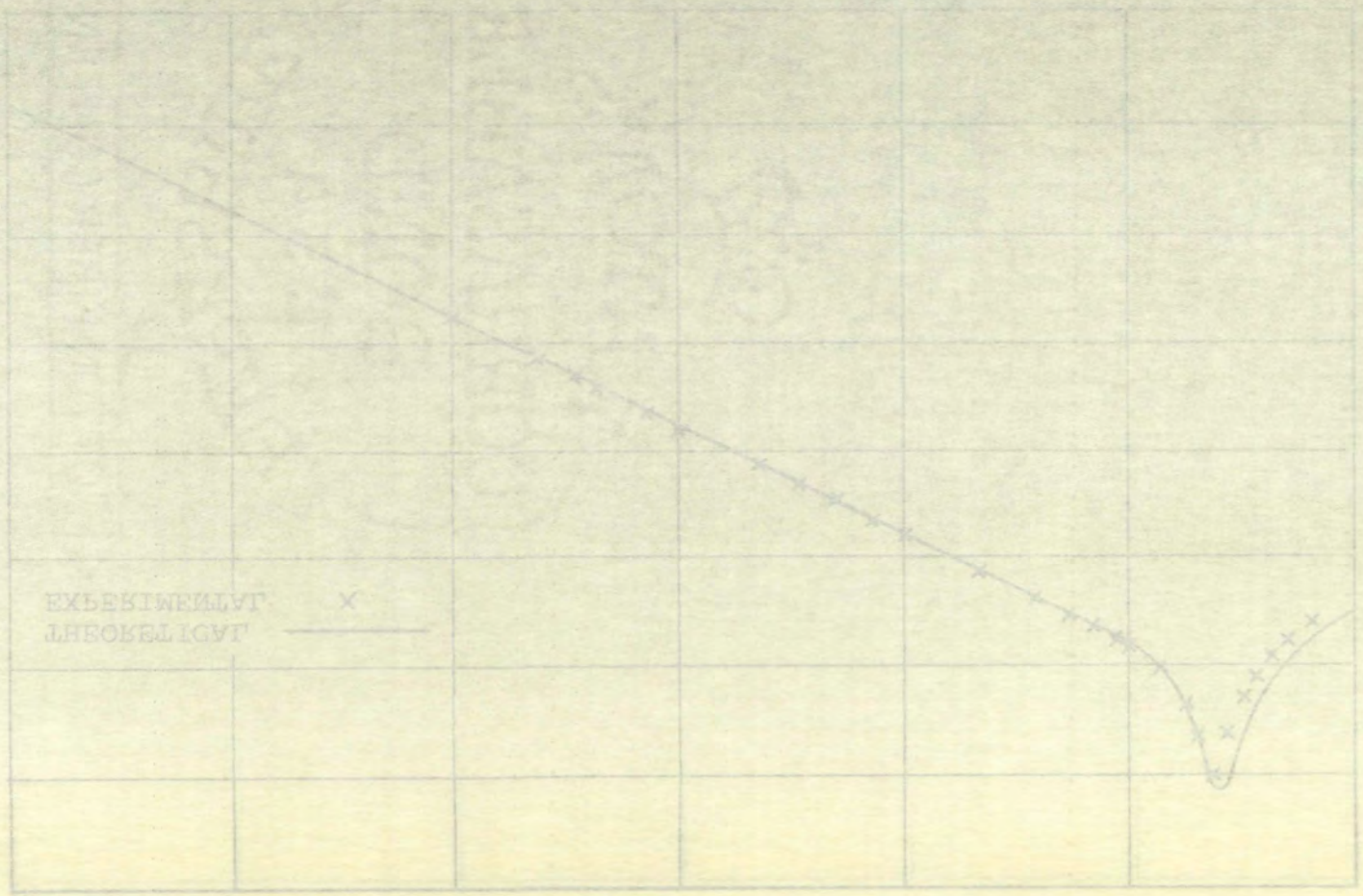
EXPERIMENTAL
THEORETICAL

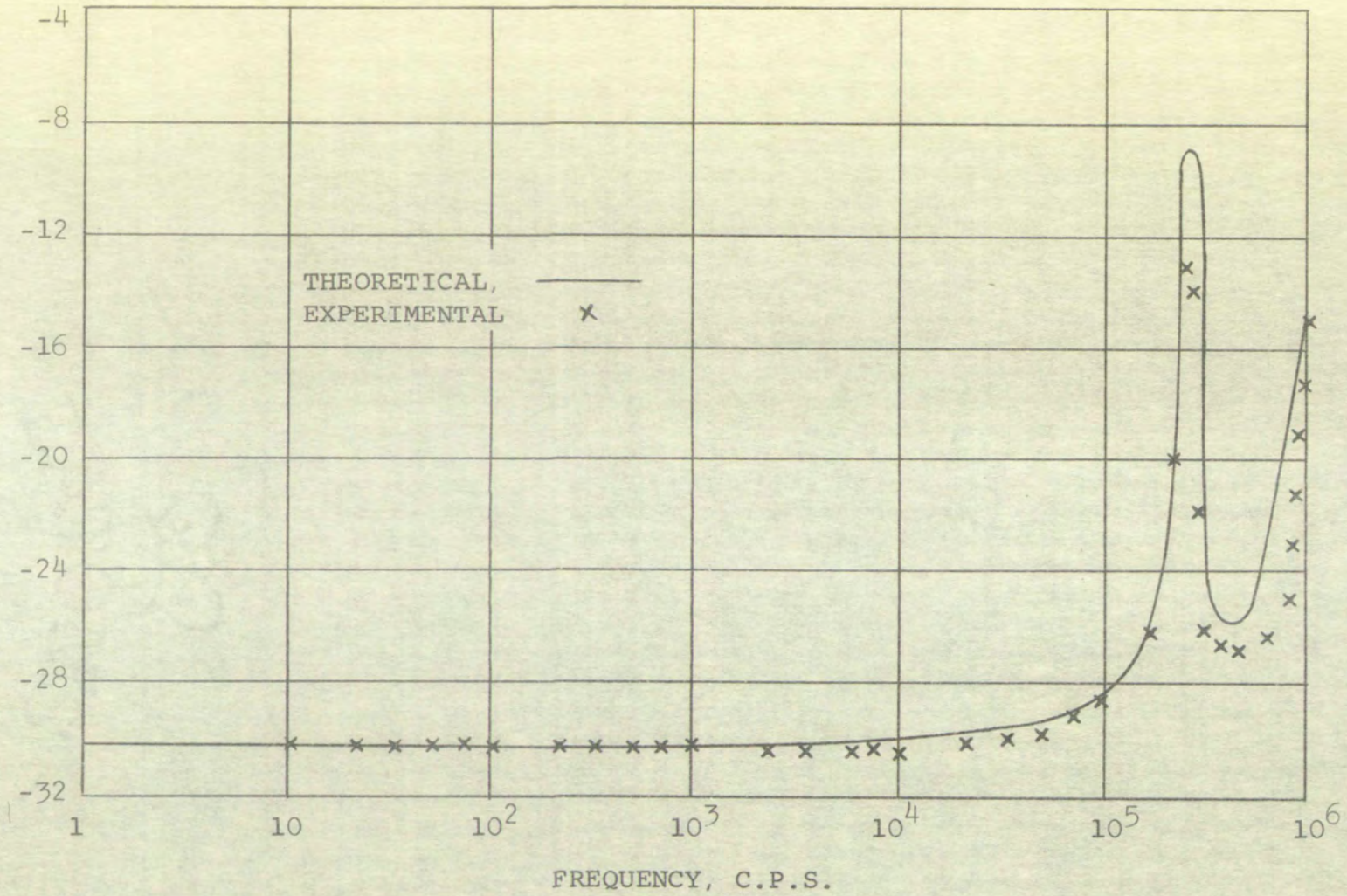

FIGURE 32

$|Z_{32}(j2\pi f)|$ VERSUS FREQUENCY

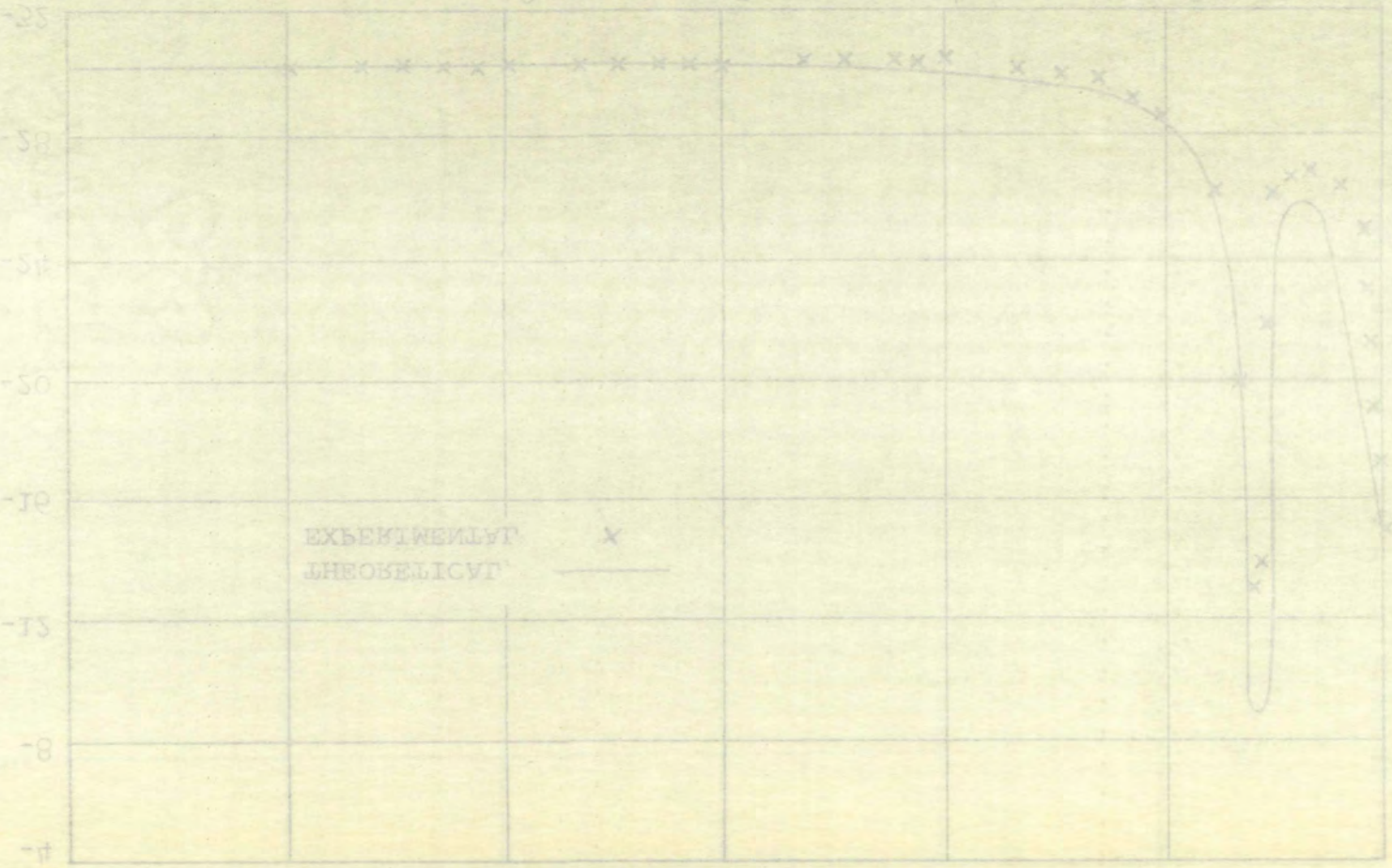
EXPERIMENTAL
THEORETICAL

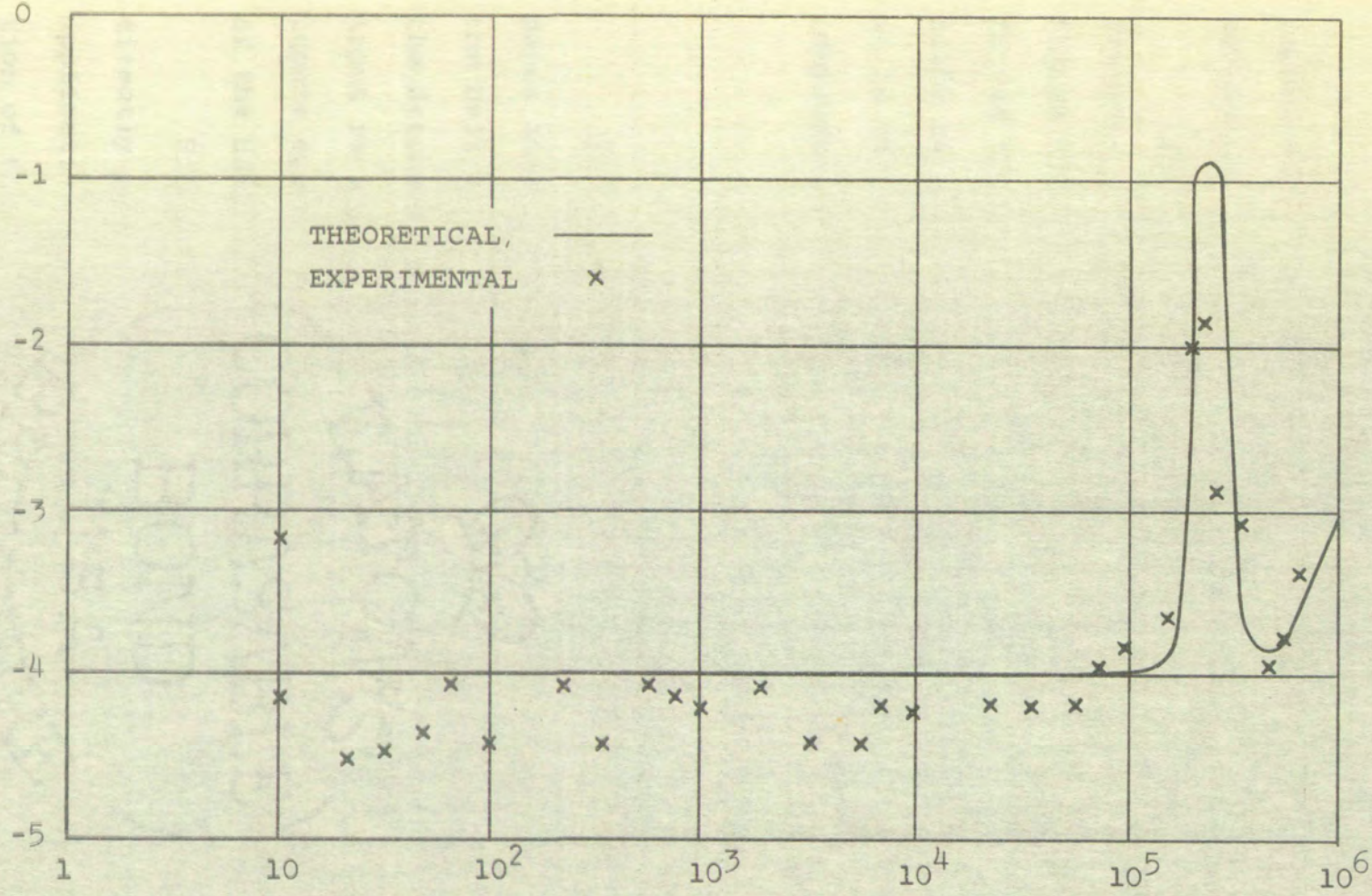

FIGURE 33

$|Z_{33}(j\pi f)|$ VERSUS FREQUENCY

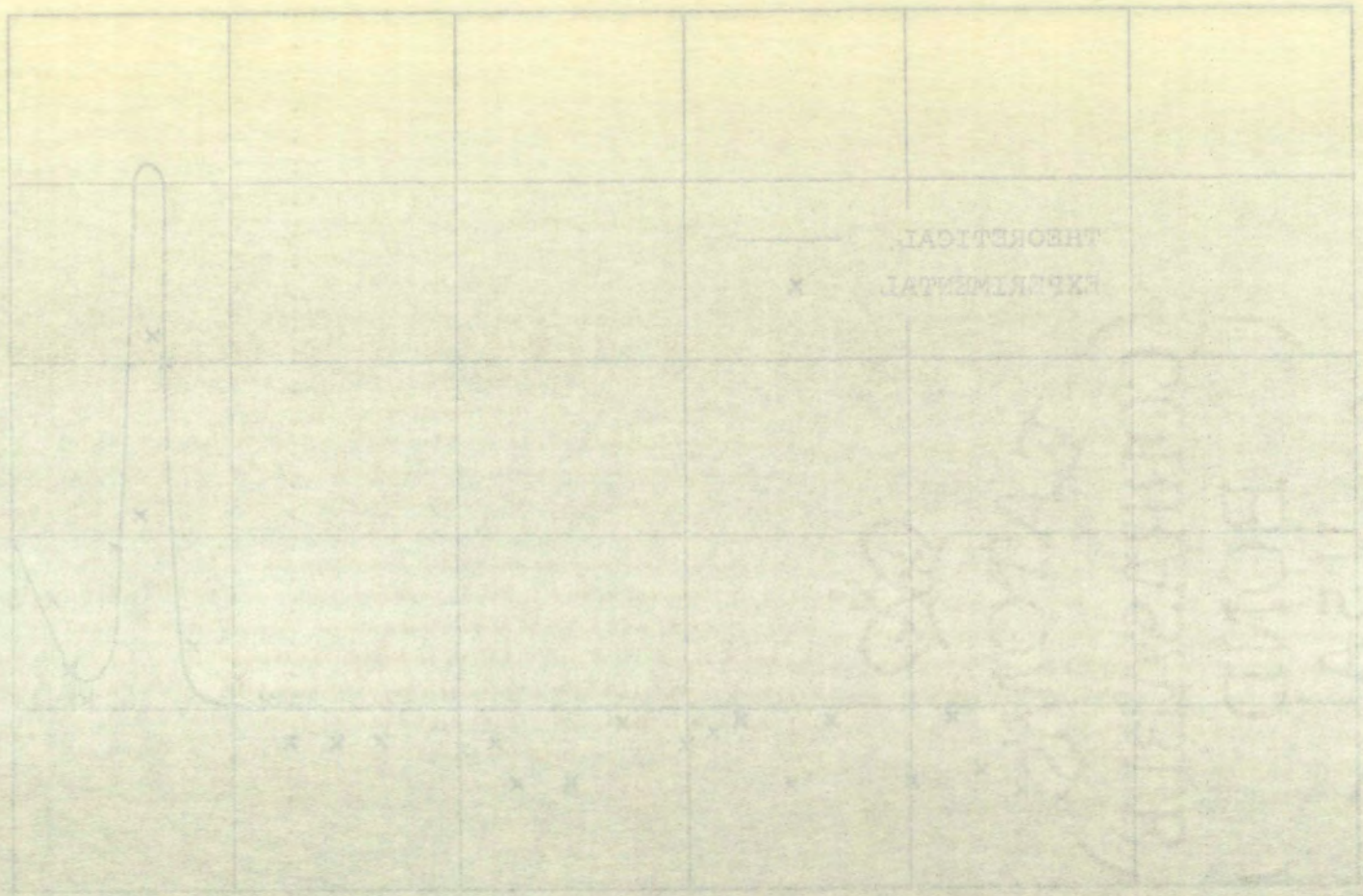

impedances agree very well with the open-circuit impedances determined theoretically from the equivalent circuit.

The open-circuit impedances were also measured at frequencies above one megacycle. As can be seen from Figure 25, the results predicted by the equivalent circuit failed to agree with experiment. The equivalent circuit could be modified to account for this discrepancy; however, it is believed that the equivalent circuit would be too complicated to be of any practical value.

II. EXTENSION OF THE OPEN-CIRCUIT IMPEDANCE APPROACH

It has been mentioned that the open-circuit impedance analysis fails to place in evidence the effects of the Hall voltage generators. This is primarily because in the determination of the open-circuit impedances only one input is applied to the system at a time. Therefore, two inputs must be applied to the system to observe the effects of the Hall voltage generators.

Since the output of the Hall voltage generators is directly proportional to the product of two currents, the application of arbitrary inputs complicates the determination of the resulting output. To avoid this difficulty the inputs were restricted to a d.c. signal and an a.c. signal.

impedances agree very well with the open-circuit impedances determined theoretically from the equivalent circuit.

The open-circuit impedances were also measured at frequencies above one megacycle. As can be seen from Figure 25, the results predicted by the equivalent circuit failed to agree with experiment. The equivalent circuit could be modified to account for this discrepancy; however, it is believed that the equivalent circuit would be too complicated to be of any practical value.

II. EXTENSION OF THE OPEN-CIRCUIT IMPEDANCE APPROACH

It has been mentioned that the open-circuit impedance analysis fails to place in evidence the effects of the Hall voltage generators. This is primarily because in the determination of the open-circuit impedances only one input is applied to the system at a time. Therefore, two inputs must be applied to the system to observe the effects of the Hall voltage generators.

Since the output of the Hall voltage generators is directly proportional to the product of two currents, the application of arbitrary inputs complicates the determination of the resulting output. To avoid this difficulty the inputs were restricted to a d.c. signal and an a.c. signal.

A d.c. voltage was applied to terminals 2-2' of the experimental model, and an a.c. voltage was applied to terminals 1-1'. The open-circuit voltage resulting at terminals 3-3' was then measured as a function of frequency. The results obtained by this procedure were then compared with the response predicted by the equivalent circuit. As may be seen from Figure 34, the response predicted from the equivalent circuit agrees very well with the response obtained experimentally.

A d.c. voltage was then applied to terminals 2-2', and an a.c. voltage was applied to terminals 1-1'. The open-circuit voltage obtained at terminals 3-3' was experimentally found to be independent of frequency. This result is also predicted by the equivalent circuit.

Therefore, it is believed that the results obtained from the open-circuit impedance approach indicate that the equivalent circuit represents the operation of the physical system under sinusoidal steady-state conditions below one megacycle.

III. TRANSIENT ANALYSIS

Since the equivalent circuit fails to predict the behavior of the system for frequencies above one megacycle, the ability of the equivalent circuit to predict transient

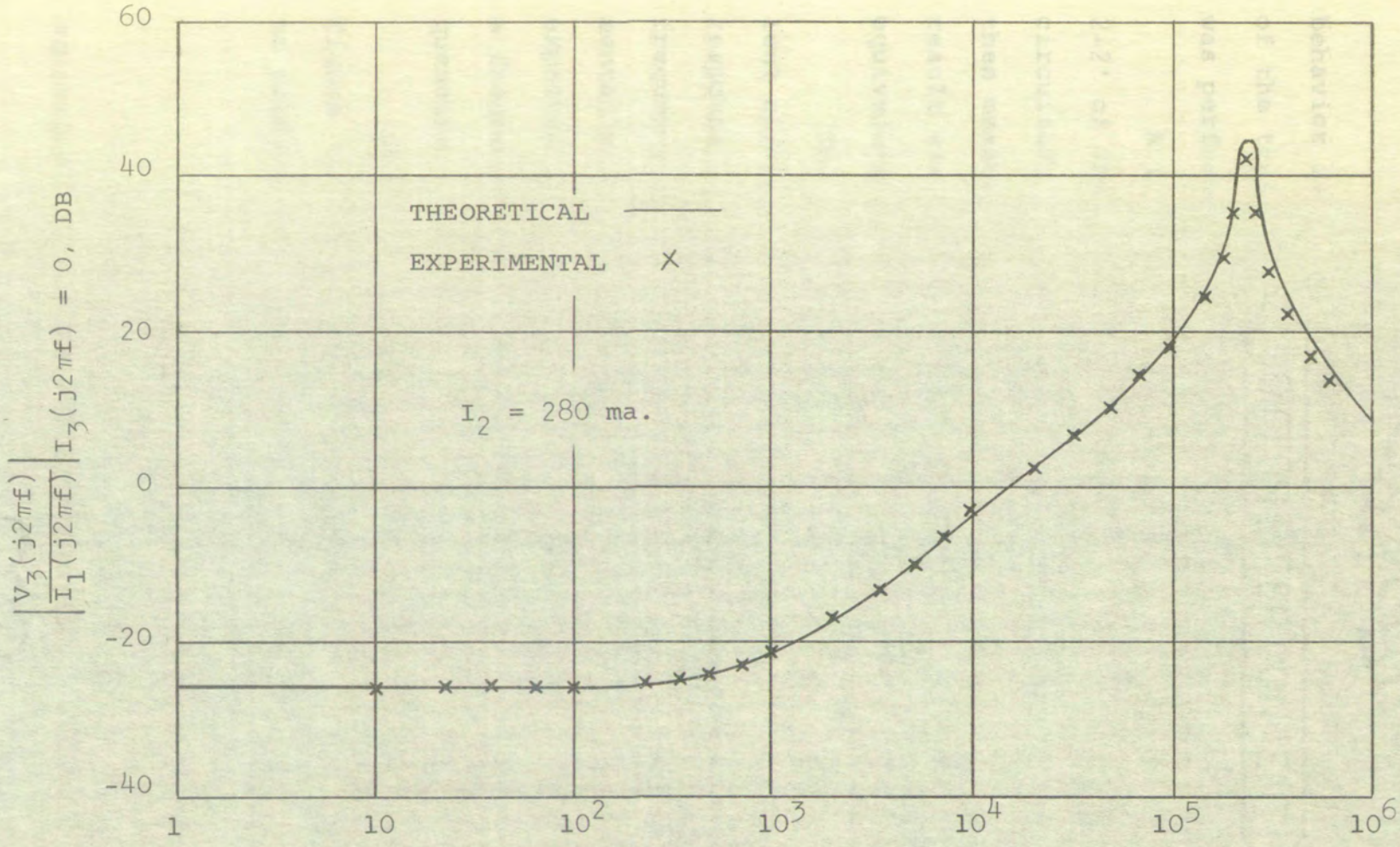

FIGURE 34

$\left|\frac{V_3(j2\pi f)}{I_1(j2\pi f)}\right| I_3(j2\pi f) = 0$ VERSUS FREQUENCY

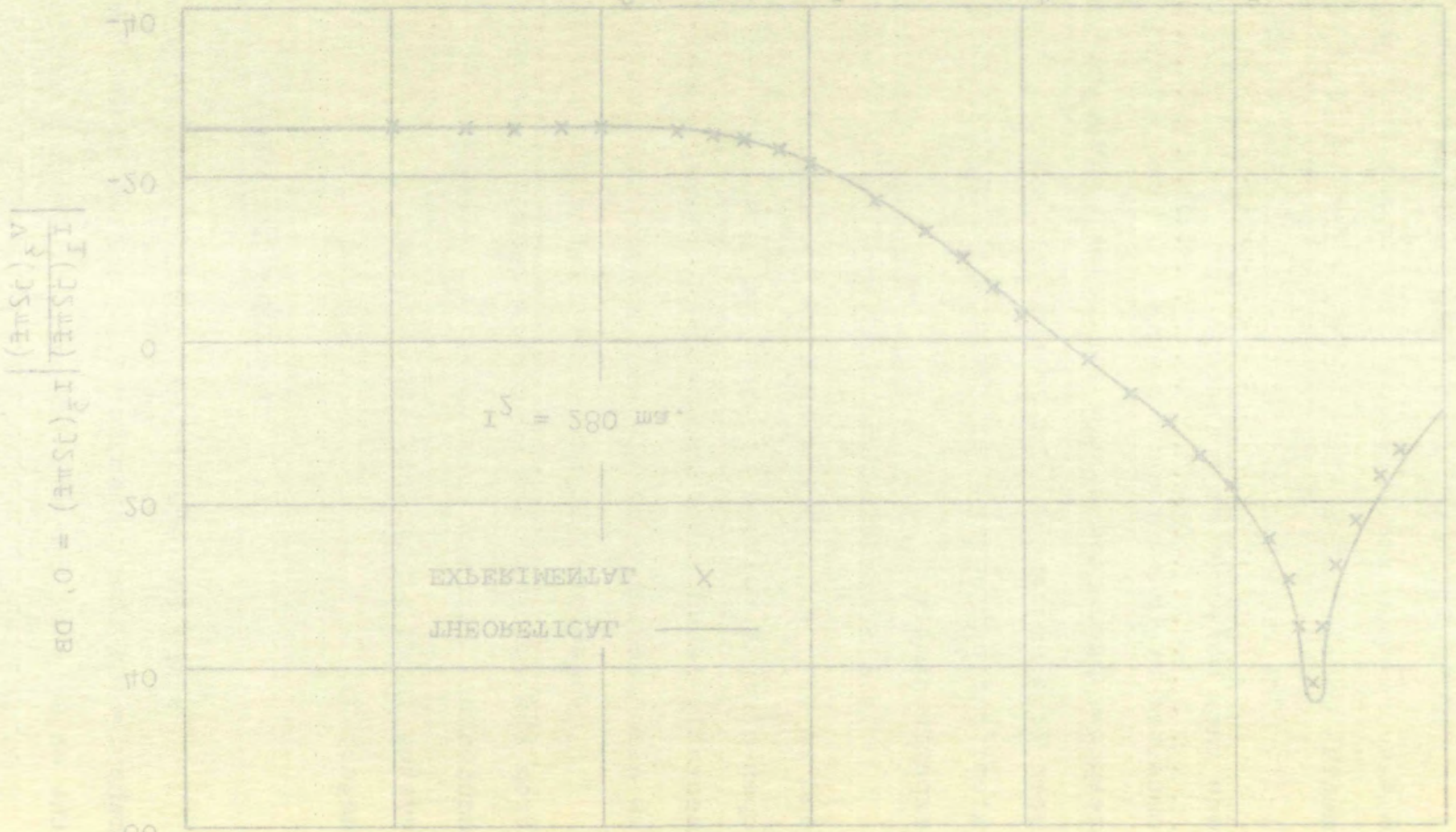
1
10
10^2
10^3
10^4
10^5
10^6
-40
-50
0
50
40
60
$L^2 = 580$ mH.
EXPERIMENTAL X
THEORETICAL ——
FREQUENCY C.P.S.

behavior is somewhat doubtful. To obtain some indication of the transient behavior of the system the following test was performed.

A unit step of current was supplied to terminals 2-2' of the system with terminals 1-1' and 3-3' open-circuited. The voltage resulting at terminals 1-1' was then measured with a Tektronix 545 oscilloscope. This result was then compared with the response predicted by the equivalent circuit. The results are shown in Figure 35.

The response obtained theoretically from the equivalent circuit agrees very well with the experimental response. The only significant difference is the high frequency low amplitude components present in the experimentally determined response. This difference is to be expected since the open-circuit impedance $Z_{12}(j\omega)$ possesses a frequency response containing a number of resonant frequencies above one megacycle.

Thus, it is believed that the results shown on Figure 35 indicate that the equivalent circuit may be used to predict the transient behavior of the system.

IV. NONLINEAR PHENOMENA

It should be noted that the application of the equivalent circuit may involve nonlinear differential

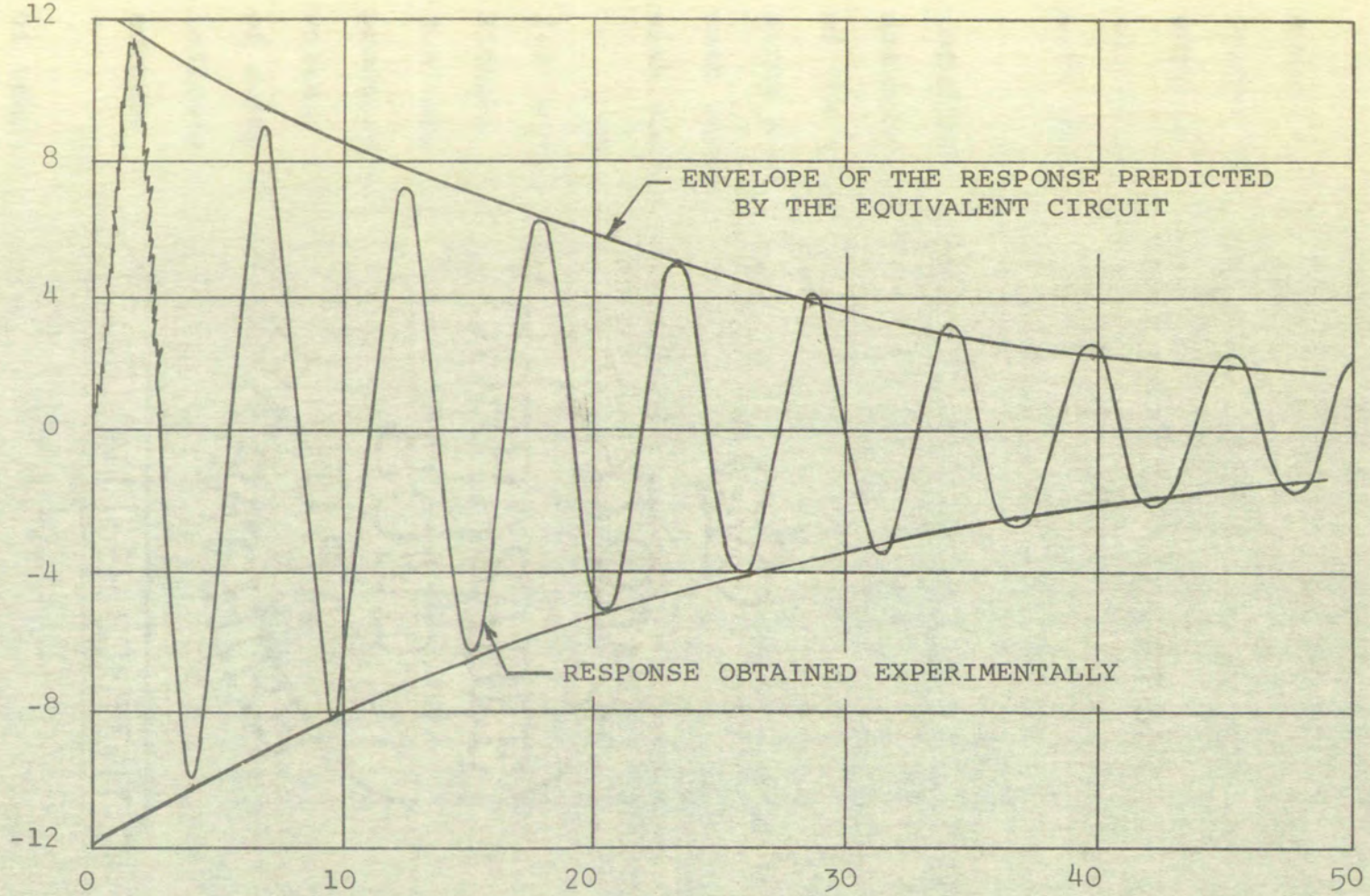

FIGURE 35

$V_1(t)$ VERSUS t

RESPONSE OBTAINED EXPERIMENTALLY
ENVELOPE OF THE RESPONSE PREDICTED BY THE EQUIVALENT CIRCUIT
-12
-8
-4
0
4
8
12
0
10
30
50
70
90

equations. The presence of the Hall voltage generators causes the nonlinearities. There are also nonlinear effects which are not evident from an inspection of the equivalent circuit. The following discussion is concerned with these nonlinearities.

In the development of the mutual inductance, self inductance, and Hall voltage generator parameters it was assumed that the magnetic flux density is a linear function of the magnetic field intensity. This is not entirely true since a magnetic material is used in the system. To obtain some indication of the variation of magnetic flux density with current in loop one the following test was performed.

A d.c. current was applied to terminals 1-1' and 2-2' with terminals 3-3' open-circuited. Under these conditions the open-circuit voltage resulting at terminals 3-3' was directly proportional to the magnetic flux density produced by the current in loop one. The open-circuit voltage of terminals 3-3' was then measured as a function of current in loop one. The results shown in Figure 36 indicate that the flux density starts to saturate when the current in loop one exceeds one ampere.

The conductivity of the semiconductor is a function of temperature and magnetic flux density. Since the conductivity of the semiconductor is involved in the parameters

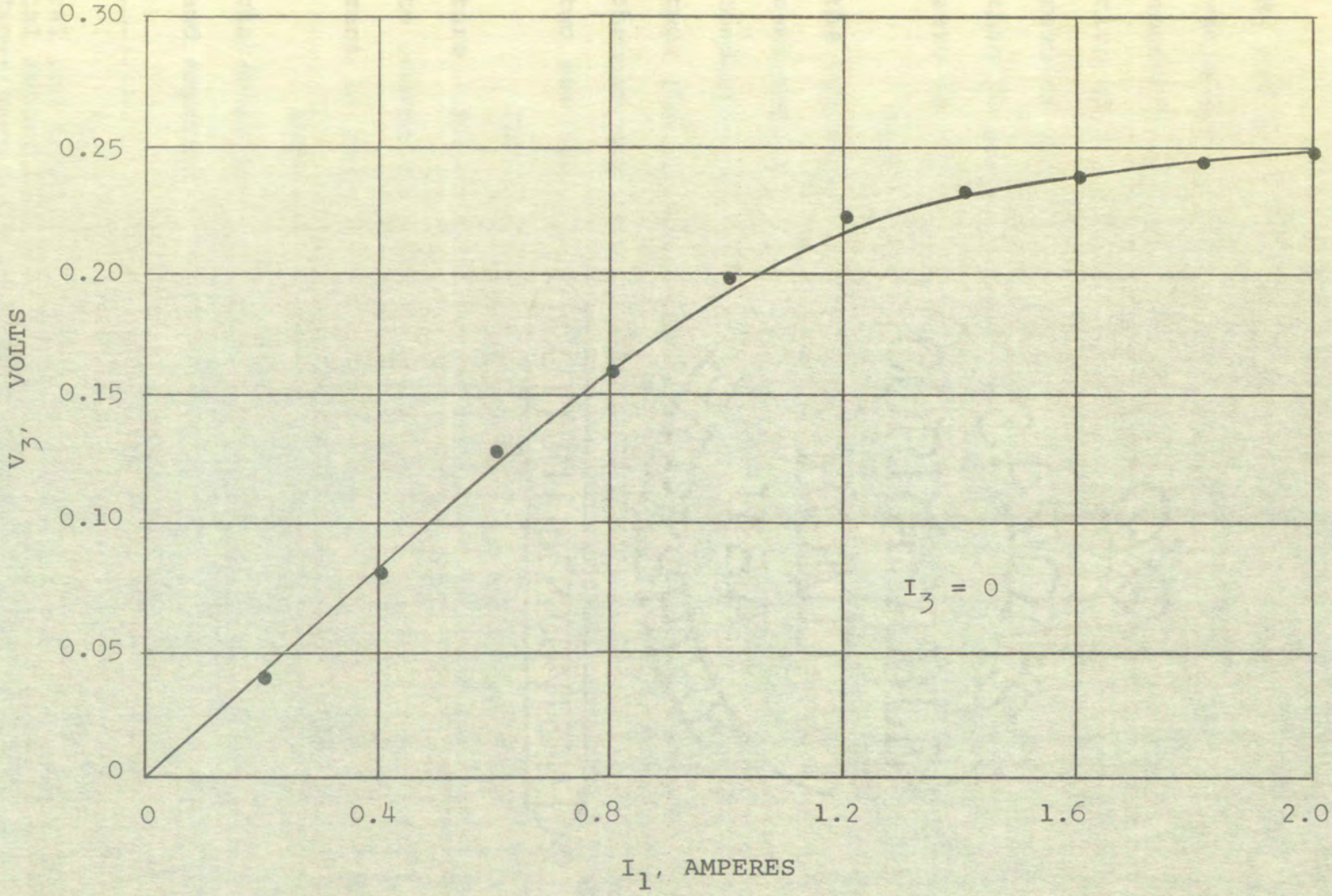

FIGURE 36

V_3 VERSUS I_1

R_2 and R_3, nonlinear effects may occur. To illustrate the variation of conductivity with magnetic flux density the conductivity of the semiconductor was measured as a function of current in loop one. As may be seen from the results shown on Figure 37, the conductivity changed less than 20 per cent as the current in loop one was varied from zero to two amperes.

Since the conductivity is a function of temperature, the current in loops two and three may cause heating of the semiconductor and hence a change in conductivity. The conductivity was measured as a function of current in loop two; the results are shown in Figure 38. The conductivity changed approximately 25 percent as the current in loop two was varied from zero to one ampere.

The Hall constant, R, is also a function of temperature. Since the Hall constant is inversely proportional to conductivity, the variation of Hall constant with current in loop two may be obtained from Figure 38.[1]

Some of the more important aspects of the nonlinear characteristics of the physical system have been discussed and experimentally investigated. It should be emphasized

---

[1]David L. Endsley and W.W. Grannemann, "A Theroetical and Experimental Analysis of a Hall Generator" (Technical Report EE-27, the University of New Mexico Engineering Experiment Station, Albuquerque, 1959), p. 19.

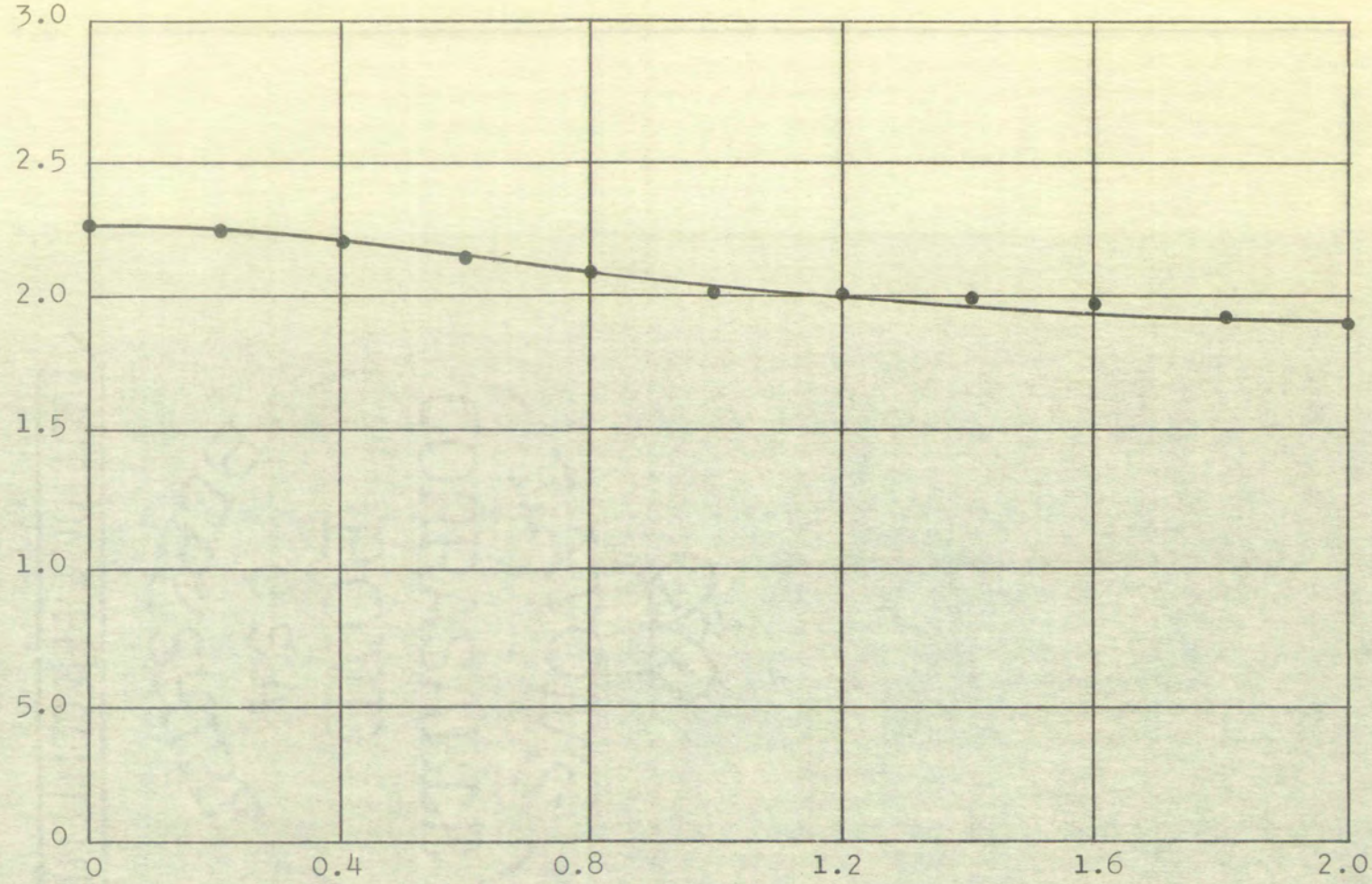

FIGURE 37

$\sigma \times 10^{-4}$ VERSUS I_1

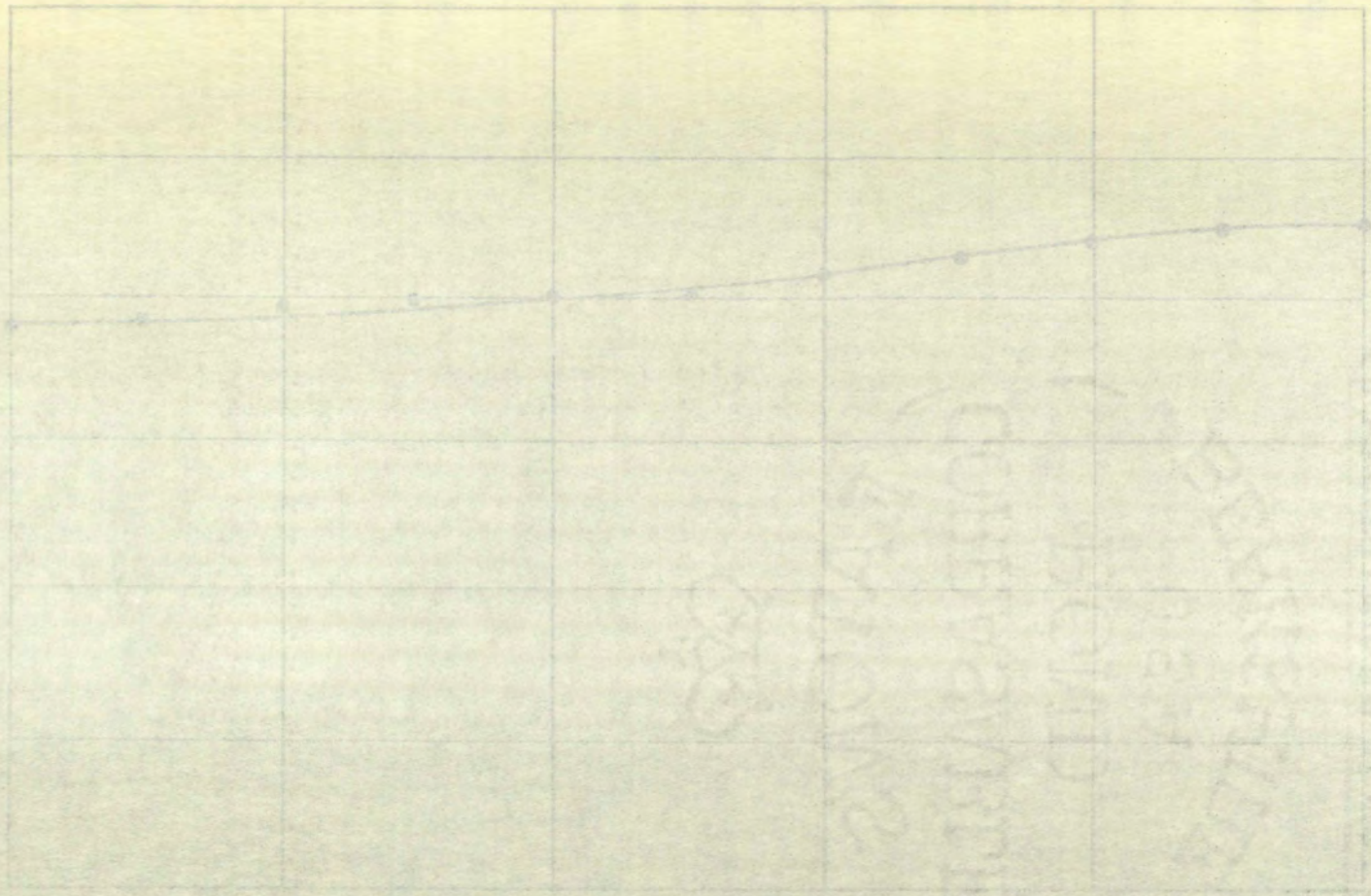

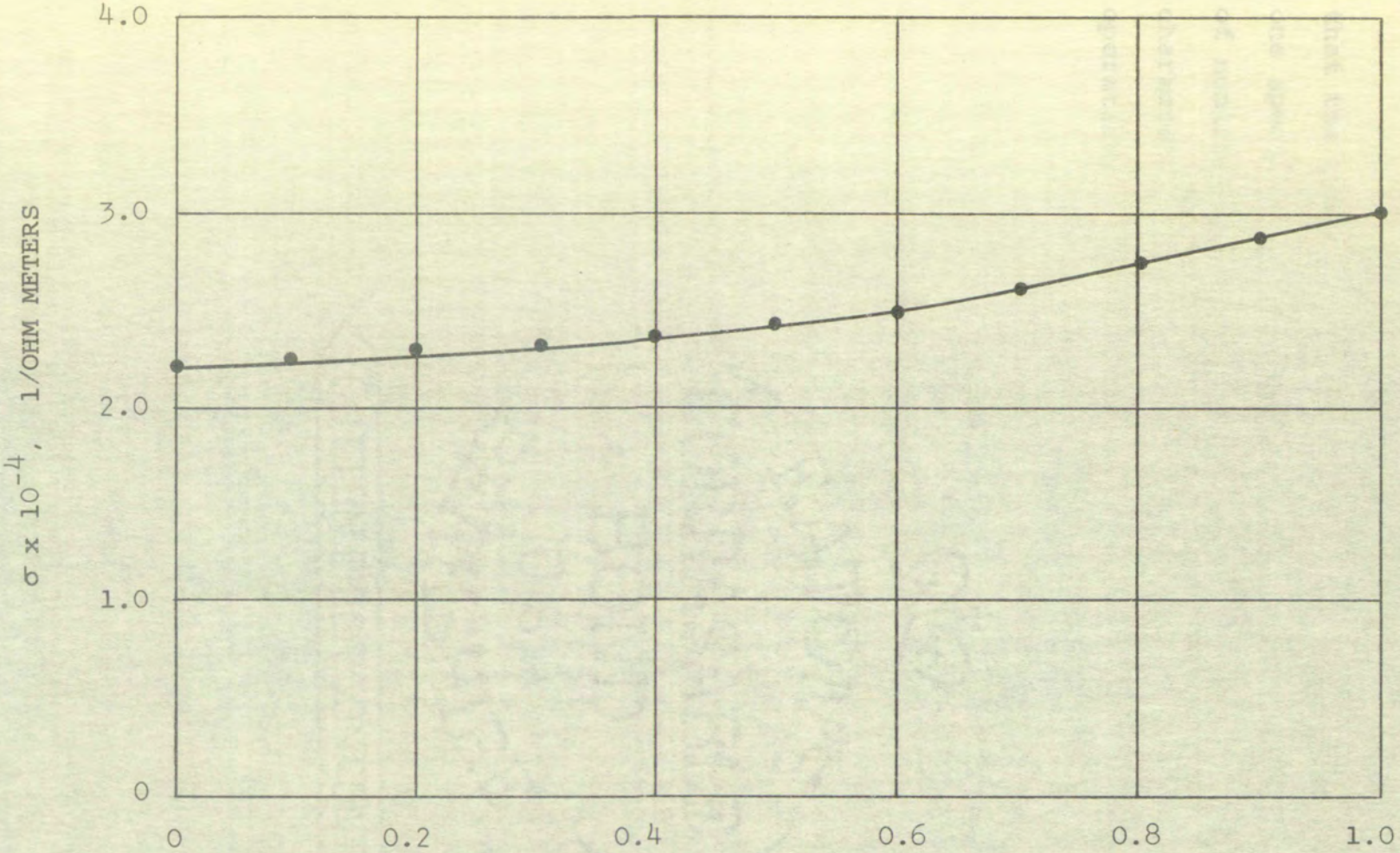

FIGURE 38

$\sigma \times 10^{-4}$ VERSUS I_2

that the results obtained experimentally are valid for only one specific model. The primary purpose of the discussion of nonlinear phenomena has been to highlight some of the characteristics which one should expect with large signal operation.

CHAPTER IV

SUMMARY AND CONCLUSIONS

I. SUMMARY

The development of high mobility semiconductors has made possible a number of new devices which utilize the Hall effect. Some of the more promising applications include clip-on ammeters, magnetic field meters, multipliers, modulators, amplifiers, impedance converters, and power meters. Many of the devices are only in an introductory state, and further study is required to determine their practical value.

The study of Hall effect devices involves a number of considerations. One must keep in mind the various impedances of the Hall generator as well as the Hall effect. The magnetic field must also be examined since it is involved in the Hall voltage equation. Furthermore, the various self and mutual inductances must be considered. An equivalent circuit based on the various dimensions and electrical characteristics of the system should prove to be useful in the analysis and design of devices which utilize the Hall effect.

Since a flux concentrator is used in many of the Hall effect devices, it was decided that its characteristics

should be included in the equivalent circuit. One of the more commonly used flux concentrators consists of a high permeability toroid. This particular flux concentrator was considered in the development of the equivalent circuit. An air gap was cut in the toroid, and the Hall generator was placed in the air gap. The leads of the Hall generator, for which the equivalent circuit was developed, formed closed loops within the air gap. This specific model is illustrated by Figure 8 which has been repeated and is shown on page 80. The results of this study may be readily extended to include situations in which other flux concentrators and other lead configurations are used.

An equivalent circuit of the system shown on Figure 8 has been developed. The result is indicated by Figure 13 which has been repeated and is shown on page 81. The parameters of the equivalent circuit involve both the dimensions and the electrical characteristics of the system. The various dimensions involved in the parameters of the equivalent circuit are indicated in Figure 8. The parameters of the equivalent circuit also involve several of the areas formed by the leads of the Hall generator. These various areas are illustrated by Figure 24 which has been repeated and is shown on page 82. The parameters of the equivalent circuit shown on Figure 13 are given by the

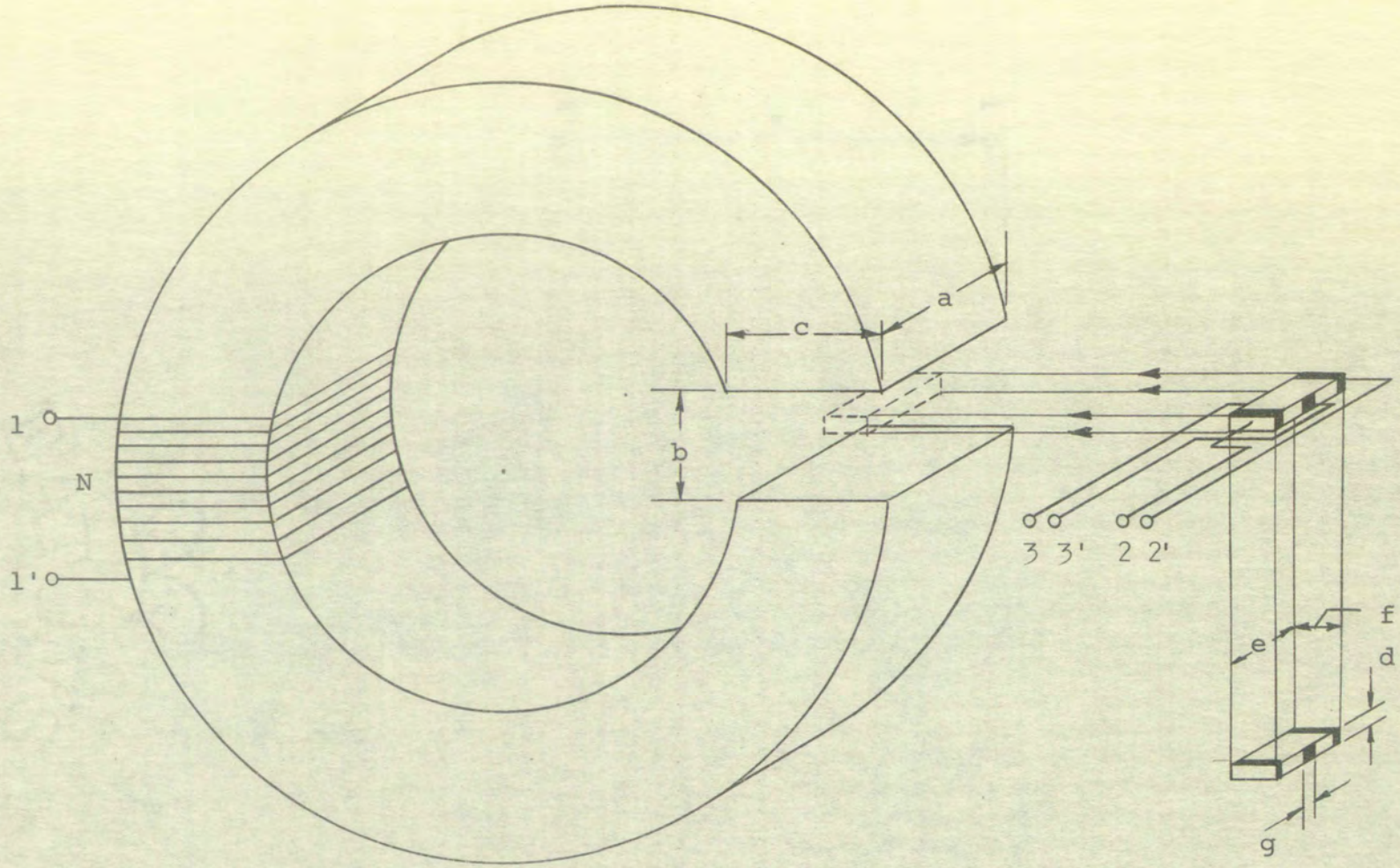

FIGURE 8 (REPEAT)

HALL GENERATOR AND FLUX CONCENTRATOR

Рисунок 8 (левый)

Half generator and flux concentrator

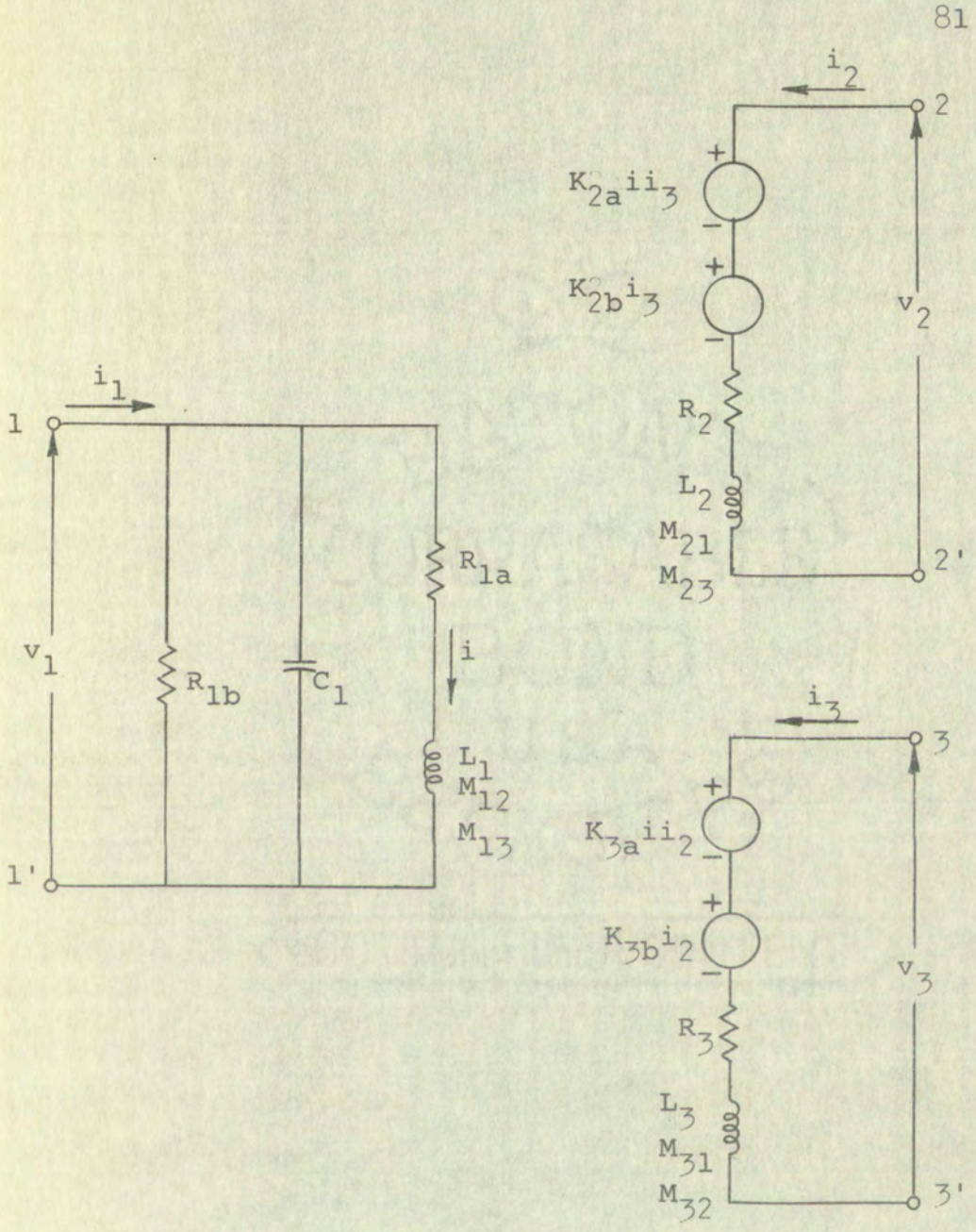

FIGURE 13 (REPEAT)

EQUIVALENT CIRCUIT OF A HALL GENERATOR
WHICH UTILIZES A FLUX CONCENTRATOR

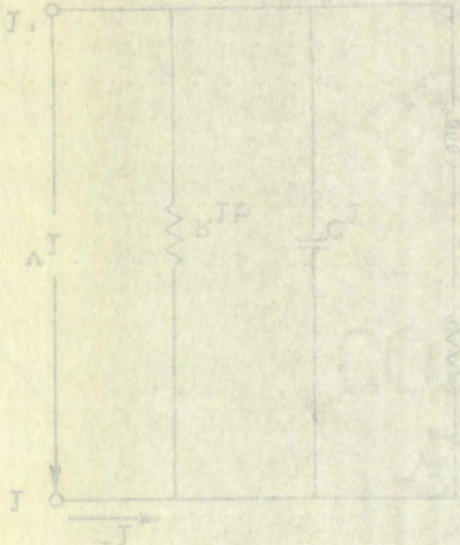

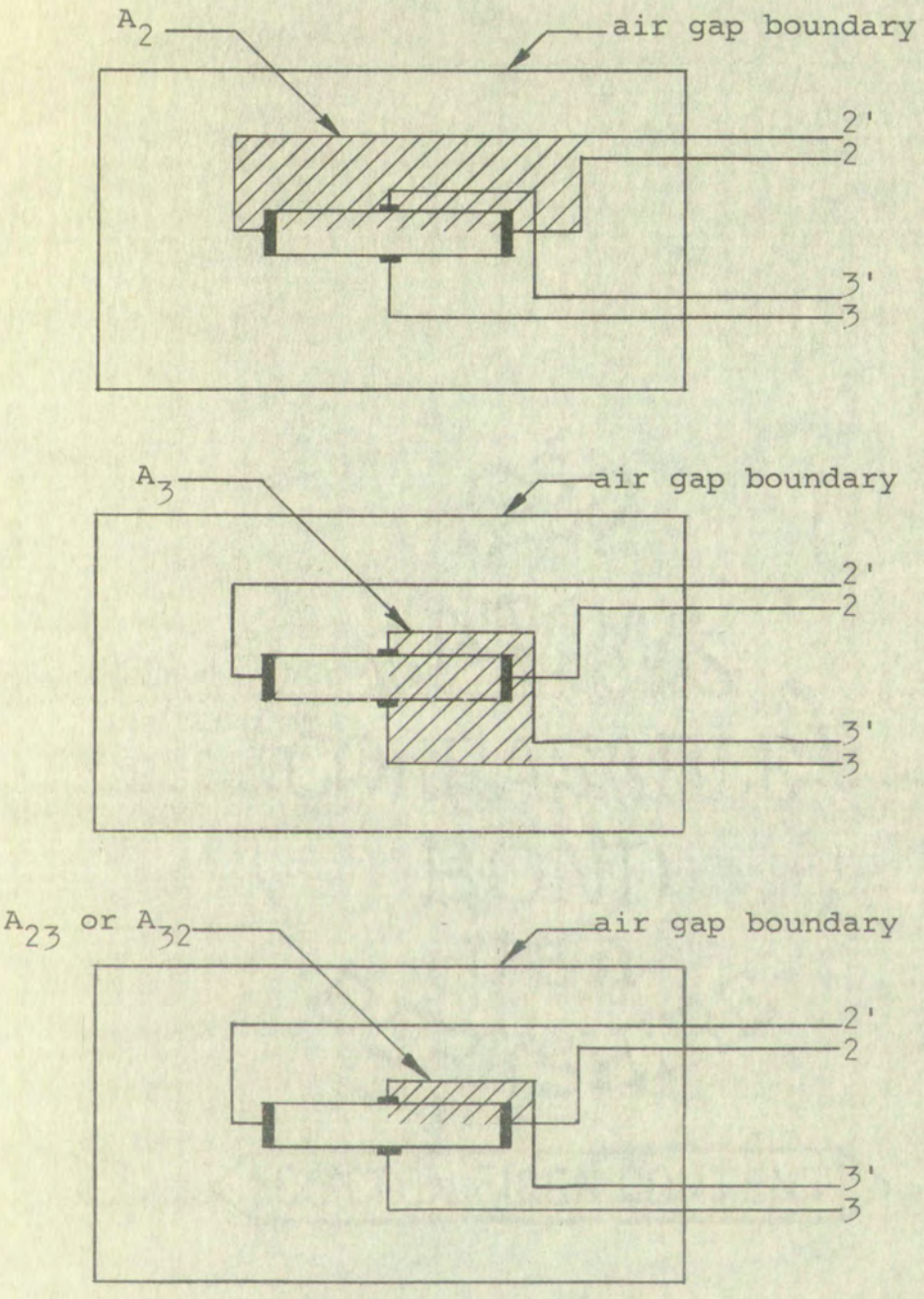

FIGURE 24 (REPEAT)
VARIOUS AREAS INVOLVED IN THE PARAMETERS
OF THE EQUIVALENT CIRCUIT

FIGURE 24 (REPEAT)

VARIOUS AREAS INVOLVED IN THE PARAMETERS

OF THE EQUIVALENT CIRCUIT

following equations:

$$L_1 = \frac{\mu_o N^2 ac}{b}, \qquad L_2 = \frac{\mu_o A_2}{b}, \qquad L_3 = \frac{\mu_o A_3}{b},$$

$$M_{12} = \frac{\mu_o N A_2}{b}, \qquad M_{13} = \frac{\mu_o N A_3}{b}, \qquad M_{21} = \frac{\mu_o N A_2}{b},$$

$$M_{31} = \frac{\mu_o N A_3}{b}, \qquad M_{23} = \frac{\mu_o A_{23}}{b}, \qquad M_{32} = \frac{\mu_o A_{32}}{b},$$

$$C_1 = \frac{1}{\omega_r^2 L_1} \qquad K_{2a} = \frac{\mu_o NR}{bd} \qquad K_{2b} = \left.\frac{V_2(j\omega)}{I_3(j\omega)}\right|_{\omega=0}, \quad (50)$$

$$K_{3a} = \frac{\mu_o NR}{bd} \qquad K_{3b} = \frac{\delta}{\sigma df}, \qquad R_{1a} = \left.\frac{V_1(j\omega)}{I_1(j\omega)}\right|_{\omega=0},$$

$$R_3 = \frac{2}{\sigma \pi d} \ln\left[\frac{\epsilon^{\pi g/f} + 1}{\epsilon^{\pi g/f} - 1}\right], \quad R_2 = \frac{e}{\sigma df}, \qquad R_{1b} = \left|Z_{11}(j\omega)\right|_{\omega=\omega_r},$$

where, R = Hall constant, meter^3/coulomb,

σ = conductivity of the semiconductor, 1/ohm meter,

μ_o = permeability of free space, henry/meter,

ω = angular frequency, radian/second,

ω_r = resonant angular frequency of the coil surrounding the toroid, radian/second,

δ = displacement of the output probes, meter,

$$Z_{11}(j\omega) = \left.\frac{V_1(j\omega)}{I_1(j\omega)}\right| I_2(j\omega) = I_3(j\omega) = 0, \text{ ohm.}$$

The set of equations (50) permits one to theoretically determine with the exception of four parameters the

following equations:

$$L_1 = \frac{\mu_o N_2^2 ac}{b},$$

$$M_{12} = \frac{\mu_o N A_2^2}{b},$$

$$M_{31} = \frac{\mu_o N A_3^2}{b},$$

$$C_1 = \frac{1}{\omega_r^2 L_1},$$

$$K_{3a} = \frac{\mu_o N R}{bd},$$

$$R_3 = \frac{2}{\sigma \pi d} \ln \left[\frac{e^{\pi d/\delta} + 1}{e^{\pi d/\delta} - 1} \right],$$

where, R = Hall constant (meter/coulomb),

σ = conductivity of the reacting plate (mho/meter),

μ_o = permeability of free space (henry/meter),

ω = angular frequency, radian/second,

ω_r = resonant angular frequency of the circuit, radians/second,

δ = displacement of the output member, meter,

$$Z_{11}(j\omega) = \frac{I_1^2(j\omega)}{V_1(j\omega)},$$

The set of equations (3-3) permits one to theoretically determine with the exception of [illegible] the

equivalent circuit of the system shown in Figure 8. The parameters R_{1b}, C_1, and K_{2b} must be determined experimentally. The parameter R_{1a} is simply the resistance of the coil surrounding the toroid, and it may be determined either experimentally or from tables. The parameter K_{2b} is nonzero only if the electrodes which supply the current to the semiconductor fail to cover its entire end faces. In the majority of applications the electrodes would cover the entire end faces of the semiconductor, and K_{2b} would be zero. If this is the case, only the parameters R_{1b} and C_1 would need to be determined experimentally.

The instructions for the experimental determination of the parameters R_{1b} and C_1 are contained in the set of equations (50). The resonant angular frequency, ω_r, of the coil surrounding the toroid may be determined from a plot of $|Z_{11}(j\omega)|$ as a function of frequency. The angular frequency for which $|Z_{11}(j\omega)|$ is a maximum is the resonant angular frequency of the coil surrounding the toroid. Therefore, the parameters R_{1b} and C_1 may be easily determined experimentally.

The determination of the equivalent circuit was based to a large extent on reasonable assumptions. Since a number of approximations were made throughout the development of the equivalent circuit, the experimental verifacation of the equivalent circuit was quite important. A

physical system consisting of a high permeability toroid and an indium antimonide Hall generator was used in the experimental verification of the equivalent circuit. The set of equations (50) was used to determine the equivalent circuit parameters. The validity of this equivalent circuit was then established by several approaches.

The first approach involved an analysis of the system from an open-circuit impedance viewpoint. The various open-circuit impedances of the system were theoretically determined as a function of frequency from the equivalent circuit, and the open-circuit impedances of the physical system were then measured as a function of frequency. For frequencies below one megacycle the results obtained from the equivalent circuit were found to agree quite well with those obtained by measurement of the physical system. The difference between the experimental and theoretical open-circuit impedances was never found to be more than 30 per cent except at frequencies near resonance. Even at frequencies near resonance the only significant difference between the experimental and theoretical results was a slight shift in the resonant frequency. This was believed to be caused by the capacitance of the equipment used in the measurements.

The usefulness of the open-circuit impedance

approach was limited by the fact that the effects of the Hall voltage generator were not placed in evidence. Indeed if they were, the concept of impedance would have no meaning since the Hall voltage is not linear with respect to voltages applied at terminals 1-1' and 2-2'. The only reason that the open-circuit impedance approach could be used was that the effect of the Hall voltage generator could be neglected in comparison with the other voltages present. This was primarily due to the fact that in the measurement of the open-circuit impedances only one voltage was impressed on the system at a time.

To place in evidence the effects of the Hall voltage generator voltages must be impressed at two different inputs. If arbitrary voltages are used, the determination of the behavior of the system is complicated by the multiplication effect of the Hall voltage generators. To avoid this difficulty it was decided that a d.c. voltage would be applied to terminals 1-1', and an a.c. voltage would be applied to terminals 2-2'. The open-circuit voltage was then measured at terminals 3-3'. Such an analysis indicated that the equivalent circuit could accurately be used to predict the voltage obtained. A d.c. voltage was then applied to terminals 2-2', and an a.c. voltage was applied to terminals 1-1'. The open-circuit voltage obtained at

terminals 3-3' was as predicted by the equivalent circuit. Thus, the results of this phase of the experimental investigation indicated that the equivalent circuit could be used to accurately represent the physical system for the case of sinusoidal steady-state operation at frequencies below one megacycle.

The open-circuit impedances were also investigated for frequencies above one megacycle. It was generally found that the equivalent circuit failed to represent the physical system. The equivalent circuit could be modified to take into consideration high frequency operation, but it is believed that the equivalent circuit would be too complicated to be of any practical value. Since the equivalent circuit fails to represent the physical system for frequencies above one megacycle, one is hesitant to state that the equivalent circuit may be used to predict the transient behavior of the system.

To obtain some indication of the ability of the equivalent circuit to predict the transient behavior of the system the following test was performed. A step of current was supplied to terminals 2-2' of the physical system with terminals 1-1' open-circuited. The voltage appearing at terminals 3-3' was then measured as a function of time and compared with the response as predicted from the equivalent

circuit. The agreement between the two was generally quite good with the exception that the response of the physical system possessed some high frequency low amplitude components which died out after several cycles of oscillation. Therefore, the equivalent circuit may be used to obtain some indication of the transient behavior of the system even though the equivalent circuit is not valid for frequencies above one megacycle.

The nonlinear properties of the system were also investigated. Since the Hall voltage generators are proportional to the product of two currents, application of the equivalent circuit may involve nonlinear differential equations. Another type of nonlinearity may occur due to the amplitudes of the currents used in the system. This particular type of nonlinearity is not evident from an inspection of the equivalent circuit and must be determined from the physical system.

Since a magnetic material is used in the system, the flux produced due to a flow of current will eventually reach saturation. The conductivity of the semiconductor is a function of magnetic field and temperature. Furthermore, the Hall constant, R, is a function of temperature. These three factors were investigated experimentally, and it was generally found that current must be confined to less than

one ampere to prevent this type of nonlinearity. These results depend upon the particular system used.

In summary it is believed that the results of the experimental analysis indicate that the equivalent circuit may be used to obtain an accurate representation of the system chosen for study provided that the frequency of operation is limited to less than one megacycle. The equivalent circuit may also be used to obtain some indication of the transient behavior of the system. The restrictions imposed on the amplitude level are not particularly severe. Although only one system was used in the experimental verification of the equivalent circuit, the results should be valid for other systems with different dimensions and electrical characteristics. The basic equivalent circuit should be applicable; however, such factors as frequency and amplitude range would be different.

II. CONCLUSIONS

The equivalent circuit developed in this study should prove to be useful in the analysis and design of Hall effect devices. By examination of the parameters of the equivalent circuit one should be able to determine how to select the various dimensions and electrical characteristics of the system to obtain optimum performance.

The frequency range and amplitude level restrictions should not seriously limit the usefulness of the equivalent circuit. Even though the equivalent circuit is not valid for frequencies above one megacycle, the transient behavior of the system may be determined. In general it is believed that the equivalent circuit represents very accurately the physical system.

Although the equivalent circuit developed in this study is limited to a specific flux concentrator and Hall generator, the results may be extended to include other configurations. For example consider a configuration which utilizes a flux concentrator and Hall generator similar to the one considered in this study with the exception that the leads of the Hall generator are brought directly out of the air gap without forming closed loops. The self and mutual inductance parameters of the equivalent circuit would need to be changed; however, the other parameters of the equivalent circuit would be the same as those developed in this study. The determination of the self and mutual inductance parameters would be based on the same principles used in this study.

The major limitation of the equivalent circuit is the possibility of nonlinear differential equations. The analytical solutions of these equations may be quite

The frequency range and amplitude level restrictions should not seriously limit the usefulness of the equivalent circuit. Even though the equivalent circuit is not valid for frequencies above one megacycle, the transient behavior of the system may be determined. In general it is believed that the equivalent circuit represents very accurately the physical system.

Although the equivalent circuit developed in this study is limited to a specific flux concentrator and Hall generator, the results may be extended to include other configurations. For example consider a configuration which utilizes a flux concentrator and Hall generator similar to the one considered in this study with the exception that the leads of the Hall generator are brought directly out of the air gap without forming closed loops. The self and mutual inductance parameters of the equivalent circuit would need to be changed; however, the other parameters of the equivalent circuit would be the same as those developed in this study. The determination of the self and mutual inductance parameters would be based on the same principles used in this study.

The major limitation of the equivalent circuit is the possibility of nonlinear differential equations. The analytical solutions of these equations may be quite

difficult unless certain assumptions are made. If non-linear differential equations are encountered, they may be solved with the aid of a computer. In fact the complete equivalent circuit may be programmed on a suitable computer and studied under various operating conditions that might occur in the application of the device.

The equivalent circuit should also be useful in the understanding of the various phenomena which occur in the system. By an examination of the equivalent circuit one should be able to write the various differential equations which describe the operation of the system as well as understand why they take the form they do. This is perhaps the most important contribution offered by this study.

BIBLIOGRAPHY

BIBLIOGRAPHY

BIBLIOGRAPHY

Dunlap, W. Crawford, Jr. An Introduction to Semiconductors. New York: John Wiley and Sons, Inc., 1957. 417 pp.

Endsley, David L., and W.W. Grannemann. "A Theoretical and Experimental Analysis of a Hall Generator." Technical Report EE-27, the University of New Mexico Engineering Experiment Station, Albuquerque, 1959.

Fox, Jerome (ed.). Proceedings of the Symposium on the Role of Solid State Phenomena in Electric Circuits. New York: Interscience Publishers, 1957. 339 pp.

Hall, E.H. "On a New Action of the Magnet on Electric Currents," American Journal of Mathematics, 2:287, 1879.

Hilsum, C. "Multiplication by Semiconductors," Electronic Engineering, 30:664-666, November, 1958.

Kittel, Charles. Introduction to Solid State Physics. New York: John Wiley and Sons, Inc., 1953. 617 pp.

Kraus, John D. Electromagnetics. New York: McGraw-Hill Book Company, Inc., 1953. 604 pp.

Lindberg, Olaf. "Hall Effect," Proceedings of the I.R.E., 40:1414-1419, November, 1952.

Löfgren, Lars. "Analog Multiplier Based on the Hall Effect," Journal of Applied Physics, 29:158-166.

Middlebrook, R.D. An Introduction to Junction Transistor Theory. New York: John-Wiley and Sons, Inc., 1957. 296 pp.

Ross, I.M., and E.W. Saker. "Applications of Indium Antimonide," Journal of Electronics, 1:223-230, June, 1955.

_____, E.W. Saker, and N.A.C. Thompson. "The Hall-Effect Compass," Journal of Scientific Instruments, 34:479-484, December, 1957.

_____, and N.A.C. Thompson. "An Amplifier Based on the Hall Effect," Nature, 175:518, March, 1955

Saker, E.W., F.A. Cunnell, and J.T. Edmonds. "Indium Antimonide as a Fluxmeter Material," British Journal of Applied Physics, 6:217-220, June, 1955.

Shive, John N. The Properties, Physics, and Design of Semiconductor Devices. Princeton, New Jersey: D. Van Nostrand Company, Inc., 1959. 487 pp.

Shockley, William. Electrons and Holes in Semiconductors. Princeton, New Jersey: D. Van Nostrand Company, Inc., 1950, 558 pp.

Spence, D.W. and C.R. Cahn. "Basic Concepts in the Analysis of Stationary Electric Circuits," A.I.E.E. Transactions on Communications and Electronics, pp. 617-624, November, 1953.

Stout, Melville B. Basic Electrical Measurements. New York: Prentice-Hall, Inc., 1950. 504 pp.

Strutt, M.J.O. "Hall Effect in Semiconductor Compounds," Electronic and Radio Engineering, 36:2-10, January, 1959.

Baker, E.W., F.A. Cunnell, and J.T. Edmonds. "Indium Antimonide as a Fluxmeter Material." British Journal of Applied Physics, 6:217-220, June, 1955.

Shive, John N. The Properties, Physics, and Design of Semiconductor Devices. Princeton, New Jersey: D. Van Nostrand Company, Inc., 1959. 487 pp.

Shockley, William. Electrons and Holes in Semiconductors. Princeton, New Jersey: D. Van Nostrand Company, Inc., 1950. 558 pp.

Spence, D.W. and C.R. Cahn. "Basic Concepts in the Analysis of Stationary Electric Circuits," A.I.E.E. Transactions on Communications and Electronics, pp. 617-624, November, 1959.

Stout, Melville B. Basic Electrical Measurements. New York: Prentice-Hall, Inc., 1950. 504 pp.

Strutt, M.J.O. "Hall Effect in Semiconductor Compounds," Electronic and Radio Engineering, 36:2-10, January, 1959.

APPENDIX

APPENDIX I

DIMENSIONS AND ELECTRICAL CHARACTERISTICS OF THE EXPERIMENTAL MODEL

$N = 155$ turns

$a = 1.9 \times 10^{-2}$ meter

$b = 7.61 \times 10^{-4}$ meter

$c = 10^{-2}$ meter

$d = 1.27 \times 10^{-4}$ meter

$e = 1.02 \times 10^{-2}$ meter

$f = 3.18 \times 10^{-3}$ meter

$g = 1.27 \times 10^{-4}$ meter

$\delta = 2.77 \times 10^{-4}$ meter

$A_2 = 4 \times 10^{-5}$ meter^2

$A_3 = 4 \times 10^{-5}$ meter^2

$A_{23} = 2 \times 10^{-5}$ meter^2

$\sigma = 2.2 \times 10^{4}$ 1/ohm meters

$R = 10^{-4}$ meter^3/coulomb

$R_{1a} = 0.613$ ohm

$f_r = 237$ k.c.p.s.

$|Z_{11}(j\omega_r)| = 142$ Kohms

APPENDIX I

DIMENSIONS AND ELECTRICAL CHARACTERISTICS OF THE EXPERIMENTAL MODEL

$N = 155$ turns

$a = 1.9 \times 10^{-2}$ meter

$b = 7.61 \times 10^{-4}$ meter

$c = 10^{-2}$ meter

$d = 1.27 \times 10^{-4}$ meter

$e = 1.02 \times 10^{-2}$ meter

$f = 3.18 \times 10^{-3}$ meter

$g = 1.27 \times 10^{-4}$ meter

$\delta = 2.77 \times 10^{-4}$ meter

$A_2 = 4 \times 10^{-5}$ meter^2

$A_3 = 4 \times 10^{-5}$ meter^2

$A_{23} = 2 \times 10^{-5}$ meter^2

$\sigma = 2.2 \times 10^{4}$ 1/ohm meters

$R = 10^{-4}$ meter^3/coulomb

$R_{1a} = 0.613$ ohm

$\varepsilon_r = 237$ k.c.p.s.

$|Z_{11}(j\omega_r)| = 142$ Kohms

APPENDIX II

PARAMETERS OF THE EQUIVALENT CIRCUIT OF THE EXPERIMENTAL MODEL

L_1 = 7.52 m henry

L_2 = 0.066 μ henry

L_3 = 0.066 μ henry

M_{12} = 10.2 μ henry

M_{13} = 10.2 μ henry

M_{21} = 10.2 μ henry

M_{31} = 10.2 μ henry

M_{23} = 0.033 μ henry

M_{32} = 0.033 μ henry

C_1 = 60 $\mu\mu$ farad

K_{2a} = 0.202 volt/ampere^2

K_{2b} = 0.0375 volt/ampere

K_{3a} = 0.202 volt/ampere^2

K_{3b} = 0.0312 volt/ampere

R_{1a} = 0.613 ohm

R_3 = 0.695 ohm

R_2 = 1.26 ohms

R_{1b} = 142 K ohms

APPENDIX III

OPEN CIRCUIT IMPEDANCES

$$Z_{11}(s) = \frac{1.67\times10^{10}(s + 81.5)}{s^2 + 1.17\times10^{5}s + 2.22\times10^{12}}$$

$$Z_{12}(s) = \frac{\pm 2.26\times10^{7}s}{s^2 + 1.17\times10^{5}s + 2.22\times10^{12}}$$

$$Z_{13}(s) = \frac{\pm 2.26\times10^{7}s}{s^2 + 1.17\times10^{5}s + 2.22\times10^{12}}$$

$$Z_{21}(s) = \frac{\pm 2.26\times10^{7}s}{s^2 + 1.17\times10^{5}s + 2.22\times10^{12}}$$

$$Z_{22}(s) = \frac{5.22\times10^{-8}(s^3 + 2.21\times10^{7}s^2 + 5.38\times10^{12}s + 4.86\times10^{19})}{s^2 + 1.17\times10^{5}s + 2.22\times10^{12}}$$

$$Z_{23}(s) = \frac{\pm 1.92\times10^{-8}(s^3 + 2.08\times10^{6}s^2 + 4.05\times10^{12}s + 4.35\times10^{18})}{s^2 + 1.17\times10^{5}s + 2.22\times10^{12}}$$

$$Z_{31}(s) = \frac{\pm 2.26\times10^{7}s}{s^2 + 1.17\times10^{5}s + 2.22\times10^{12}}$$

$$Z_{32}(s) = \frac{\pm 1.92\times10^{-8}(s^3 + 1.75\times10^{6}s^2 + 4.01\times10^{12}s + 3.61\times10^{18})}{s^2 + 1.17\times10^{5}s + 2.22\times10^{12}}$$

$$Z_{33}(s) = \frac{5.22\times10^{-8}(s^3 + 1.22\times10^{7}s^2 + 4.22\times10^{12}s + 2.68\times10^{19})}{s^2 + 1.17\times10^{5}s + 2.22\times10^{12}}$$

APPENDIX III

OPEN CIRCUIT IMPEDANCES

$$Z_{11}(s) = \frac{1.6\gamma\times10^{10}(s + 81.5)}{s^2 + 1.17\times10^5 s + 2.22\times10^{12}}$$

$$Z_{12}(s) = \frac{\pm2.26\times10^7 s}{s^2 + 1.17\times10^5 s + 2.22\times10^{12}}$$

$$Z_{13}(s) = \frac{\pm2.26\times10^7 s}{s^2 + 1.17\times10^5 s + 2.22\times10^{12}}$$

$$Z_{21}(s) = \frac{\pm2.26\times10^7 s}{s^2 + 1.17\times10^5 s + 2.22\times10^{12}}$$

$$Z_{22}(s) = \frac{5.22\times10^{-8}(s^3 + 2.21\times10^7 s^2 + 5.38\times10^{12} s + 4.86\times10^{19})}{s^2 + 1.17\times10^5 s + 2.22\times10^{12}}$$

$$Z_{23}(s) = \frac{\pm1.92\times10^{-8}(s^3 + 2.08\times10^6 s^2 + 4.05\times10^{12} s + 4.29\times10^{18})}{s^2 + 1.17\times10^5 s + 2.22\times10^{12}}$$

$$Z_{31}(s) = \frac{\pm2.26\times10^7 s}{s^2 + 1.17\times10^5 s + 2.22\times10^{12}}$$

$$Z_{32}(s) = \frac{\pm1.92\times10^{-8}(s^3 + 1.73\times10^6 s^2 + 4.01\times10^{12} s + 3.61\times10^{18})}{s^2 + 1.17\times10^5 s + 2.22\times10^{12}}$$

$$Z_{33}(s) = \frac{5.22\times10^{-8}(s^3 + 1.22\times10^7 s^2 + 4.22\times10^{12} s + 2.68\times10^{19})}{s^2 + 1.17\times10^5 s + 2.22\times10^{12}}$$

APPENDIX IV

DERIVATION OF $Z_{23}(s)$

The determination of the open-circuit impedance $Z_{23}(s)$ involves a consideration of the voltage produced at terminals 2-2' due to a current in loop three. Assume that the current in loop three is given by,

$$i_3(t) = I_3 \sin\omega t \tag{51}$$

where, $i_3(t)$ = current in loop three, ampere,

I_3 = peak value of current in loop three, ampere,

ω = angular frequency, radian/second.

An inspection of the equivalent circuit shown on Figure 13, page 23 indicates that the voltage produced at terminals 3-3' is expressible as,

$$\begin{aligned} v_2(t) = {} & \pm M_{23}\frac{d}{dt} i_3(t) \pm M_{21}\frac{d}{dt} i(t) \\ & \pm K_{2b} i_3(t) \pm K_{2a} i(t) \cdot i_3(t) \end{aligned} \tag{52}$$

where, $v_2(t)$ = voltage produced at terminals 2-2',

$i(t)$ = current which results in loop one due to a current in loop three, ampere.

The current produced in loop one due to a current in loop three may be shown to be,

$$i(t) = \left|H(j\omega)\right| I_3 \sin(\omega t + \phi) \tag{53}$$

where,
$$H(j\omega) = \left|H(j\omega)\right| \angle \phi \tag{54}$$

and,
$$H(j\omega) = \frac{\pm j\omega(M_{13}/L_1)(j\omega + 1/R_{1b}C_1)}{-\omega^2 + j\omega\left(\frac{1}{R_{1b}C_1} + \frac{R_{1a}}{L_1}\right) + \frac{R_{1a}+R_{1b}}{R_{1b}L_1C_1}}. \tag{55}$$

Equations (52) through (55) may now be combined to give,

$$v_2(t) = I_3\Big[\pm \omega M_{23}\cos\omega t \pm \omega M_{21}\left|H(j\omega)\right| \cos(\omega t + \phi) \pm K_{2b}\sin\omega t \pm K_{2a}\left|H(j\omega)\right|^2 I_3 \sin(\omega t + \phi)\sin\omega t\Big] \tag{56}$$

Consider the terms,

$$\pm K_{2a}\left|H(j\omega)\right|^2 I_3 \sin(\omega t + \phi)\ \sin\omega t$$

$$\text{and, } \pm K_{2b}\sin\omega t.$$

If the parameters of the equivalent circuit of the experimental model are substituted into these terms it is seen that the coefficients vary with frequency as indicated by Figure 39. Figure 39 further indicates that if the current in loop three is less than one ampere, then

$$K_{2a}\left|H(j\omega)\right|^2 \ll K_{2b}. \tag{57}$$

Therefore the term,

$$\pm K_{2a}\left|H(j\omega)\right|^2 I_3 \sin(\omega t + \phi)\sin\omega t$$

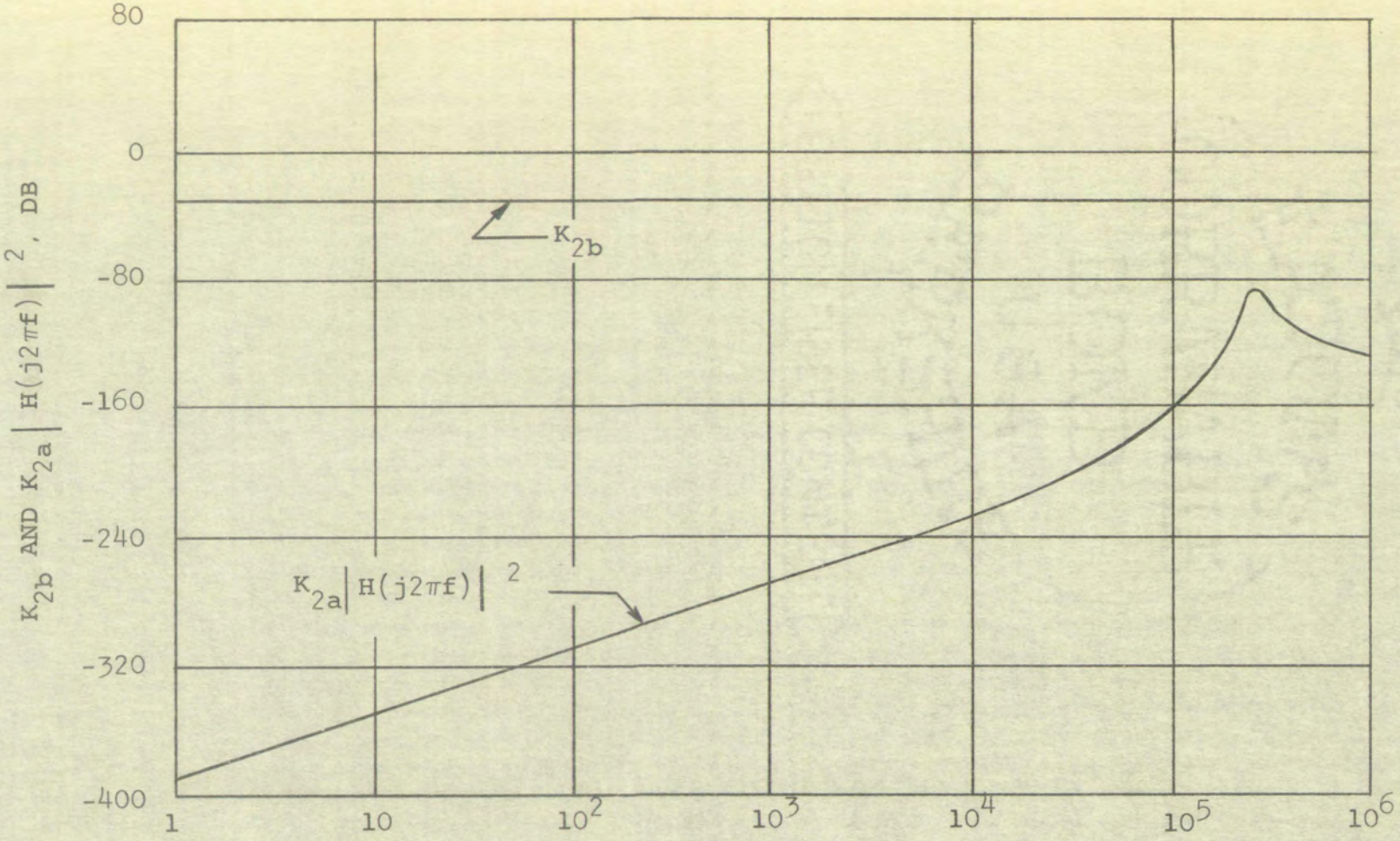

FIGURE 39

K_{2b} and $K_{2a}\left|H(j2\pi f)\right|^2$ VERSUS FREQUENCY

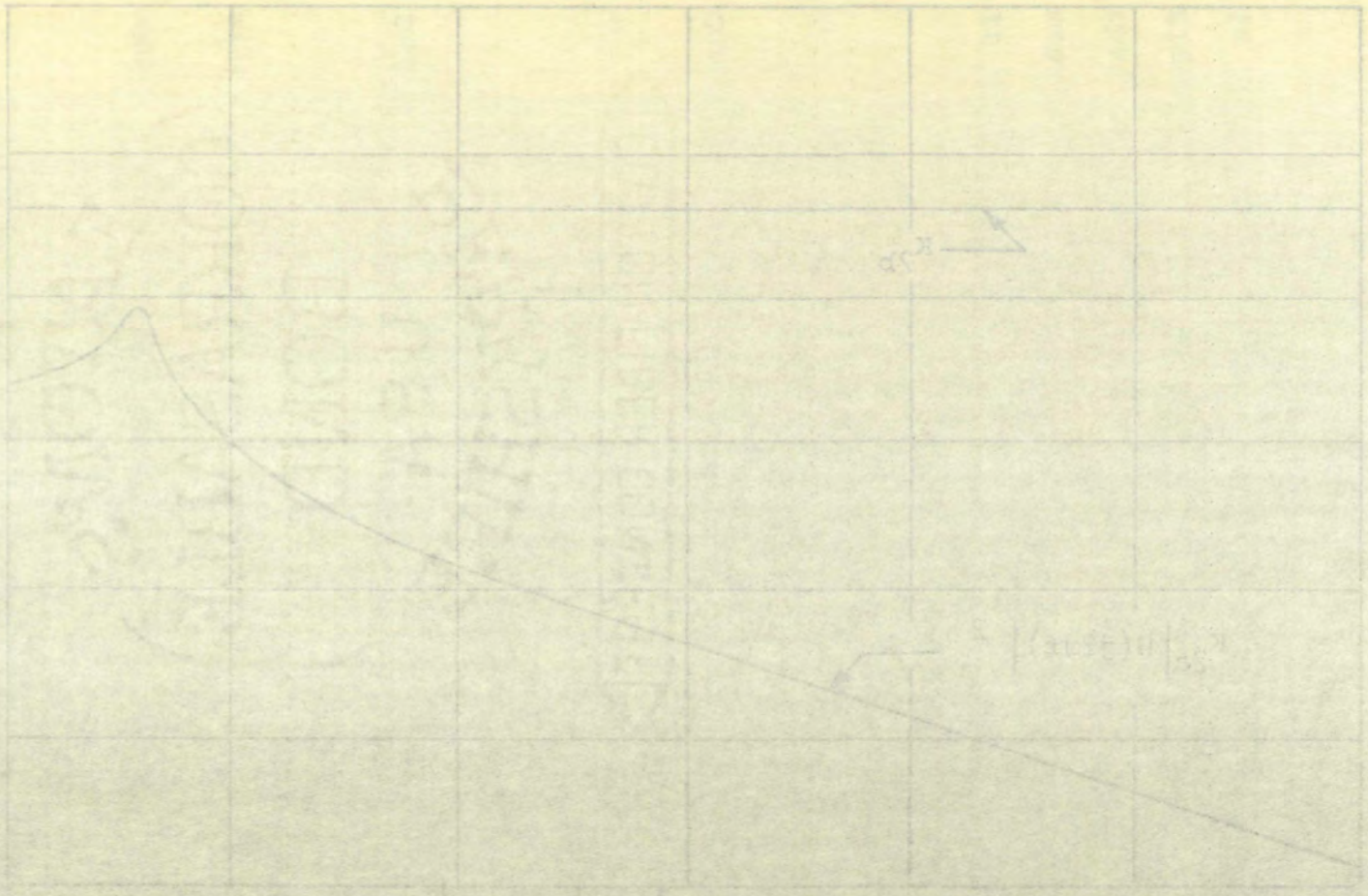

may be neglected in equation (56). If this approximation is made, the derivation of $Z_{23}(s)$ is quite straightforward. It should be emphasized that the assumption made in this derivation is valid only for the experimental model considered in this study. The assumption should be valid for a number of other configurations: however, each case must be examined individually.

may be neglected in equation (56). If this approximation is made, the derivation of $Z_{23}(s)$ is quite straightforward. It should be emphasized that the assumption made in this derivation is valid only for the experimental model considered in this study. The assumption should be valid for a number of other configurations; however, each case must be examined individually.

IMPORTANT!

Special care should be taken to prevent loss or damage of this volume. If lost or damaged, it must be paid for at the current rate of typing.

DATE DUE

AUG 13 1962			
AUG - 6 RECD			
GAYLORD			PRINTED IN U.S.A.